Identification of the PH Domain of Adaptor Protein SH2B1 as a Critical Regulator of Energy Balance and Glucose Metabolism

by

Anabel Flores Arenas

A dissertation submitted in partial fulfillment
of the requirements for the degree of
Doctor of Philosophy
(Cellular and Molecular Biology)
in the University of Michigan
2019

Doctoral Committee:

Professor Christin Carter-Su, Chair
Professor Malcolm J. Low
Professor Martin G. Myers Jr.
Associate Professor Brian Pierchala

Anabel Flores Arenas

anabelf@umich.edu

ORCID iD: 0000-0003-1764-4278

Dedication

This dissertation is dedicated to my lovely family.

Acknowledgements

I would like thank my mentor, Christin Carter-Su. She is not only a great scientist but also an exceptional mentor. It is a true privilege to have a mentor guide me through the many challenges I have faced as a graduate student. She has helped me grow as a scientist and personally. She has helped me write grants, manuscripts, and analyze data, for that I will always be grateful. She has taught me to learn to take a seat at the table as a minority woman in science and to find passion in my profession. She is a truly inspiring woman who was more than a mentor to me. I am truly blessed to have Christy as a role model.

I would like to thank my committee members Drs. Martin G. Myers Jr., Malcolm J. Low, and Brian Pierchala. Special thanks to Martin for being like a co-mentor throughout my graduate career and for helping with our animal studies. Thank you all for the exchange of ideas and positive motivation during my committee meetings, which were invaluable contributions that improved my experiments. All of you have been excellent role models during my graduate school studies. Your advice and guidance has been well appreciated.

I would like to thank past and present members of the Carter-Su Lab. Larry Argetsinger for his guidance and support. I have not met a person more kind and willing to go out of his way to help others. Thank you for helping me troubleshoot experiments and for your words of wisdom throughout my graduate career. I am grateful for your great stories that inspired me to travel to beautiful places in the Upper Peninsula of Michigan. Joel Cline for keeping the lab operating and his great stories about Ollie and Coby. I am grateful to Barbara Hawkins and Sarah

Cain for their support throughout my graduate career. I thank past and current members of the lab Liliya Mancour, Ray Joe, Jessica Cote, Michael Ellis, Nadya Svezhova, Erik Clutter and Abby Cacciaglia for their scientific support and day-to-day conversations that have made life in the lab enjoyable. I thank the past and current students I mentored Lauren DeSantis, Yixin Xu, Gowry Chandresakar, Alvaro Malaga, Paul Vander, Amanda Beyer, and Nicole Pohlman. I am really grateful for your help in my projects! Special thanks to Lauren DeSantis (Ms. Hyper-personality) and Paul Vander for their great contribution towards my project and for making the Carter-Su Lab such a joyful place to work in. Also, I thank the undergraduate work study students: Michelle Kim, Kaitlyn Kuder, and Tahrim Choudhury, whose help have made life in the lab easier. I thank the past and current members of the Yin lab: Lei, Tony, Deqiang, Pei, Meichan, Claire, Omar, and Nick; for helpful scientific feedback and help to improve my scientific communication.

I want to thank my friends, Susana Chan, Macy Veiling, Brittany Flores, Sierrah Grigsby for being great friends and for their support so that I could accomplish my doctoral goals.

I would like to thank other mentors that have supported me throughout my education. Ms. Maria Grieve, my elementary school principal who wend above and beyond her job to make sure my sisters and I thrived in a new school system. Ms. Socorro Ceja, Mr. Dennis Mendoca and Mr. Rafael Barboza for their support throughout high school. Dr. Bruce Prins and Dr. Dennis Bideshi, Professors at California Baptist University, are the persons who got me interested in research. I express my gratitude towards past research mentors: Drs. Joan Heller Brown (UCSD), Nicole Purcell (UCSD), Francisco Villarreal (UCSD), George Kulik (Wake Forest University), and Sazzad Hassan (Wake Forest University). I would definitely not have pursued a Ph.D. if it were not for them.

I would like to thank my beautiful family. First, my wonderful mother Petra for her patience, understanding, and love. She is the super glue that holds our family together. I would like to extend my gratitude to both of my parents for raising six children and sending them all to college. My siblings are the best gift my parents have given me! My big brother Yasmany, for teaching me how to read as a child and for setting a good example for the rest of us. My older sister Cristina, for inspiring me to be a scientist, to fly out of the nest, and explore the world. My twin Lourdes, for all the great adventures and her company throughout high school, college, and graduate school. My young sister Yolanda, for her kindness and for the intellectual conversations. Thank you for being my companion in my international adventures. My baby sister Zenaida, for her free spirit and bringing so much joy into our lives. Thank you, sisters, you are my best friends!

The work for my dissertation was supported by NIH grants R01-DK54222, R01-DK107730, T32-GM008322 and 5P60-DK20572; HHMI Gilliam Fellowship; and Rackham Graduate School Merit Fellowship.

Table of Contents

List of Tables

List of Figures

Abstract

Obesity is a growing epidemic but the cellular and molecular mechanisms underlying obesity are still not well understood. Mutations in the adaptor protein SH2B1 have been identified in individuals with severe early-onset childhood obesity, insulin resistance, and hyperphagia. Adaptor proteins have protein binding domains that link protein binding partners and therefore facilitate the creation of larger signaling complexes. This phenotype is also seen in mice lacking SH2B1 (SH2B1-KO mice). Furthermore, experiments using SH2B1-KO mice and cultured neurons suggest that neuronal SH2B1 is critical for this phenotype. Three of the human obesity-associated mutations are located in the pleckstrin homology (PH) domain of SH2B1, suggesting that the PH domain is important for the overall function of SH2B1. The aims of this thesis work were to gain insight into how SH2B1 regulates energy balance and glucose metabolism, and the contribution of its PH domain to these functions by using two novel mouse models. The first model contained one of the human obesity-associated mutations (P322S). Body weight, food intake, glucose tolerance and insulin tolerance were not substantially altered by the P322S mutation when mice were fed normal chow. However, the P322S mutation decreased glucose tolerance in mice challenged by a high fat diet. No effect on insulin tolerance was noted. In contrast, a second mouse model with a two-amino acid deletion (ΔP317,R318) in the PH domain of SH2B1 showed an obese phenotype. The ΔP317,R318 mice showed significantly increased body weight, adiposity, plasma leptin levels and plasma insulin levels, and decreased glucose and insulin tolerance. In females, the reduced glucose tolerance and increased plasma insulin levels appeared even before the onset of obesity, suggesting that the ΔP317, R318 mutation

results in impaired glucose homeostasis independent of the obese phenotype. At the cellular level, deleting P317, R318 changed the localization of SH2B1β from being primarily in the cytoplasm and plasma membrane to being primarily in the nucleus. Deleting P317, R318 also impaired the ability of SH2B1β to enhance nerve growth factor-induced neurite outgrowth in preneuronal PC12 cells. This work provides evidence that the PH domain is a key regulator of SH2B1 subcellular localization, neurite outgrowth, and the control of energy balance and glucose homeostasis.

Chapter 1 Introduction

The Adaptor Protein SH2B1

Adaptor proteins form part of the signaling cascade downstream of cell surface receptors. Adaptor proteins are diverse proteins composed of multiple modular interaction domains (1). They play a role in helping to relay messages from the plasma membrane to the nucleus and other parts of the cell by serving as docking sites for multiple protein partners in the cascade. Their resulting proximity allows proteins in the cascade to find their partners quickly. Some adaptor proteins are docked by proteins in the cascade even before an activated membrane receptor sends a message to them. However, other adaptor proteins remain unloaded until a message from an activated membrane receptor reaches them and then they are docked by other proteins in the cascade. Some of these cell surface receptors include receptor tyrosine kinases. Ligand binding activates the enzymatic activity of these receptor tyrosine kinases producing phosphotyrosine residues that can serve as docking sites for proteins with Src homology 2 (SH2) domains (2). SH2B1 (SH2-B, PSM) is a member of a family of three adaptor proteins that also includes SH2B2 (APS) and SH2B3 (Lnk). The three proteins share common domains including dimerization, pleckstrin homology (PH) and SRC homology 2 (SH2) domains (3-5). The *SH2B1* gene is alternatively spliced into 4 isoforms (α, β, γ, and δ). The isoforms are identical and differ only in the C-terminal region after the SH2 domain (Figure 1.1) (6) SH2B1 is recruited to, and plays a role in, the signal transduction process of multiple receptor tyrosine kinases including receptors for nerve growth factor (NGF) (7,8), brain-derived neurotrophic factor (BDNF) (7), insulin receptor (9,10), insulin-like growth factor (IGF-I) (11), glial cell line-derived

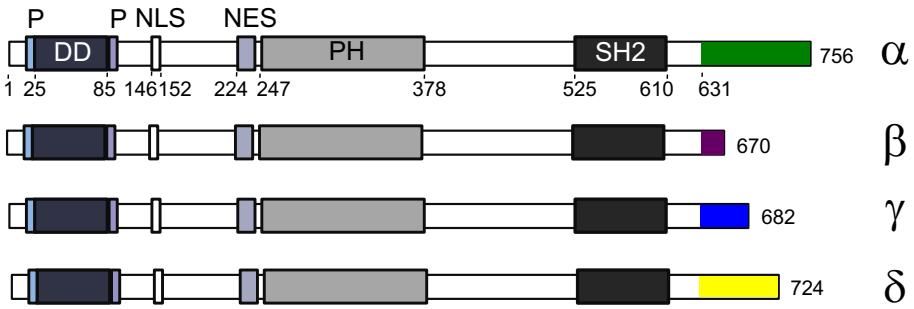

Figure 1.1 Schematic of the four human SH2B1 isoforms.

Shown are the proline-rich regions (P), dimerization domain (DD), nuclear localization sequence (NLS), nuclear export sequence (NES), pleckstrin homology (PH) domain, Src-homology 2 domain (SH2), and tyrosines (Y). Unique C-terminal tails are depicted in different colors.

neurotrophic factor (GDNF) (12), platelet-derived growth factor (PDGF) (13), and fibroblast growth factor (FGF) (14). SH2B1 is also recruited to activated JAK family members complexed to ligand-bound cytokine family receptors (15-18).

Mechanisms of interaction of SH2B1 with different receptors

The mechanisms by which SH2B1 interacts with these different receptors and mediates signal transduction have been investigated to varying degrees. In this thesis, I will limit my discussion to receptors for NGF (TrkA), BDNF (TrkB), leptin (in complex with JAK2), insulin, and IGF-1 because those are the most pertinent to my project. SH2B1 has been implicated in TrkA and TrkB signaling. SH2B1β/γ and family member SH2B2 were identified to interact with TrkA and TrkB in yeast two-hybrid screens (7,17). SH2B1α, β and γ have been shown to co-precipitate with active TrkA and SH2B1β with TrkB (19,7,13,20). NGF and BDNF stimulation lead to the dimerization of TrkA and TrkB, respectively (21) and subsequent autophosphorylation of several tyrosines in the cytoplasmic domain of TrkA and TrkB (22). The interaction of SH2B1β/γ or SH2B2 with TrkA takes place via phosphorylated tyrosines in the kinase activation loop of TrkA (7,17). This phosphotyrosine-dependent interaction between SH2B1 and TrkA was confirmed via GST pull down assays in cells treated with NGF (interaction was not seen in cells without treatment). The SH2 domain appears to be required for this interaction since it was not seen when the SH2 domain was mutated (8). I helped show that in response to NGF, TrkA phosphorylates tyrosine 753 in SH2B1α and tyrosines 55 and 439 in both SH2B1α and SH2B1β (19). I have also shown that SH2B1β is phosphorylated by TrkB (data not shown) but have not yet identified the sites of phosphorylation. While SH2B1β and γ appear to have similar functions *in vitro*, Joe et al. (19) showed that SH2B1α has different effects on NGF signaling. In contrast to the β tail, the unique α tail inhibits the ability of SH2B1

to: 1) cycle through the nucleus; 2) enhance NGF-mediated neurite outgrowth; 3) enhance NGF-mediated gene expression; 4) enhance phosphorylation of AKT and phospholipase C gamma (PLC-γ); and 5) enhance autophosphorylation of TrkA. The function of SH2B1α appears to be regulated by phosphorylation of tyrosine 753 in the C-terminal tail since the functions listed above were restored when tyrosine 753 was mutated to a phenylalanine (Y753F). Furthermore, SH2B1α may act as an inhibitor of the actions mediated by SH2B1β. Co-expression of SH2B1α inhibited the ability of SH2B1β to enhance neurite outgrowth. This was not the case when SH2B1α Y753F was co-expressed with SH2B1β.

Shc and PLC-γ are phosphorylated in response to NGF and recruited to TrkA (7,8). Phosphorylation of PLC-γ leads to activation of its enzymatic activity (23). However, tyrosyl phosphorylation of SH2B1 is thought to create docking sites for the formation of protein complexes at the receptor which in turn mediate signal transduction cascades. Tyrosyl phosphorylation of Shc by TrkA results in the recruitment of Grb2-SOS complexes leading to the activation of the Ras-ERK signaling cascade (24,22). SH2B1γ has been reported to interact with Grb2 by one group (7) which raises the possibility that SH2B1 may be playing a similar role as Shc in signaling by NGF.

SH2B1 function in neuronal differentiation and survival

SH2B1β and γ have been implicated in NGF- and BDNF-induced neuronal differentiation and survival. Overexpression of SH2B1β/γ enhances NGF-induced neurite outgrowth in neuron-like PC12 cells while knockdown of all 4 isoforms of SH2B1 by shRNA significantly decreases NGF-induced neurite outgrowth (25). Interestingly, unlike overexpression of SH2B1β/γ, overexpression of SH2B1α does not enhance the ability of NGF to promote neurite outgrowth in PC12 cells (26). Furthermore, rat neonatal sympathetic neurons cultured

with NGF had significantly reduced survival rates when anti-SH2B1 antibodies were injected intracellularly to reduce the activity of endogenous SH2B1 (7). Sympathetic neurons also showed degeneration of the axons when transfected with cDNA encoding a truncated SH2B1 mutant while overexpression of SH2B1γ promoted long, branched axonal growths (7). Qian has hypothesized that SH2B1γ is able to promote neuronal differentiation by increasing TrkA activity, recruiting Grb2 and initiating Ras-dependent signaling, resulting in prolonged ERK 1/2 phosphorylation (7). However, Rui et al. provide evidence that SH2B1β may be promoting neuronal differentiation by a different mechanism. SH2B1β was shown to enhance neuronal differentiation in PC12 cells while SH2B1β R555E (mutant lacking the SH2 domain) inhibited neuronal differentiation (13). However, neither SH2B1β nor SH2B1β R555E altered NGF-induced TrkA autophosphorylation or phosphorylation of downstream proteins including ERK1/2 (13), suggesting that SH2B1β could be regulating NGF-induced neuronal differentiation through a different pathway and may not be directly activating TrkA.

BDNF and TrkB are highly expressed in the central nervous system (CNS) (brain and spinal cord) and peripheral nervous system (PNS) (cranial and spinal ganglia) and have been shown to play a role in neurite outgrowth, neuronal survival, and growth. shRNA knock-down of SH2B1 decreases BDNF-induced neurite outgrowth and branching in neonatal cortical neurons while overexpression of SH2B1β enhances BDNF-induced neurite outgrowth and branching in hippocampal neurons (20). Similarly, SH2B1 knock-down in PC12 cells stably expressing TrkB results in decreased neurite outgrowth, while overexpression of SH2B1β enhances BDNF-induced neurite outgrowth (20). The SH2 domain seems to be required for the function of SH2B1β in enhancing BDNF-induced neurite outgrowth since this function was significantly impaired when PC12 cells stably expressed the SH2B1β R555E mutant lacking the SH2 domain

(20). Shih et al. (20) also showed that pharmacologic inhibitors that prevent phosphorylation of ERK 1/2 or AKT inhibit the ability of SH2B1β to enhance BDNF-induced neurite outgrowth indicating that the MEK-ERK and PI3K-AKT signaling pathways are required for SH2B1 enhancement of BDNF-induced neurite outgrowth. However, they do not clarify whether SH2B1β actually acts via these pathways. SH2B1 also mediates signals for other neurotrophic factors including GDNF. SH2B1 has been shown to interact with the co-receptor for GDNF, RET, and facilitates GDNF-induced neurite outgrowth in PC12 cells and mesencephalic neurons (12). Thus, SH2B1 has a broad role in enhancing neurotrophic signaling and development.

Nuclear localization of SH2B1

While the SH2 domain has been shown to be important for the interaction of SH2B1 with different receptors at the plasma membrane, SH2B1β has been shown to cycle through the nucleus. A nuclear localization sequence (NLS) (25) and a nuclear-export sequence (NES) shared by all 4 isoforms were identified (27). At steady state, SH2B1β localizes to the plasma membrane and to the cytosol (28) but when cells are treated with the nuclear export inhibitor leptomycin B, SH2B1β accumulates in the nucleus (27). When the NES is mutated or deleted, SH2B1β also accumulates in the nucleus (27). These results indicate that at steady state, the rate of nuclear export of SH2B1β exceeds the rate of nuclear import. When either the NES or the NLS are mutated, SH2B1β loses its ability to enhance neurite outgrowth, suggesting cycling through the nucleus is important for SH2B1β enhancement of NGF-induced neurite outgrowth. The NLS (as well as the dimerization domain) has also been shown to be important for the localization of SH2B1 to the plasma membrane (28). Phosphorylation of SH2B1β at Ser161 and Ser165 near the NLS appear to release SH2B1β from the plasma membrane and enable it to translocate to the nucleus (28). A potential role of nuclear SH2B1 is enhancement of gene

expression. Expression of a sub-set of NGF-induced genes is enhanced by SH2B1β as shown by a microarray analysis of PC12 cells expressing GFP, GFP-SH2B1β WT or GFP-SH2B1β R555E before and after NGF treatment (29). SH2B1β-regulated genes included *Plaur*, *Mmp3*, and *Mmp10*, which encode for the proteins urokinase plasminogen activator (uPAR), matrix metalloproteinase 3 (MMP3), and MMP10, respectively. These proteins have been shown to be involved in extracellular matrix degradation crucial for neurite outgrowth in differentiating neurons (30-33). uPAR binds the inactive pro-form of urokinase plasminogen activator (pro-uPA) which is then cleaved by cathepsins and becomes activated. Activated uPA cleaves inactive plasminogen to form enzymatically active plasmin, which can then cleave inactive pro-MMPs to form active MMPs. This pathway has been implicated in neurite outgrowth and cell differentiation (34). uPAR is also considered an early NGF response gene whose function may be required to induce secondary response genes important for neuronal differentiation including *Mmp3* (31,35). When the NLS of SH2B1β is mutated, the ability of SH2B1to promote NGF-induced expression of these genes is impaired. The finding that mutating the NLS and/or NES impairs the ability of SH2B1β to enhance NGF-induced gene expression and neurite outgrowth suggest that shuttling in and out of the nucleus seems to be important for at least some of the functions of SH2B1.

SH2B1 and JAK2

The interaction of SH2B1 and JAK2 and the mechanism by which SH2B1 affects signaling by JAK2 has been widely investigated. SH2B1 has been shown to bind to activated JAK2 via the SH2 domain of SH2B1 and phosphotyrosine 813 in JAK2 (36). Binding of SH2B1 to JAK2 in 293T cells has been shown to enhance activation and autophosphorylation of JAK2. Two proposed mechanisms have been hypothesized for how SH2B1 enhances JAK2 activity.

One is that dimerization of SH2B1 leads to dimerization of JAK2 which enhances JAK2 activity (15). The other one is that SH2B1 binds to active and autophosphorylated JAK2 which leads to a conformational change that keeps JAK2 in an active state (37). In support of the second mechanism, only the SH2 domain of SH2B1β, which lacks the SH2B1 dimerization domain, has to be bound to JAK2 to increase its activity. Mutational analysis suggests that SH2B1 directly increases JAK2 activity without competing for an inhibitor or recruiting another activator to enhance JAK2 activity. JAK2 has been shown to phosphorylate SH2B1β on tyrosines 439 and 494 (38), suggesting that its phosphorylation by JAK2 may allow it to recruit SH2 domain-containing proteins.

JAK2 is known to interact with the receptor for the satiety hormone leptin, LEPRb. Leptin binds to its receptor, which activates JAK2, leading to the initiation of downstream pathways including STAT3 and the IRS/phosphatidylinositol 3 kinase (PI3K) pathways (39-41). Disruption of these pathways has been associated with obesity in mice (42). The function of SH2B1 in modulating leptin action important for energy balance will be discussed in a later section of this chapter.

Role of SH2B1 in insulin and IGF-1 signaling

The role of SH2B1 in insulin and IGF-1 signaling has been investigated *in vitro* and *in vivo*. SH2B1 has been shown to bind to phosphotyrosines in the activation loop of the insulin receptor via its SH2 domain and become tyrosyl phosphorylated (43,9,44,10). SH2B1 enhances insulin receptor activity and cellular responses, including mitogenesis and glucose uptake (45,46). Overexpression of SH2B1 isoforms stimulates insulin receptor activity leading to increased IRS phosphorylation and PI3K signaling, as well as extracellular regulated kinase (ERK) signaling (47,48,10). SH2B1 expression delays dephosphorylation of insulin receptor and

IRS (47) and protects IRS from phosphatases (48). The role of SH2B1 in insulin sensitivity and glucose homeostasis *in vivo* will be discussed in another section of this chapter.

SH2B1 also associates, via its SH2 domain, with the related IGF-I receptor (49,11). Insulin receptor and IGF-I receptor belong to the same family of receptors and major cellular targets are shared between the two including IRS-1, IRS-2, IRS-3, and Shc (50-53). SH2B1 has been suggested to enhance IGF-I actions important for the growth and maturation of the ovaries in mice (49).

SH2B2 and SH2B3 family members

As mentioned previously, SH2B1 is one of a family of three proteins. The other two are SH2B2/APS and SH2B3/LNK. These proteins have conserved structures of a dimerization, PH, and SH domain. Furthermore, these family members share high sequence homology. SH2B1 is ubiquitously expressed in peripheral tissues and the central nervous system. Like SH2B1, SH2B2 is widely expressed in multiple tissues including leptin and insulin targets (brain, liver, muscle, and adipose tissue) (54-56). SH2B3 is found primarily in hematopoietic cells (57). SH2B1 and SH2B2 are able to form hetero- and homo-dimers via their N-terminal dimerization domains. SH2B2, like SH2B1, is involved in mediating neurotrophic signaling. Similar to SH2B1, SH2B2 is able to bind phosphotyrosines 679, 683, and 684 in TrkA in response to NGF, interact with TrkB in response to BDNF, be phosphorylated by both TrkA and TrkB, and promote neurite outgrowth in PC12 cells (7). Interestingly, SH2B3 has been shown to have the opposite effect of SH2B1 and SH2B2. It inhibits NGF-induced neurite outgrowth in PC12 cells and cortical neurons (58). Furthermore, overexpression of SH2B3 reduces the interaction between SH2B1β and TrkA (58). The inhibitory role of SH2B3 in NGF signaling suggests that

while SH2B1 and SH2B2 are positive regulators of neurotrophic factor-induced neurite outgrowth, SH2B3 may be an inhibitor competing for Trk binding.

SH2B2 and JAK2

In the context of cytokine receptor signaling via JAK2, like SH2B1, SH2B2 binds via its SH2 domain to phosphotyrosine 813 in JAK2, potentiating the activity of JAK2 overexpressed in cultured cells (16,17,59). However, compared to SH2B1, SH2B2 only modestly activates overexpressed JAK2 compared to the robust activation of JAK2 by SH2B1 (60,16). The fact that SH2B2 is recruited to JAK2 raises the possibility that SH2B2, like SH2B1, may regulate leptin sensitivity in mice. However, SH2B2-deficient mice did not show altered body weight, feeding, energy expenditure, adiposity, or plasma leptin levels with either a standard chow or a high fat diet (61). These findings suggest that SH2B2 does not play a major role in leptin regulation of energy balance and adiposity.

SH2B2 and insulin signaling

Similar to SH2B1, SH2B2 seems to play a role in the regulation of insulin signaling. SH2B2 binds to the insulin receptor (62) and SH2B2 becomes tyrosyl phosphorylated to an even greater extent than SH2B1 in response to insulin (47). Moreover, the insulin receptor phosphorylates SH2B2 at Tyr618, which binds directly to c-Cbl (63). SH2B2 is required for tyrosine phosphorylation of c-Cbl by the insulin receptor and subsequent activation of the c-Cbl pathway, which has been reported to be required for insulin-stimulated Glut4 translocation to the plasma membrane and glucose uptake in adipocytes (64-66,63). Also, like SH2B1, SH2B2 binds to the activated IGF-I receptor and is phosphorylated by IGF-1 receptor (67). To complicate things further, the Rui lab identified a new isoform of SH2B2. This new isoform, SH2B2β, has a dimerization domain and PH domain but lacks an SH2 domain (68). SH2B2β was shown to bind

to SH2B2 (renamed by the authors as SH2B2α) and SH2B1 *in vitro* and in intact cells and to attenuate the ability of SH2B2α and SH2B1 to activate JAK2 and insulin signaling, including the phosphorylation of downstream target IRS1 (68). SH2B2β may be an endogenous inhibitor of SH2B2α and/or SH2B1 by acting as a negative regulator of JAK2. In contrast to SH2B1, deletion of SH2B2 increases insulin sensitivity in mice (55). However, SH2B2 does not seem to affect high fat diet (HFD)-induced insulin resistance and reduced glucose tolerance (61). Furthermore, deleting *Sh2b2* in *Sh2b1 KO* mice does not further aggravate insulin resistance compared to *Sh2b1 KO* mice (61). Thus, unlike SH2B1, SH2B2 does not seem to be required for the maintenance of glucose homeostasis or energy balance.

Role of SH2B2 in erythropoietin signaling

Tyrosyl phosphorylation of SH2B2, presumably through JAKs, is stimulated by ligands other than leptin, including erythropoietin (EPO), interleukin 5 (IL-5), IL-3, and granulocyte-macrophage colony stimulating factor (69,70,67). EPO and EPO receptor are crucial for the production of red blood cells. EPO activates JAK2 and the activated JAK2 phosphorylates tyrosines in EPO receptor which leads to activation of signal transducers and activators of transcription 5 (STAT5), and the RAS/mitogen activated protein kinase (MAPK) and PI3K/AKT pathways (71). SH2B2 has been shown to bind via its SH2 domain to phosphotyrosine 343 of EPO receptors (70) and is phosphorylated on tyrosine 618 which is able to bind to c-Cbl. SH2B2 is therefore able to recruit c-Cbl E3 ligase to EPO receptors, which results in the inhibition of JAK2/STAT5 pathway in hematopoietic cell lines (70). SH2B2 is also known to co-localize with B cell antigen receptors (BCRs) and negatively regulate BCR signaling, presumably as a consequence of phosphorylation of tyrosines on SH2B2 (72,69,5). Whereas deletion of SH2B1 does not seem to affect the development of T and B lymphocytes and mast cells (49), *Sh2b2 KO*

mice show increased B-1 cell number (72,69) and deletion of SH2B2 in mast cells leads to increased degranulation, a key process that releases antimicrobial cytotoxic molecules (73). Conversely, overexpression of SH2B2 in lymphocytes impairs BCR-induced B cell proliferation (72) and overexpression of SH2B2 in mice reduces the number of B-1 cells (72,69). These findings suggest that SH2B2 is involved in the regulation of signaling of certain cytokines and immune responses, more specifically serving as a negative regulator of a subset of immune cells.

SH2B3

While SH2B2 shares many functions with SH2B1, curiously SH2B3 seems to have opposite functions of SH2B1. Like SH2B1 and SH2B2, SH2B3 can also form homo dimers when it is over expressed *in vitro* (74). SH2B3 is known for its role in regulating cytokine signaling in lymphohematopoiesis (Gery and Koeffler 2013) but recently it was shown to play a role in adipose inflammation and pathogenesis of diabetes. SH2B3-deficient mice showed adipose inflammation as well as reduced glucose tolerance and insulin resistance. The reduced glucose tolerance phenotype was attributed to expansion and increased activity of interleukin-15-dependent cells and the JAK/STAT5 pathway in adipose tissue since the phenotype was rescued with genetic interleukin-15 deficiency or JAK inhibitor treatment (75). These results indicate that SH2B3 regulates glucose homeostasis in adipose tissue by regulating expansion and activation of adipose innate-lymphoid tissues. Thus, SH2B3 plays a role in the regulation of glucose homoeostasis although it may be in a different fashion than the role of SH2B1 (discussed later).

Role of SH2B3 in hematopoiesis

Unlike SH2B1, SH2B3 has been shown to play a major role in hematopoiesis. SH2B3 is expressed in hematopoietic cells and has been implicated in the integration and regulation of multiple signaling events. Like SH2B1 and SH2B2, SH2B3 interacts via its SH2 domain with

EPO receptor and JAK2 (76-78). Functional inactivation studies revealed that its SH2 domain is important for the inhibitory function of SH2B3. The PH domain also seems to be important for its activity (79,74,78). SH2B3-deficient mice show inhibition of the proliferation of hematopoietic stem cells, B lymphocytes, and myeloid progenitors (57,80,81). Mice lacking SH2B3 show features of myeloproliferative disorders, presumably due in part to hypersensitivity to cytokines. These mice also show increased hematopoietic stem cells with enhanced self-renewal capacity, suggesting that SH2B3 controls hematopoietic stem cell numbers by regulating quiescence, cell self-renewal, proliferation, and apoptosis (82). SH2B3-deficient mice also revealed a role for SH2B3 in B-cell proliferation. These mice showed selective expansion of pro and pre-B and immature B cells in bone marrow and spleen (80). SH2B3 has also been shown to inhibit erythropoiesis (78). Like SH2B1, SH2B3 binds to phosphotyrosine 813 of activated JAK2 and to a lesser extent to phosphotyrosine 613 (76). This allows SH2B3 to downregulate the catalytic activity of JAK2 (76). SH2B3 also binds to non-phosphorylated JAK2 via its N-terminal domain and maintains the kinase in an inactive state in the absence of cytokine stimulation (83). Thus, SH2B3 is a negative regulator of EPO signaling by downregulating JAK2 activation.

PH domain of SH2B3 and myeloproliferative neoplasms

Constitutively active JAK2 has been associated with pathogenesis of myeloproliferative neoplasms, polycythemia vera, essential thrombocythemia, and primary myelofibrosis (84). Aberrant JAK-STAT signaling in myeloproliferative neoplasms has been attributed to JAK2V617F mutation in over 50% of the cases of polycythemia vera, primary myelofibrosis, and essential thrombocythemia. SH2B3 has been shown to downregulate JAK2V617F *in vitro* (85). *In vivo*, in a transduction-transplant murine model, SH2B3 deficiency was found to

aggravate development of myeloproliferative neoplasms induced by JAK2V617F (10). Interaction between SH2B3 and JAK2V617F was required to restrain polycythemia vera/primary myelofibrosis expression in this transduction-transplant model. Interestingly, mutations in the PH domain and SH2 domain or PH domain alone of SH2B3 have been identified in patients with JAK2V617F negative myeloproliferative neoplasms (86). Furthermore, identification of a mutational hot spot in the PH domain of SH2B3 in patients with myeloid malignancies suggests that this domain may be playing an important role in the inhibitory role of this protein. Similar to JAK2V617F, these mutations are associated with expansion of myeloid progenitor population by cytokine-responsive pSTAT3/5 expression. Within the last 10 years, at least 11 point mutations (E208Q/E, S213R, A215V, G220V/R, A223V, G229S, T274A, D234N, F287S) have been identified in the PH domain of SH2B3 in patients with myeloproliferative neoplasms, polycythemia vera, essential thrombocythemia and/or primary myelofibrosis (87,88,71,89-91). Mutations in the PH domain of SH2B1 have also been identified in patients exhibiting early onset childhood obesity (92) and will be discussed further in a later section of this chapter. This points to the importance of an intact PH domain for the function of SH2B family members. Clustal analysis of the PH domains of SH2B1, SH2B2, and SH2B3 reveals that the PH domains are highly-conserved. We took advantage of the high conservation of the PH domain and have used NMR from the PH domain of SH2B2 to model the PH domain of SH2B1, which will be discussed in Chapter 2.

Regulation of Body Weight

Obesity is a growing epidemic but the cellular and molecular mechanisms underlying obesity and associated co-morbidities like diabetes are still not well understood. A complete understanding of the molecular mechanisms underlying obesity is important for the development

of new therapeutics. Obesity results from an imbalance of energy intake and energy expenditure. Energy balance is primarily regulated by the central nervous system, more specifically, in the arcuate nucleus in the hypothalamus, a region of the brain where nutrient, hormonal, and neuronal signals are received, coordinated and processed (93,94). The neurons in the arcuate nucleus of the hypothalamus connect to other neuronal subpopulations within the hypothalamus as well as other brain regions including the paraventricular hypothalamic nucleus (PVH), dorsomedial hypothalamus (DMH), lateral hypothalamus (LH), and ventromedial hypothalamus (VMH), which allows for a coordinated response (94). Distinct neuronal populations within the arcuate nucleus of the hypothalamus sense nutrient status and integrate signals from peripheral hormones such as leptin to regulate food intake and energy expenditure (95). This ability to sense nutrient status and respond to peripheral hormones is possible due to the close proximity of the arcuate nucleus to the median eminence, an organ rich in capillaries that lead to the leaky blood brain barrier (BBB), which facilitates transport of peripheral hormonal signals from the blood into the brain (96). Leptin is produced by adipocytes proportional to the energy stores (triglycerides) in the body and acts to regulate energy balance by reducing appetite and increasing thermogenesis (94). Leptin binds to and activates its long form receptor (LEPRb) in the hypothalamus. This activates several intracellular signaling pathways including the STAT3 and PI3K pathway (97,98). These pathways play a crucial role in mediating leptin regulation of energy balance since inhibition of STAT3 or PI3K results in leptin resistance and obesity (99). When leptin signaling is genetically disrupted, satiety is impaired, and food intake increases (hyperphagia). Several mutations in genes encoding leptin or leptin receptor (LepR) have been identified in patients that exhibit extreme obesity and hyperphagia (40,100,101).

Role of POMC and AgRP/NPY in feeding behavior

Leptin receptor-expressing neurons project to other groups of neurons within the arcuate nucleus of the hypothalamus that also play a role in the regulation of food intake and energy balance. One group are pro-opiomelanocortin (POMC) neurons that produce melanocyte stimulating hormone (α-MSH), which is anorexigenic. POMC is cleaved to α-melanocyte-stimulating hormone (α-MSH), which is released from axons and activates melanocortin 3 and 4 receptors (MC3/4R) in neurons in a variety of brain regions including the paraventricular hypothalamic nucleus, dorsomedial hypothalamus, lateral hypothalamus, and ventromedial hypothalamus (102,103). Neurons in these different areas process the information and project to neurocircuits distal to the hypothalamus that lead to a decrease in food intake and increase in energy expenditure. A second group of leptin receptor-expressing neurons in the arcuate nucleus express orexigenic neuropeptide Y (NPY) and agouti-related peptide (AgRP) (104). AgRP is an antagonist of MC3R and MC4R (105). NPY stimulates food intake by exerting its effects through G-protein coupled receptors including Y1, Y2, Y4, and Y6 (106). High levels of NPY are found in obese rodents as well as humans (107), demonstrating a role for NPY in eating disorders. AgRP/NPY neurons project to the paraventricular hypothalamic nucleus and lateral hypothalamus to mediate their action (108). Thus, leptin decreases food intake and increases energy expenditure by activating POMC neurons and inhibiting NPY/AgRP neurons (105). Deficiencies in POMC or MC4R expression or activity result in early-onset obesity and hyperphagia in humans (109).

Role of BDNF in feeding behavior

One downstream mediator thought to be involved in transducing the effects of MC4R activation on food intake regulation is BDNF (110). BDNF is a neurotrophic factor shown to promote survival of neurons, induce differentiation of neurons in developing and adult central

nervous systems and promote the formation of appropriate neuronal connections at central synapses (111,112). Activation of MC4R stimulates synthesis of BDNF in dendrites. BDNF has been shown to bind to TrkB to regulate feeding and energy expenditure in the paraventricular hypothalamic nucleus, ventromedial hypothalamus, and NTS (113-115). Mutations in children with severe obesity have been identified in the genes encoding BDNF and its receptor TrkB (116). Conditional deletion of BDNF leads to hyperphagia and obesity in mice (117). The obese phenotype seen in BDNF and TrkB mutant animals may be attributed to neurodevelopmental anomalies as well as impaired signaling in adults (114). Together, these findings suggest that BDNF, like POMC, acts as an anorexigenic signaling molecule.

Regulation of Glucose Metabolism

We obtain glucose primarily from the food that we eat. Stimulation of appetite is driven in part by the "hunger hormone" ghrelin. This hormone is primarily released by the stomach, although small amounts are also known to be released by the small intestine, pancreas, and brain. Ghrelin travels in the bloodstream and acts at the level of the hypothalamus to increase appetite, promote food intake, and promote the release of insulin from β-cells in the pancreas (118).

Insulin and glucagon work together to maintain peripheral glucose homeostasis during fed and fasted states, respectively. Food intake and high glucose levels in the blood stimulate the pancreas to release insulin from β-cells in the pancreas and inhibit the release of glucagon from pancreatic α-cells (118). Insulin and glucagon have opposite roles in the regulation of glucose metabolism. Insulin lowers blood glucose by increasing the rate of glucose uptake and utilization by tissues in the body including skeletal muscle and adipocytes. It does so by binding to its membrane receptor, which is a receptor tyrosine kinase, and causing a cytosolic pool of GLUT4 glucose transporters to be recruited to the plasma membrane. During the fed state, insulin also

acts indirectly to increase glucose uptake in the liver. Insulin activates the enzyme hexokinase, which phosphorylates glucose and traps it in the cell. Then, insulin stimulates the storage of glucose in the form of glycogen by activating enzymes involved in glycogen synthesis, including phosphofructokinase and glycogen synthase. Insulin also suppresses hepatic glucose production (119,120). During the fasting state, glucagon is the primary regulator of glucose metabolism in the liver. Glucagon stimulates the synthesis of glucose from non-carbohydrate precursors such as lactic acid, glycerol, and amino acids. Glucagon also signals the liver to break down glycogen into glucose and transport it out into the blood (120).

Insulin also acts at the level of the central nervous system. Insulin receptors are widely expressed in the brain and insulin has been shown to act on NPY/AgRP- as well as POMC-expressing neurons (121-123). Insulin action in AgRP/NPY neurons has been shown to be required for insulin to suppress hepatic glucose production during hyperinsulinemic-euglycemic clamps. This is thought to occur as a consequence of insulin hyperpolarizing AgRP neurons, which reduces the release of AgRP and other neurotransmitters, affecting peripheral hepatic innervation, which results in increased interleukin (IL)-6 expression in liver cells. IL-6 decreases expression of glucose-6-phosphatase and thereby reduces gluconeogenesis in the liver (124). Hypothalamic insulin also functions in conjunction with leptin to regulate glucose homeostasis (94,125). Deletion of both insulin and leptin receptors in POMC neurons impairs glucose homeostasis and leads to systemic insulin resistance (126). However, leptin and insulin appear to act on different subpopulations of POMC neurons (127).

BDNF is highly expressed in neurons in the ventral medial hypothalamus, where it acts on neurons to regulate blood glucose levels (128). BDNF reduces hepatic glucose production by inhibiting gluconeogenic enzymes such as glucose-6-phosphatase and phosphoenolpyruvate

carboxykinase (128). Consistent with this, injection of BDNF into the ventromedial hypothalamus lowers fasting blood glucose levels without affecting energy intake. One possible mechanism by which this occurs is that BDNF activates SF-1 neurons within the ventromedial hypothalamus, which leads to excitation of the neurons in the paraventricular hypothalamus and dorsomedial hypothalamus, which in turn decrease glucagon secretion, which decreases liver glucose production (129). Interestingly, ventromedial hypothalamus neurons do not only respond to BDNF but some also produce BDNF (130). This production of BDNF is upregulated by glucose, leptin, and melanocortins (131,114,110). Some studies also postulate that BDNF is a mediator of leptin's action on glucose homeostasis (128). However, the ability of leptin to increase peripheral glucose uptake in addition to being able to decrease hepatic glucose production points to other key mediators of leptin action independent of BDNF (128).

Regulation of Body Weight by SH2B1

Growth, survival, and reproduction of organisms is dependent on nutrient availability and storage. Two main forms of nutrients essential for tissues and organs are lipids and glucose. Our neuroendocrine system has evolved to maintain lipid and glucose homeostasis. One of the major regulators of this metabolic system is the hypothalamus. Given that SH2B1 enhances the function of a number of receptors in the hypothalamus that regulate feeding behavior and/or energy expenditure (41,61,132,133,17), it is not surprising that in mice, deletion of SH2B1 results in obesity, leptin resistance and hyperphagia (54,61,48,56). SH2B1 has been shown to be a key molecule that positively regulates leptin sensitivity *in vitro* (134,54) and leptin signaling in hypothalamic neurons (56). Deletion of SH2B1 impaired leptin-stimulated JAK2 activation and tyrosine phosphorylation of leptin receptor's downstream targets of STAT3 and IRS2 in the hypothalamus. Because both the STAT3 and IRS2/PI3 kinase pathways are required for leptin

regulation of food intake and body weight, reduction in these signaling pathways seem likely to contribute to the hyperphagia and obesity seen in the *Sh2b1 KO* mice. Expression of SH2B1β driven by the neuron-specific enolase promoter largely corrects the obese phenotype and leptin resistance seen in *Sh2b1 KO* mice (133). Furthermore, neuron-specific restoration of SH2B1 also corrects the overexpression of NPY and AgRP neuropeptides observed in *Sh2b1 KO* mice. These data strongly suggest that decreased neuronal signaling via SH2B1 is important for the obese phenotype in *Sh2b1 KO* mice (133). Consistent with neuronal SH2B1 being critical for SH2B1's effects on energy balance, neuron-specific overexpression of SH2B1β is able to protect against high fat diet-induced obesity (133).

The above studies were carried out using an *Sh2b1 KO* mouse line produced by the Rui lab (Duan 2004, Ren 2005, Ren 2007). Another research group, the Yoshimura lab, generated an independent line of *Sh2b1 KO* mice by homologous recombination (49). This group did not report an obese phenotype for the *Sh2b1 KO* mice. This second line of *Sh2b1 KO* mice actually showed reduced levels of fat mass and adipogenic genes (e.g. PPARγ) in white adipose tissue (135). These authors concluded that SH2B1 regulates adipogenesis at least in part by regulating the insulin/IGF-1/PPARγ pathway (135). The discrepancies in the findings between the two groups (Rui and Yoshimura) may be due to the background of the mice and/or the conditions in which the mice were kept. The Yoshimura lab also reported that the *Sh2b1 KO* mice are infertile (49). The infertility was attributed to immaturity of the reproductive organs and a reduced ability of oocytes to respond to follicle stimulating hormone (FSH) and IGF-1 (49). A reduced response to IGF-1 in *Sh2b1 KO* mice would be consistent with *in vitro* studies showing that SH2B1 can bind to the IGF-1 receptor and enhance at least some IGF-1 functions (10,45).

The ability of SH2B1 to regulate energy balance and glucose metabolism is conserved in

species as evolutionarily distant as insects (136). Disruption of dSH2B, the *Drosophila* homolog of SH2B1, leads to increased whole body glucose and lipid levels in flies. Consistent with SH2B1 being an important regulator of energy balance, single nucleotide polymorphisms in the *SH2B1* gene are associated with obesity in American, Asian, and European populations (137-140). Further, studies utilizing the Genetics of Obesity Study (GOOS) cohort have identified mutations in SH2B1 in multiple individuals with severe childhood obesity (92,26). Like the *Sh2b1 KO* mice, these individuals are hyperphagic. Insulin resistance greater than expected from the level of obesity is also exhibited in the humans with rare mutations in SH2B1 (92,26). One of the human mutations identified was SH2B1 P322S. The P322S mutation is located within the PH domain of SH2B1 and is therefore present in all four known isoforms of SH2B1. Due to the lack of a large number of human patients with the P322S mutation in SH2B1, the metabolic phenotype associated with SH2B1 P322S is difficult to investigate in human patients. As described in Chapter 2, we have generated and characterized a mouse model that encodes one of these obesity-associated human mutations (P322S). We have also generated a second mouse model in which SH2B1 has a 2-amino acid deletion. The effects on the cellular actions of SH2B1 of human obesity-associated mutations identified in SH2B1 will be discussed in Chapter 2 of this dissertation.

Regulation of Glucose Metabolism by SH2B1

SH2B1 is expressed in multiple tissues involved in glucose homeostasis including the brain, pancreas, adipose tissue, liver, and skeletal muscle (141,142,54,68,10). The role of SH2B1 in these different tissues has been studied to varying degrees, except in the skeletal muscle. To investigate the role of SH2B1 in glucose homeostasis, the Rui lab first generated a full body *Sh2b1 KO* mouse model. Consistent with SH2B1 playing a role in glucose homeostasis, deletion

of SH2B1 in mice results in insulin resistance (54,56). *Sh2b1 KO* mice develop age-dependent hyperinsulinemia, hyperglycemia, reduced glucose tolerance and reduced insulin sensitivity (54). Deletion of SH2B1 impaired insulin receptor activation, insulin-stimulated tyrosyl phosphorylation of IRS1 and IRS2 in the liver, skeletal muscle, and fat, and activation of the PI3K pathway (41). This suggests that the hyperinsulinemia, hyperglycemia, reduced glucose tolerance and insulin sensitivity seen in the *Sh2b1 KO* mice is due, at least in part, to the inability of SH2B1 to enhance insulin receptor activation and tyrosine phosphorylation of IRS1 and IRS2. Interestingly, neuron-specific restoration of SH2B1 rescued the reduced glucose tolerance, insulin resistance, and increased adiposity seen in the *Sh2b1 KO* mice (56), suggesting that the regulation of glucose homeostasis by SH2B1 takes place primarily in the central nervous system.

The finding that SH2B1 is highly expressed in pancreatic β-cells (10) triggered interest in studying the role of SH2B1in the regulation of glucose homeostasis within the pancreas. Glucose homeostasis requires the secretion of insulin from pancreatic β-cells, which promotes glucose uptake in skeletal muscle and adipose tissue and inhibits hepatic gluconeogenesis. Both insulin and IGF-1 promote β-cell expansion by stimulating β-cell proliferation and inhibiting β-cell death (143-145). Pancreas-specific deletion of SH2B1 results in impaired insulin secretion, β-cell survival, β-cell proliferation, islet expansion, and glucose tolerance in mice fed a high fat diet (142). Since SH2B1 has been shown to be required for the activation of the PI3K/Akt pathway in β-cells *in vitro* and *in vivo* (142), the impaired glucose tolerance phenotype may be due, at least in part, to impaired PI3K/Akt signaling in β-cells.

The Bernal-Mizrachi lab further investigated the role of SH2B1 in glucose homeostasis in β-cells. Nutrient environment in states of overnutrition such as in obesity are known to play a role in the adaptation of β-cells to insulin resistance. One of the molecules responsible for

integrating signals from nutrients and growth factors to regulate β-cell size and proliferation is the mammalian target of rapamycin complex 1 (mTORC1) (143,146). mTORC1 controls β-cell growth and proliferation through phosphorylation of 4E-binding proteins (4E-BP) (147). 4E-BP2 deletion in mice induces translation of SH2B1 and promotes the formation of an SH2B1 complex with IRS2 and JAK2, preventing IRS2 ubiquitination. This suggests that SH2B1 is a major regulator of IRS2 stability. Increased IRS2 stability would be expected to increase cell cycle progression of β-cells, β-cell survival, and β-cell mass (148).

β-cells secrete insulin in response to high glucose blood levels such as those after a meal. Insulin expression and secretion are regulated by nutrients and hormones. SH2B1 is one of the proteins that mediate insulin synthesis and secretion. Knockdown of SH2B1 reduced insulin expression, insulin content, and glucose-stimulated insulin secretion in both rat INS 832/13 β-cells and in mouse islets (141). Similarly, heterozygous deletion of SH2B1 aggravates the decreased pancreatic insulin content and plasma insulin levels in leptin-deficient ob/ob mice. Overexpression of JAK2, the kinase that mediates the action of the leptin receptor, increased the activity of an insulin promoter, and SH2B1 enhanced that ability (141). SH2B1 also increases the expression of transcription factor Pdx1, which activates the insulin promoter and insulin expression in β-cells (141). These findings suggest that SH2B1 promotes insulin synthesis and secretion in β-cells by enhancing JAK2 activation and Pdx1 expression.

Since the liver is a key organ in controlling glucose homeostasis and SH2B1 is highly expressed in the liver, the Rui lab investigated the role of SH2B1 in the function of the liver to regulate glucose homeostasis. The liver produces glucose through gluconeogenesis and glycogenolysis. This key role is essential to provide glucose to vital organs, including the brain, during fasting periods to meet their metabolic demands. Insulin controls glucose homeostasis by

stimulating glucose uptake and by suppressing hepatic glucose production. During insulin resistance, the ability for insulin to suppress hepatic glucose production is impaired, resulting in production of excess glucose, which contributes to hyperglycemia and reduced glucose tolerance (149). Rui and colleagues generated mice with specific deletion of SH2B1 in the liver. Blood glucose levels, plasma insulin levels, glucose tolerance and insulin sensitivity were normal in these mice fed either standard chow or a high fat diet (150). This suggests that SH2B1 in the liver does not appear to be required to maintain normal insulin sensitivity and glucose metabolism.

Adult-onset deletion of SH2B1 from the liver reduces hepatic steatosis and expression of the lipogenic gene diacylglycerol acyltransferase-2 (DGAT2) while increasing the expression of the lipolytic enzyme adipose triglyceride lipase (ATGL) (150). Furthermore, deletion of both SH2B1 and SH2B2 in the liver in mice fed a high fat diet reduces very low density lipoprotein (VLDL) secretion. VLDL secretion is important for exporting triglycerides from the liver to other tissues (150). This ability of liver SH2B1 to regulate adiposity may contribute to the ability of SH2B1 to regulate body weight.

Use of CRISPR-cas9 to Generate Novel Mouse Models

The ability to modify the genome in a precise and targeted manner is key to determining genetic contributions to disease as well as the contributions of specific proteins to normal physiological function and disease states. In recent years, a number of technologies designed to modify the genome have emerged, including clustered regularly interspaced short palindromic repeats (CRISPR)/cas9 genome editing. CRISPR/cas9 was originally identified in bacteria that use it as a defense mechanism against phage infection and plasmid transfer (151). CRISPR/cas9 has been modified to make it a powerful tool for stimulating targeted double-strand breaks

(DSBs) in eukaryotic cells (152). Cas9 nuclease from *Streptococcus Pyogenes* (Sp) is directed via Watson-Crick base pairing by a ~20 nucleotide RNA-guide to any target genomic locus (153-155). One of the requirements in the selection of the Cas9 target site is the presence of a Protospacer Adjacent Motif (PAM) sequence 3' of the ~20-nucleotide target sequence (156). The SpCas9 requires a 5'- NGG PAM sequence. The specificity of the Cas9 depends on the 20 nucleotide RNA guide. Each base within the 20 nucleotide RNA guide sequence contributes to specificity; mismatches between the RNA guide and the complementary target DNA can happen depending on the quantity, position, and base identity of the targeted sequences (157). These mismatches can lead to potential off-target cleavage activities and random insertions and deletions. Several online CRISPR design Tools exist that allow for prediction of off-target genomic modifications for each RNA guide including (156). Upon cleavage by cas9, the double-strand break is repaired by one of two repair mechanisms. Non-homologous end joining (NHEJ) is the most common repair mechanism but is prone to errors resulting in random insertions or deletions. Homologous directed repair occurs at a lower frequency but is a high-fidelity repair mechanism that can be exploited to generate precise modifications at a target locus in the presence of an exogenously introduced donor template (156). The donor template can be a double-stranded DNA targeting construct with homology arms flanking the insertion sequence or a single- stranded DNA oligonucleotide. Single-stranded DNA oligonucleotides provide the advantage of being able to make small edits in the genome including single nucleotide mutations (158). Using CRISPR/cas9 to make genome edits through homologous directed repair provides a more effective method than non-homologous end joining, because unlike non-homologous end joining, homologous directed repair generally occurs only in dividing cells (159). This latter method was the method I used to create the two mouse models in Chapter 2.

Pleckstrin Homology Domains

PH domains were first identified in the platelet protein pleckstrin (160). PH domains are defined as regions of approximately 100 residues that are involved in signaling, cytoskeletal organization, membrane trafficking, and phospholipid processing (161,162). Structurally, PH domains are seven-stranded structures formed by 2 anti-parallel β-sheets curving to form a β-barrel configuration with a C-terminal α-helix blocking one end of the barrel (163,162). Early investigations of PH domains describe their affinity for phospholipids, however, more recent studies (162,164) show that the majority of PH domains do not share this function and that PH domains are more versatile than initially thought. For example, some PH domains have been reported to bind via protein-protein interactions to phosphotyrosine- or polyproline helice -containing peptides (162). Using truncation analysis, our lab showed previously that the PH domain of SH2B1β is not required to localize SH2B1β to the plasma membrane (25). Furthermore, in NIH 3T3 cells, live cell translocation experiments showed that the PH domain of SH2B1 mainly localizes in the cytoplasm and is not recruited to the plasma membrane of PDGF-stimulated cells in contrast to PH domains that bind to PIP3 (165). These results indicate that its PH domain does not recruit SH2B1 to an organelle-specific phospholipid, making it likely that the PH domain of SH2B1 has a function other than recruiting SH2B1 to phospholipids at the plasma membrane. Consistent with this, a series of experiments using N- and C-terminally truncated SH2B1β constructs determined that the PH domain of SH2B1 contributes to the binding of SH2B1β to inactive JAK2 (59,18). Rui et al hypothesized that the prior localization of SH2B1β to inactive JAK2 would enhance the likelihood that SH2B1β would subsequently bind, via its SH2 domain, to phosphoTyr813 in activated JAK2, an interaction that is essential for JAK2-dependent SH2B1β function. It seems likely that the PH domain of SH2B1 functions

in a similar fashion when cells are stimulated by ligands such as leptin that utilize JAK2. Nothing is known about how the PH domain of SH2B1 functions within the context of SH2B1 bound to the other receptors implicated in regulating energy balance or glucose homeostasis such as the receptors for insulin, IGF-1, and BDNF. However, consistent with the importance of an intact PH domain for the function of SH2B family members, in patients with myeloproliferative neoplasms, more than 11 point mutations have been identified in the highly-conserved PH domain of the SH2B1 orthologue SH2B2/Lnk. My studies described in Chapter 2 tested the importance of the SH2B1 PH domain *in vivo* by generating and studying mice containing human obesity-associated (P322S) or engineered (in-frame deletion of P317 and R318 (ΔPR)) mutations in the SH2B1 PH domain. My results demonstrate that the SH2B1 PH domain plays multiple crucial roles *in vivo*, including the control of energy balance and glucose homeostasis.

Chapter 2 Crucial Role of SH2B1 PH Domain Function for the Control of Energy Balance and Metabolism

Abstract

Mutations in the adaptor protein SH2B1 have been identified in individuals with severe childhood obesity and insulin resistance, a phenotype seen in mice lacking SH2B1. Three of the mutations are in the PH domain of SH2B1, suggesting that this domain is important for SH2B1 function. Here, we examine the impact of PH domain mutations on SH2B1 regulation of energy balance and glucose metabolism. We show that the P322S human obesity-associated mutation modestly alters glucose tolerance in mice with diet-induced obesity. A nearby two-amino acid deletion leads to an obese phenotype, promotes SH2B1β localization in the nucleus and impairs SH2B1β enhancement of neurite outgrowth. These results and structural analysis of a model of the PH domain of SH2B1 and SH2B3/Lnk suggest that the PH domain of SH2B1 is a key regulator of energy balance and glucose homeostasis, perhaps by promoting proper subcellular localization of SH2B1 and enhancing neuronal circuits or function.

Introduction

Human patients with mutations in the adaptor protein SH2B1 exhibit severe obesity, hyperphagia and insulin resistance disproportionate for their obesity (92,26). Consistent with SH2B1 playing a key role in regulating energy balance and glucose homeostasis, $SH2B1^{-/-}$ mice are obese and have impaired glucose homeostasis (54,56). Expression of *Sh2b1β* driven by the neuron-specific enolase promoter largely corrects the obese and glucose-intolerant phenotypes

seen in *Sh2b1*$^{-/-}$ mice (133), suggesting that decreased neuronal signaling via SH2B1 is important for these phenotypes.

At the cellular level, SH2B1 binds to phosphorylated tyrosines in numerous ligand-activated receptor tyrosine kinases and JAK family members complexed to cytokine family receptors and enhances the function of those receptors (36,132,44,7,10,17,20). Some of these receptors, including receptors for the satiety hormone leptin, brain-derived neurotrophic factor (BDNF) and insulin reside in the hypothalamus and regulate feeding behavior, energy expenditure and/or glucose homeostasis (166).

The four known isoforms of SH2B1 (Figure 2.1a) share 631 N-terminal amino acids that contain dimerization, pleckstrin homology (PH) and SH2 domains, a nuclear localization sequence (NLS) and a nuclear export sequence (NES). They differ only in their C-termini (27,25,6). The SH2 domain recruits SH2B1 to phosphotyrosines in tyrosine kinases (167). The NLS and NES enable SH2B1 to shuttle between the plasma membrane, cytosol, and nucleus. The NLS and dimerization domains localize SH2B1 to the plasma membrane (27,25). However, the function of the PH domain in SH2B1 remains largely unknown.

PH domains are the 11th most common domain in the human proteonome (168). They are known mainly for their ability to bind phosphoinositides in plasma membranes and organelle membranes (169,170). However, 90-95% of all human PH domains do not bind strongly to phosphoinositides (168). Truncation analysis reveals that the PH domain of SH2B1β is not required for localization of SH2B1β to the plasma membrane (25,171) nor does the PH domain itself localize to the plasma membrane (165). The findings that 3 human obesity-associated mutations are in the PH domain of SH2B1 (92,172,173) and at least 11 point mutations associated with myeloproliferative neoplasms are in the PH domain of the SH2B1 orthologue

SH2B3/Lnk (86,90) highlight the importance of an intact PH domain for the function of SH2B family members.

Here, we test the importance of the PH domain to SH2B1 regulation of energy balance and glucose homeostasis. CRISPR/Cas9 genome editing was used to disrupt the PH domain of SH2B1 by introducing the human obesity-associated P322S mutation or a 2-residue deletion of P317 and R318 (ΔPR). In mice with diet-induced obesity, P322S modestly impaired glucose tolerance. The ΔPR deletion caused SH2B1β to mislocalize to the nucleus, impaired the ability of SH2B1β to enhance neurotrophic factor-mediated neurite outgrowth, produced substantial obesity, and impaired glucose homeostasis. Modeling of the structure of the PH domains of SH2B1 and SH2B3/Lnk based on NMR structure of SH2B2 with visualization of the locations of SH2B1 P322S, the ΔPR deletion, and the human mutations in SH2B3/Lnk identified a regulatory hot spot in the PH domains of SH2B family members. Taken together, our results reveal the importance of the PH domain of SH2B1 in localizing SH2B1 and regulating energy balance and glucose homeostasis.

Results and Discussion

Generation of SH2B1 P322S mice

To gain insight into the role of the PH domain of SH2B1 and the impact of the human mutations in SH2B1 on energy balance and glucose metabolism, we used CRISPR-based genome editing to introduce the human obesity-associated P322S mutation located in the PH domain of SH2B1 into C57BL/6J mice. We chose this mutation for multiple reasons: 1) its presence in the PH domain; 2) its strong association with obesity in the proband family (92); 3) the obese humans with the P322S mutation are heterozygous for the mutation; 4) its inhibitory effect on the ability of SH2B1β to enhance nerve growth factor (NGF)-stimulated neurite

outgrowth and growth hormone (GH)-stimulated macrophage motility (92); 5) its evolutionary conservation in mammals; 6) the conservation of P322 in the SH2B family member SH2B2/APS; and 7) programs that predict whether an amino acid substitution would have an impact on the biological function of the target protein (Provean, RRID:SCR_002182; PolyPhen, RRID:SCR_013189) predict that the P322S mutation would be "probably damaging". To create the SH2B1 P322S mouse model, two individual sets of CRISPR/Cas9 guides and donor template (Figure 2.1b) were designed using http://tools.genome-engineering.org (156) and injected into oocytes from C57BL/6J mice. The oocytes were then implanted into C57BL/6J mice. DNA sequencing confirmed germline transmission of the Guide 2-mediated P322S edit in the N1 generation (Figure 2.2a). Insertion of the P322S mutation does not affect the mRNA levels for the four different isoforms of SH2B1 (α, β, γ, δ) in either in the three tissues tested (brain, liver, heart) (Figure 2.2b). Consistent with results in human tissues showing ubiquitous expression of the β and γ isoforms (92), mRNA for the β and γ isoforms is found in all three tissues from wild-type (WT), SH2B1 P322S/+ and SH2B1 P322S/P322S mice, although only a minimal amount of mRNA for the γ isoform was visible in the brain. Also, consistent with results using human tissues, mRNA for the α and δ isoforms are present in the brain tissue, absent in the liver and present only to a minor extent in the heart from WT, SH2B1 P322S/+ and SH2B1 P322S/P322S mice. We also examined whether the SH2B1 P322S mutation alters SH2B1 protein levels in brain tissue (Figure 2.1c). Immunoblotting whole brain lysates with an antibody made against a region of SH2B1 shared by all 4 isoforms (αSH2B1) revealed three bands corresponding to SH2B1. None of the bands were present in brains from SH2B1 KO mice. Based on the migration of myc-tagged isoforms of SH2B1 expressed in 293T cells (data not shown), the upper band co-migrates with overexpressed SH2B1α and the middle band with overexpressed

SH2B1δ, while the lower band migrates appropriately for SH2B1β and SH2B1γ. We further confirmed that all the observed bands correspond to SH2B1 by immunoprecipitating SH2B1 from whole brain lysates using αSH2B1 before immunoblotting with αSH2B1 (Figure 2.2c) and by immunoblotting with a different polyclonal antibody made against amino acids 1-631 shared by all four isoforms (data not shown). Both the immunoblots of whole brain lysates and of protein immunoprecipitated from whole brain lysates using αSH2B1 revealed similar levels and profiles of SH2B1 isoforms in brains from WT and P322S/P322S mice, indicating that the P322S mutation does not affect the expression of the SH2B1 isoforms.

Interestingly, we noticed that as we expanded the SH2B1 P322S mouse colony, the P322S/P322S mice were born at approximately half the expected Mendelian ratio (Figure 2.2d). The SH2B1 KO mice are infertile, which has been hypothesized to be due to immaturity of the reproductive organs and a reduced response in oocytes to follicle stimulating hormone (FSH) and IGF-1 (49). A reduced response to IGF-1 in KO mice would be consistent with *in vitro* studies showing that SH2B1 can bind to the IGF-1 receptor and enhance at least some IGF-1 functions (10,45). The P322S mutation in SH2B1 does not seem to have as drastic an effect on fertility as deleting SH2B1 since the P322S/P322S mice are fertile (data not shown). However, the fact that P322S/P322S mice are born at about half of the expected Mendelian ratio suggests that SH2B1 is important for implantation and/or the embryonic development of the pups with the P322S/P322S mutation.

The effect of the SH2B1 P322S mutation on body weight, food intake, adiposity, and leptin levels

The amino acid sequence of the PH domain in SH2B1, which contains P322, is 94% conserved between mouse and human, suggesting that the P322S mutation in mice would have

the same impact on SH2B1 function as the P322S mutation is believed to have in humans. Because the P322S SH2B1 mutation in humans was identified in an individual with severe childhood obesity (92), we first examined whether the P322S SH2B1 mutation causes obesity in mice. Mice were fed a 9% fat standard chow, individually housed at week 4, and weighed weekly for 26 weeks. Male and female homozygote (P322S/P322S) and heterozygote (P322S/+) mice showed no statistically significant difference in body weight compared to their sex-matched WT littermates (Figure 2.1d). Due to the low number of homozygous mice generated and because in human patients the obese individuals are heterozygous for the P322S SH2B1 mutation (92), subsequent experiments examined the effect of the P322S mutation in heterozygous mice. Consistent with the observed lack of difference in body weight, we found that there was no difference in food intake between male or female P322S/+ mice and their sex-matched WT littermates (Figure 2.1e). Similar to body weight and food intake, fat mass (Figure 2.1f) and lean mass (Figure 2.3a) of male and female P322S/+ mice assessed at week 30 using nuclear magnetic resonance (NMR) were comparable to that of their WT littermates. There was also no statistically significant difference in the weight of the brain, heart, kidney, or perigonadal fat from male or female P322S/+ mice or testis from P322S/+ male mice due to the P322S mutation (Table 2.1).

SH2B1 has been shown to be a positive regulator of signaling via the satiety hormone leptin (56,133). The primary source of leptin in an animal is adipose tissue. Although leptin levels are generally thought to reflect the amount of adipose tissue present in the animal (174,94), if a defect in SH2B1 P322S signaling leads to leptin resistance, then elevated leptin levels might compensate for the defect. However, we detected similar serum levels of leptin measured at week 30 between male P322S/+ mice and their respective WT littermates (Figure

2.3b). Thus, in contrast to the obesity and hyperphagia seen in humans with the P322S variant (92), our results indicate that the SH2B1 P322S mutation does not appear to detectably affect the ability of SH2B1 to regulate energy balance or leptin sensitivity of C57BL/6J mice fed standard chow.

Effect of the P322S mutation in SH2B1 on insulin-regulated glucose metabolism

In addition to obesity, the human patients with the P322S SH2B1 mutation exhibit a disproportionate degree of insulin resistance for their obesity (92). We therefore examined whether glucose metabolism in the P322S/+ mice is impaired. In 28-week-old mice after a 4-hour fast, neither male nor female P322S/+ mice fed standard chow showed statistically significant differences in basal glucose levels compared to their WT littermates (Figure 2.4a). To determine if either glucose tolerance or insulin sensitivity are reduced, glucose tolerance and insulin tolerance tests were performed. To assess glucose tolerance, glucose was injected intraperitoneally into 28-week-old mice following a 4-hour fast. In contrast to what we predicted from the human patients, glucose tolerance was not altered in either male or female P322S/+ mice (Figure 2.1g & Figure 2.4b). When insulin tolerance tests were performed in 29-week-old mice after a 6-hour fast, the changes in glucose levels after the insulin injection were similarly not statistically altered in either male or female P322S/+ mice (Figure 2.1h & Figure 2.4c). Plasma insulin levels after an overnight fast were also comparable between 13-week-old male P322S/+ mice and their control littermates (Figure 2.1i). These data suggest that the P322S mutation in SH2B1 does not significantly affect glucose metabolism or insulin sensitivity in mice fed standard chow.

The effect of the P322S mutation in SH2B1 on body weight in mice fed a high fat diet

Eating a diet that is high in fat is one of the main factors contributing to the development of human obesity (175). We therefore thought it possible that the effect of the P322S mutation in SH2B1 on energy balance might only become evident in mice with diet-induced obesity. To test this hypothesis, we fed the mice a high fat diet (60% fat) for 24 weeks (weeks 6-30). Although both male and female mice gained significantly more weight on a high fat diet (compare Figure 2.5a to Fig. 2.1d), neither male nor female P322S/+ mice showed a greater body weight gain than their WT littermates (Figure 2.5a). For both male and female mice on a high fat diet, the P322S/+ mice and their sex-matched WT littermates also consumed comparable amounts of food, assessed in 27-week-old mice (Figure 2.5b).

In contrast to mice fed normal chow, both male and female mice (29-week-old) fed a high fat diet exhibited a modest but statistically significant higher basal glucose level after a 6 hour fast than their WT littermates (Figure 2.6a). Consistent with an impaired ability to handle glucose, both male and female P322S/+ mice assessed at 28 weeks and fasted for 4 hours displayed reduced glucose tolerance in response to an intraperitoneal injection of glucose (Figure 2.5c). This impaired ability to handle glucose was also detected in female mice when the area under the curve was calculated (Figure 2.6b). In the males, an upward trend was evident although the area under the curve did not reach statistical significance when compared to WT littermates. However, despite their decreased glucose tolerance, neither the male nor the female P322S/+ mice showed decreased insulin sensitivity compared to their sex-matched WT littermates assessed using an insulin tolerance test (Figure 2.5d and Figure 2.6c). Plasma insulin levels obtained after an overnight fast were also not statistically different between P322S/+ mice and their sex-matched controls (Figure 2.5e), consistent with the P322S mutation not affecting insulin sensitivity. Because glucose tolerance is impaired by the accumulation of fat (176,177),

we evaluated if the reduced glucose tolerance seen in the high-fat-diet-fed P322S/+ mice might have resulted from increased adiposity. We analyzed body composition using NMR. For both male and female mice, the P322S/+ mutation did not affect either the level of adiposity (Figure 2.5f) or lean body mass (Figure 2.7a). Similarly, the P322S mutation in SH2B1 had no effect on the weight of brain, heart, kidney, perigonadal fat or testis (Table 2.2). These data suggest that in mice fed a high fat diet, the P322S mutation in SH2B1 modestly attenuates the positive effect of SH2B1 on glucose homeostasis.

Disruption of the PH domain alters the subcellular localization of SH2B1

While the P322S mouse did not show the obese phenotype we predicted from the human patients, we hypothesized that a different PH domain mutation might result in a more profound phenotype and provide insight into the importance of the PH domain of SH2B1 in the regulation of energy balance and glucose homeostasis. While making the P322S mouse model, we generated a second mouse model in a C57BL/6 background that disrupts the PH domain of SH2B1 with a two-amino acid deletion (ΔP317,R318) (ΔPR) (Figure 2.1a). DNA sequencing confirmed germline transmission of the ΔPR edit (Figure 2.9a). We first confirmed that this deletion would not significantly affect the ability of SH2B1 to be expressed using an *in vitro* system. We first looked at expression of GFP-SH2B1β vs SH2B1β ΔPR in transiently transfected PC12 cells, a cell line that sends out neurite outgrowths and expresses neuron-specific genes when stimulated by the neurotrophic factor nerve growth factor (NGF) (178). Levels of GFP-SH2B1β and GFP-SH2B1β ΔPR were similar (Figure 2.8a), indicating that the ΔPR deletion is not, to a significant extent, preventing SH2B1β from being expressed or affecting its stability. We next used live cell confocal microscopy of SH2B1β to determine whether the two-amino acid deletion alters the subcellular localization of SH2B1β. Figure 2.8b

and 2.8c illustrate that GFP-SH2B1β localizes primarily to the plasma membrane and cytoplasm of both 293T and PC12 cells, consistent with previous results (28). Surprisingly, in contrast to SH2B1β WT, when SH2B1β ΔPR is expressed in either 293T cells (Figure 2.8b) or PC12 cells (Figure 2.8c), some localizes at the plasma membrane but most localizes to the nucleus. Although WT SH2B1β has been shown to shuttle between the nucleus and cytoplasm, no SH2B1β is visible in the nucleus under steady state conditions (27,28), indicating that the rate of nuclear export of SH2B1β must greatly exceed the rate of nuclear import. Interestingly, 293T cells expressing GFP-SH2B1β WT showed a nuclear localization after being treated with an inhibitor of nuclear export, leptomycin B, however, cycling of GFP- SH2B1β P322S into the nucleus was significantly impaired (Doche 2012, Figure 2B and Supplemental Figure 1). The nuclear localization of SH2B1β ΔPR suggests that the ΔPR mutation alters SH2B1 cycling through the nucleus to favor retention in the nucleus.

We next examined whether the disruption to the PH domain affects the ability of SH2B1β to enhance neurotrophic factor-mediated neurite outgrowth. SH2B1β has been shown to enhance the ability of neurotrophins such as nerve growth factor (NGF) and BDNF to promote neurite outgrowth and/or branching in PC12 cells, hippocampal, and/or cortical neurons (29,167,7,8,20). We transiently expressed GFP-SH2B1β WT or GFP-SH2B1β ΔPR in PC12 cells, added NGF for two days, and determined the percentage of transfected cells exhibiting neurite outgrowths two times the length of the cell body (Figure 2.8d). The ΔPR mutation impairs the ability of SH2B1β to enhance NGF-induced neurite outgrowth. Together, these results show that disruption of the PH domain by the ΔPR mutation alters the subcellular distribution of SH2B1β and impairs the ability of SH2B1β to enhance neurotrophic factor-induced neurite outgrowth. This raises the possibility that the PH domain helps keep SH2B1 out

of the nucleus, thereby enhancing SH2B1's ability to act at the plasma membrane to enhance the ability of hormones and neurotrophic factors to stimulate neuron function (e.g., by enhancing the formation of appropriate neuronal projections).

SH2B1 ΔPR mice develop obesity and impaired glucose metabolism

Due to the robust and interesting phenotype that the SH2B1 ΔPR mutant showed at the cellular level, we were convinced that SH2B1ΔPR was an active protein. We proceeded to investigate the effect of the ΔPR disruption of the PH domain of SH2B1 on energy balance and glucose homeostasis in mice. We first determined whether the ΔPR mutation affects the relative abundance of mRNA of the different SH2B1 isoforms in the brain and in peripheral tissue (e.g. heart). Like the P322S mutation, the ΔPR deletion does not appear to affect the relative abundance of mRNA of any of the SH2B1 isoforms in either of the tissues tested (Figure 2.10a). We also examined whether the ΔPR deletion alters levels of SH2B1 protein in brain tissue (Figure 2.10b). The ΔPR deletion had only a modest effect on protein levels and no effect on the relative levels of the different SH2B1 isoforms in the brain. We also found that in contrast to the P322S mice, the ΔPR mice are born at close to the expected Mendelian frequency (Figure 2.9b).

Having established that the protein expression of SH2B1 isoforms is not substantially affected by the ΔPR deletion in mice, we turned our attention to the effect of the ΔPR deletion on energy balance and glucose homeostasis. In contrast to the P322S mice, both male and female ΔPR mice fed standard chow exhibited significantly increased body weight and fat mass compared to their WT littermates (Figure 2.10c and 2.10d). When body weight was measured over time (Figure 2.10e), ΔPR/ΔPR and ΔPR/+ male mice at 20 weeks were 15 grams (>40%) and 3 grams heavier, respectively, than their WT littermates and the ΔPR/ΔPR female mice were approximately 9 grams (~35%) heavier. The weight gain of the male and female ΔPR/ΔPR mice

was comparable to the weight gain of the KO mice (56,133). To determine if the increased body weight seen in the ΔPR mice was a result of hyperphagia, food intake of individually housed mice was monitored from weeks 18-20 (Figure 2.10f). Both the ΔPR/ΔPR and ΔPR/+ male mice and ΔPR/ΔPR female mice showed statistically significant increased food intake compared to their WT littermates. To determine whether energy expenditure is also contributing to the obesity seen in the ΔPR mice, we measured 24-hour oxygen consumption (normalized to lean body mass) (Figure 2.10g), respiratory exchange ratio (RER) (Figure 2.11a), locomotor activity in both horizontal (activity-x total) (Figure 2.11b) and vertical axis (activity-z total) (Figure 2.11c), fat oxidation (data not shown), and glucose oxidation (data not shown) using the Comprehensive Lab Animal Monitoring System (CLAMS) in 11-12-week-old mice. The ΔPR/ΔPR mice showed a modest increase in vertical locomotor activity (Figure 2.11c). However, ΔPR/ΔPR and ΔPR/+ male and female mice showed no difference in any of the other parameters compared to their WT littermates. These data suggest that the ΔPR mutation causes obesity in mice primarily as a consequence of increased food intake and not decreased energy expenditure.

Increased weight can be due to increased overall size, lean body mass, adipose tissue, or some combination thereof. We therefore used NMR to assess lean body mass and fat mass. Body fat mass, assessed in absolute grams, was essentially doubled in both male and female ΔPR/ΔPR mice and ~50% increased when assessed as a percentage of body weight when compared to their WT littermates (Figure 2.12a and Figure 2.13a). Lean mass was much more modestly increased in both ΔPR/ΔPR male (by ~16%) and female (by ~6%) mice compared to WT littermates (Figure 2.13b) and was actually decreased in ΔPR/ΔPR male mice when normalized to body weight (Figure 2.12b). No statistically significant change in either fat mass or lean mass was

seen in ΔPR/+ male or female mice when compared to WT littermates (Figure 2.12a, 2.12b and Figure 2.13a, 2.13b).

When individual fat depots were dissected and weighed (Table 2.3), inguinal fat mass was found to increase by 120% and 20% for the ΔPR/ΔPR and ΔPR/+ male mice, respectively and perigonadal fat mass by 50% and 40%, respectively. The increase in inguinal and perigonadal fat mass was even more dramatic in the ΔPR female mice. Inguinal fat mass increased by 220% and 40% in the ΔPR/ΔPR and ΔPR/+ female mice, respectively while perigonadal fat mass increased by 280% and 60%, respectively. Brown fat was also significantly increased in ΔPR/ΔPR male mice compared to their WT littermates. In contrast, there was no difference in the weight of brain or heart from ΔPR/+ or ΔPR/ΔPR mice vs their WT littermates (Table 2.3). The modest increase in the weight of the liver from male ΔPR/ΔPR mice seems likely to be due to increased fat deposition resulting from the increased adiposity. These data suggest that the increased body weight in the ΔPR mice is primarily due to increased fat mass.

Consistent with the increased adiposity observed at 24-26 weeks of age, plasma leptin levels were significantly higher in ΔPR/ΔPR male and female mice and ΔPR/+ male mice (Figure 2.12c). To confirm that the increased leptin levels are due primarily to increased adiposity, we measured leptin concentrations and body composition at a younger age when the fat mass of the ΔPR mice may not have started to accumulate to a level higher than that of their littermate controls. Consistent with the elevated leptin levels seen in the 24-26-week old ΔPR/ΔPR mice being primarily due to elevated adiposity, leptin levels measured in 7-week old mice were not elevated in female ΔPR/ΔPR and ΔPR/+ mice and male ΔPR/+ mice (Figure 2.14a), which exhibited similar fat and lean body mass compared to their WT littermates at 11-12 weeks of age (Figure 2.13c, d & 2.14b, 6c). Only the ΔPR/ΔPR male mice, which started to

exhibit increased fat mass as early as 6-7 weeks, exhibited elevated leptin levels. Interestingly, by the time (12-14 weeks) we sacrificed that cohort of ΔPR/ΔPR mice, the perigonadal fat was doubled in weight in both males and females compared to littermate controls (Table 2.4). Liver weight was also increased in ΔPR/ΔPR and ΔPR/+ female mice compared to control littermates, consistent with increased adiposity (Table 2.4). Brain weight was not altered (Table 2.4).

Disruption of the PH domain in SH2B1 causes hyperglycemia, reduced glucose tolerance, and insulin resistance in mice

To gain insight into whether disruption of the PH domain in SH2B1 also affects SH2B1 regulation of insulin-regulated glucose metabolism, we measured blood glucose levels after a 4-hour fast at week 18. Both male and female ΔPR/ΔPR mice exhibited statistically significant hyperglycemia compared to their WT littermates (Figure 2.16a). Challenging the mice with an exogenous bolus of glucose via an intraperitoneal injection confirmed impaired glucose tolerance in both male and female ΔPR/ΔPR mice and male ΔPR/+ mice (Figure 2.15a and Figure 2.16b). The ability of exogenous insulin to lower blood glucose levels during insulin tolerance tests was also significantly impaired in ΔPR/ΔPR male mice (Figure 2.15b and Figure 2.16c) but not in female ΔPR/ΔPR mice or male or female ΔPR/+ mice. Together, these results suggest that after the onset of obesity, the SH2B1 ΔPR mice have an impaired ability to regulate glucose homeostasis.

Disruption of the PH domain in SH2B1 causes hyperglycemia, hyperinsulinemia, and reduced glucose tolerance in mice prior to the onset of obesity

Because the ΔPR mutation causes obesity and obesity itself can cause impaired glucose homeostasis, we examined whether the ΔPR deletion causes impaired glucose tolerance independent of obesity. At 8 weeks of age, before the onset of adiposity in females and when

adiposity as judged by leptin levels was still relatively modest in the males, both the ΔPR/ΔPR male and female mice showed hyperglycemia compared to their WT littermates after a 4-hour fast (Figure 2.17a). Furthermore, the ΔPR/ΔPR male and female mice showed reduced glucose tolerance compared to their WT littermates when exogenous glucose was administered intraperitoneally during a glucose tolerance test (Figure 2.16c and Figure 2.17b). The ΔPR/+ male and female mice tolerated glucose normally (Figure 2.16c and Figure 2.17b). In contrast, insulin sensitivity assessed by an insulin tolerance test at week 9 was similar in both ΔPR/ΔPR and ΔPR/+ male and female mice compared to their WT littermates (Figure 2.16d and Figure 2.17c). However, compared to WT littermates, both ΔPR/ΔPR male and female mice exhibited hyperinsulinemia at 8 weeks of age after a 6 hour fast (Figure 2.16e) suggesting that at this age, which is several weeks before the weight of the ΔPR/PR mice starts to increase above that of the WT mice (Figure 2.10e), the ΔPR mice are starting to develop insulin resistance. Together these data suggest that even before the onset of obesity, the disruption of the PH domain by the ΔPR deletion significantly impairs the ability of SH2B1 to regulate glucose homeostasis, in addition to impairing energy balance.

Modeling and analysis of the 3-D structure of the PH domain in the region of P317, R318, and P322

To gain insight into how the SH2B1 P322S mutation or deletion of residues P317 and R318 in SH2B1 might regulate the function of the PH domain in SH2B1, we analyzed the NMR structure of the PH domain of the SH2B1 family member SH2B2/APS (1V5M) (179). Clustal analysis of the PH domains of these three SH2B family members reveals that the PH domains are highly-conserved and identifies the residues corresponding to the P317 and R318 residues responsible for the ΔPR deletion and the P322S mutation in SH2B1 as P71, K72 and P76 in

SH2B2/APS, respectively (Figure 2.18a). The residues that are homologous or functionally homologous (black and cyan) in the ClustalW are colored green in Figure 2.18b-d. Non-conserved residues are colored orange. The minimal number of orange-colored residues in the region surrounding the residues P71, K72 and P76 in the SH2B2/APS structure, corresponding to P317, R318, and P322S in SH2B1, suggests that the structure in this region will be a good model for SH2B1. In the SH2B2/APS structure, the residues corresponding to P317, R318, and P322S in Sh2B1 are on an exterior surface of the PH domain. This surface is presumably a binding interface that interacts with either another region in SH2B1 or another protein (Figure 2.18b). Because the residues corresponding to P317 and R318 in SH2B1 (P71 and K72 in SH2B2/APS) are on the surface of the PH domain and do not substantially change the direction of the loop, the P317, R318 deletion in SH2B1 is not expected to severely damage the structure. However, the deletion would be expected to diminish stabilization of the turn between P71 (P317 in SH2B1) and the nearby β-pleated sheet that is provided by the predicted pi stacking between residues P317 and F309 in SH2B1 (P71 and F63 in SH2B2/APS). In addition, the deletion would be expected to substantially alter the shape of the interface surface in the region of P317 and R318 in SH2B1 (P71 and K72 in SH2B2/APS). With respect to the P322S mutation (P76 in SH2B2/APS), the proline to serine mutation would be expected to increase the motion of the peptide backbone at this residue. The mutation to serine also opens up the possibility of changes due to phosphorylation.

Consistent with the importance of an intact PH domain for the function of SH2B family members, at least 11 point mutations (E208Q/E, S213R, A215V, G220V/R, A223V, G229S, T274A, D234N, F287S) have been identified in the PH domain of the SH2B1 orthologue SH2B3/Lnk in patients with the myeloproliferative neoplasms, polycythemia vera (PV), essential

thrombocythemia (ET), and/or primary myelofibrosis (PMF) (87,88,71,89-91)(Figure 2.18a). In addition, the mutations E208Q, S213R, A215V, and T274A in SH2B3/Lnk have been identified in JAK2 mutation–negative patients with idiopathic erythrocytosis who had normal/subnormal erythropoietin levels (71,180). Residues in the SH2B2/APS structure (C45, L48, A52, and R57) that correspond to five of the human mutations in SH2B3/Lnk (G220V, G220R, A223V, G229S, and D234N) and V53 in the SH2B2/APS structure that corresponds to the human E229G mutation in SH2B1 are in close proximity to the P71, K72 or P76 (P317, R318, or P322 in SH2B1 respectively) (Figure 2.18a, c, d). The concentration of human patient mutations in this region, along with the pi stacking and extensive hydrogen bonding that stabilizes this region of the PH domain, suggest that small structural changes in this region due to mutation or other modification have the potential to produce substantial functional consequences. In addition, beyond the 8 mutation sites discussed above, two additional residues (D31 and A40 [E208Q, A215V mutations in SH2B3/Lnk]) are also on the PH domain surface and suggest that this surface might be a protein binding interface. Taken together, the human SH2B3/Lnk mutations (G220R, G220V, A223V, G229S, and D234N), the human SH2B1 mutations (E299G and P322S) and the P317, R318 deletion in SH2B1 identify a regulatory hot spot in the PH domains of the SH2B family members that is critical for the function of the PH domain.

Discussion

Although the PH domain is among the most common domains in proteins (162), the function of most PH domains remains unknown. What is known has primarily been gained from in vitro studies; few studies have been carried out in animal models in which alterations in the PH domain have resulted in identifiable changes in phenotype. The finding here that a relatively small deletion in the PH domain, predicted to have only a minor effect on the structure of the PH

domain, causes a rather profound effect on SH2B1β localization at the cellular level and energy balance and glucose homeostasis at the whole animal level provides some of the first real evidence of the importance of this domain in SH2B1 function. While SH2B1β has been shown to cycle through the nucleus, it is generally found at the plasma membrane and in the cytoplasm (27,167,25). The dramatic accumulation of SH2B1β ΔPR in the nucleus indicates that the ΔPR deletion greatly alters the ratio between nuclear import and nuclear export of SH2B1β. One explanation consistent with our structural model of the PH domain of SH2B1 (Figure 2.18) is that the ΔPR mutation alters a putative protein binding interface of SH2B1 and affects the ability of the PH domain to bind to another protein or another region of SH2B1. The resulting altered protein-protein interaction either blocks the NES, enhances the accessibility of the NLS, or both. The fact that the PH domain is shared among all isoforms of SH2B1 suggests that the PH domain of SH2B1 is likely to be similarly critical in determining the subcellular distribution of all the isoforms. We predict that such a drastically altered subcellular distribution would have an important impact on the function of each of the different SH2B1 isoforms. Consistent with this, the ΔPR mutation impairs the ability of SH2B1β to promote neurotrophic factor-induced neurite outgrowth of PC12 cells. Because neurite outgrowth in PC12 cells shares many properties with the formation of axons and/or dendrites (178), one possibility for the substantial shift in energy balance seen in the ΔPR mice is an impaired ability of the neurons that regulate feeding behavior to form the proper neuronal projections. Because SH2B1 is recruited to a variety of receptors implicated in feeding behavior, including the receptors for leptin (132), insulin (44,10) and BDNF (7,20), it will be interesting to determine whether the PH domain of SH2B1 impairs the outgrowth of neurons expressing each of these receptors, and whether a change in subcellular distribution or some other impaired function responsible for the drastic change in energy balance

observed in the SH2B1 ΔPR mice. It will also be interesting to determine if the primary effect of the PH domain on glucose homeostasis is mediated via SH2B1 acting centrally or peripherally.

Regarding the P322S mouse, we showed that in mice fed a standard 9% fat diet or a high fat diet, the P322S mutation in SH2B1 does not affect body weight, food intake or insulin sensitivity of heterozygous mice. Studies using a smaller cohort (3-4 animals) of homozygous mice fed a standard 9% fat diet gave similar results, i.e. no effect of the P322S mutation on body weight, food intake or insulin sensitivity in male or female mice (Fig. 1d and data not shown). Although the P322S mutation in SH2B1 in mice also did not seem to affect glucose tolerance or insulin sensitivity under standard chow conditions, the P322S mutation did decrease glucose tolerance when the mice were challenged with a high fat diet. However, in contrast to humans with the P322S mutation and SH2B1 KO mice, the P322S/+ mice did not show decreased sensitivity to insulin, as judged by a normal insulin tolerance test. The finding that pancreas-specific deletion of SH2B1 in mice impairs glucose tolerance under high fat diet conditions, presumably due to increased apoptosis and decreased rate of proliferation of beta cells (142), raises the possibility that under high fat diet conditions, the P322S mutation may impair the function of SH2B1 in glucose metabolism by diminishing the protective function of SH2B1 in beta cells. The reduced rate of survival of neonatal mice with the P322S mutation in SH2B1 suggests a further problem with reproduction. Taken together, our data suggest that, in mice, the P322S mutation does not replicate the full spectrum of effects seen in humans with the SH2B1 P322S mutation. Because environmental factors such as diet, exercise and other behavioral patterns greatly increase the prevalence of obesity in a population (181), it is possible that other environmental conditions or genetic backgrounds may reveal a phenotype in mice with the SH2B1 P322S mutation that more closely resembles the obese, insulin-resistant phenotype

ascribed to humans with the P322S mutation. Our combined studies with the SH2B1 P322S mice and the SH2B1ΔPR mice in conjunction with analysis of the structure of the PH domain of SH2B1, SH2B2/APS and SH2B3/Lnk highlight the importance of the PH domain in SH2B1 in a variety of cellular and whole animal metabolic functions, and suggest the importance of follow-up studies at both the cellular and whole animal level.

Methods

Study approval

All procedures were approved by the University Committee on the Use and Care of Animals at the University of Michigan and followed the Public Health Service guidelines for the humane care and use of experimental animals.

Animal care

Mice were housed in ventilated cages under controlled temperature (23°C) on a 12 hour light, 12 hour dark cycle (from 6:00 to 18:00) in the Unit for Laboratory Animal Medicine at the University of Michigan. Mice were fed standard chow (20% protein, 9% fat, PicoLab Mouse Diet 20 5058, catalog#0007689) *ad libitum* with free access to tap water.

Generation of SH2B1 P322S and ΔP317, R318 mice

CRISPR/Cas9 genome editing was used to insert the P322S mutation into mice. The reverse complement of the genomic SH2B1 sequence in C57BL/6J mice (accession # NC_000073, GRC m38) was used when designing the reagents for CRISPR. CRISPR/Cas9 genome editing requires an RNA guide and a donor template for homology-directed repair. Two sets of RNA guides (Guides 1 and 2) were selected from the guides predicted using the website described in Ran et al. (156). Guides were selected that cut within 40 nt of the codon for P322 and had a high inverse likelihood of off-target binding. The guides were expressed using the pX330 vector

(152,156). The pX330 vector contains a chimeric guide RNA expression cassette and the hSpCas9 expression cassette. The oligos required for expressing the guides were purchased from Integrated DNA Technologies (IDT). The two oligos for guide 1 (nt 3325-3344) were: (1st strand, 5'-AAACcgtaggcgtcccgaccccgtC-3' containing the reverse complement of the guide sequence flanked by an AAAC overhang for subcloning into a Bbs1 site and a 3' C for initiating transcription by U6 polymerase), and (2nd strand, 5'-CACCGacggggtcgggacgcctacg-3' containing the guide sequence flanked by a CACCG overhang for subcloning into a Bbs1 site with a G for initiating transcription by U6 polymerase). The two oligos for guide 2 (nt 3337 - 3356) were: (first strand, 5'-AAACgaccccgtctcagcattccc-3' and (2nd strand, 5'-CACCgggaatgctgagacggggtc-3'). The pair of oligos for each guide was annealed, and subcloned into the Bbs1 site in the chimeric guide RNA expression cassette in the pX330 vector. The resulting construct was expressed in DH5 ✔ cells. Colonies were selected, DNA isolated, and the sequence verified in the region of the inserted guide sequence. The donor template for homology-directed repair (HDR) (from IDT) was designed to code for a mutated version of the 180 nt region between nt 3264-3443 of SH2B1. The donor template introduced the C>T mutation into the codon for P322 to produce the human disease mutation, SH2B1 P322S. Silent mutations were introduced to create a diagnostic Xbal site and to disrupt guide RNA binding and prevent further cleavage by Cas9 following HDR (Fig. 1a). Top (sense) strand of donor template: (nt 3264) 5-gaatggagggagatacagttagatttgacacacc aaaaactgattcttcttccctttcccgcgt[guide#1cut site]aggcg**tcTAga**c[guide#2cut site]cTAg Actcagcatt**Tcc**tgctctactattactgatgtccgcacagccacagccctagagatgcctgacagggagaacacgtttgtggttaaggtag gaacccca-3' (nt 3443). Bottom (antisense) strand: 5'-tggggttcctaccttaacca

caaacgtgttctccctgtcaggcatctctagggctgtggctgtgcggacatcagtaatagtagagca**gg**A**a**atgctgagTcTAgg**tcT**

Agacgcctacgcgggaaagggaagaagaatcagtttttggtgtgtcaaatctaactgtatctccctccattc-3'.

The pX330 plasmid containing the guide sequence was purified using an endotoxin-free PureLink HiPure maxiprep kit (Life Technologies #K210006). The plasmid DNA was eluted with EB buffer (10 mM Tris, pH 8.5) and further purified using a Qiaprep miniprep column (QIAGEN; #27106). All buffers used with the miniprep column were filtered using Anotop 0.02 μm filters (Whatman #6809-1002). The miniprep column was washed with PE buffer. DNA concentrations were determine using a NanoDrop One spectrophotometer (Thermo Scientific). DNA (100 μg) eluted from the maxiprep was solubilized in 1.5 ml of PE buffer and loaded onto the miniprep column 2X. The column was washed 4 times with 0.75 ml of PE and the DNA eluted with 50 μl of EB buffer. To prepare the donor template, the oligonucleotides were solubilized in microinjection buffer (RNAse-, DNAse-free 10 mM Tris, 0.1 mM EDTA, pH 7.4, filtered with Anotop 0.02 μm filters) and annealed. A Millipore dialysis filter (#VMWP02500) was floated shiny side up on 10 ml of microinjection buffer and 75 μl of the annealed template subjected to spot dialysis for 45 minutes. The concentrations of the purified pX330 plasmid containing the guide sequence and the donor template were determined. The constructs and the template were diluted with microinjection buffer to 5 ng/μl and 10 ng/μl, respectively, and transferred to the University of Michigan Transgenic Animal Model Core for testing in blastocysts. DNA obtained from stage 8 blastocysts was genotyped by PCR followed by digestion with XbaI restriction enzyme (see below). PCR analysis and DNA sequencing showed that 8 of 23 Guide 1 and 17 of 27 Guide 2 blastocysts contained the P322S edit. Each guide/template combination was then injected into ~75 oocytes from C57BL/6J mice. The injected oocytes were then implanted into C57BL/6J mice by the University of Michigan

Transgenic Animal Model Core. The genotype of the resulting pups was determined by PCR and XbaI digestion, and confirmed by DNA sequencing. Of the five pups born from mice implanted with oocytes injected with Guide 1, 4 pups were wild-type (WT) and 1 pup contained an indel. Of the six pups born from mice implanted with oocytes injected with Guide 2, 2 pups contained the P322S edit and 4 pups had indels. P322S founders were backcrossed against C57BL/6J mice to breed out off-target effects. DNA sequencing confirmed germline transmission of the P322S edit (Supplemental Fig. 1a). N2 mice from one founder were used for experiments in Figure 1 and Supplemental Table 1. N5 mice from the same founder were used for experiments in Figure 2 and Supplemental Table 2. One of the indels encoded SH2B1 ΔP317, R318 (ΔPR). The ΔPR founder was backcrossed against C57BL/6J mice to breed out off-target effects. DNA sequencing confirmed the germline transmission of the ΔPR deletion (Supplemental Fig. 2a). N3 mice were used for experiments in Figures 4-5, Figure 6A-B, and Table 1 and N4 mice were used for experiments in Figure 6C-E and Figure 7.

Genotyping and PCR

To genotype the mice, tails were collected from mice prior to 21 days of age and boiled at 95°C for 1 hour in 75ul Buffer 1 (0.2 mM EDTA, 25 mM NaOH). Buffer 2 (75ul, 40 mM Tris HCI, pH 8.0) was then added (Biotech, 2000). A 556 nt product was amplified from purified mouse tail DNA and digested with Xbal (P322S mice) or purified with QIAquick PCR purification kit (QIAGEN; #28106) and submitted for Sanger DNA sequencing at the University of Michigan DNA Sequencing Core (P322S and ΔPR mice). The following primers were used (10 nM final concentration)

5’ –TATTGCTGTCCTGGGTTCAGTGCTAACTGT-3’ and

5’ -AAGACTCAAAGCCCCCGACATATACTCATC- 3’.

To determine relative levels of SH2B1 gene expression, total cellular RNA was extracted using TRIzol Reagent (Ambion; Life Technologies). cDNA was synthesized from the RNA using Taqman Reverse Transcription Reagent Kit (Applied Bio-Systems; N808-0234) per manufacturer's instructions. PCR was performed using GoTaq DNA polymerase (Promega, Catalog #M3005) using the following parameters: 95°C 2 minutes, 95°C 15 seconds, 63°C 30 seconds, 72°C 1:20 minutes, repeat 42 cycles, 72°C 4 minutes, 4°C.

PCR primers (each 10 mM concentration) used for detection of all SH2B1 isoforms were 5' TTCGATATGCTTGAGCACTTCCGG 3' and 5'GCCTCTTCTGCCCCAGGATGT 3'.

Body weight

P322S mice were individually housed at 4 (standard chow) or 6 (high fat diet) weeks of age and body weight was assessed weekly on the same day of the week and at the same time. ΔPR mice were individually housed at 5 weeks of age and body weight was assessed weekly on the same day of the week and at the same time. Food intake, GTT, ITT, and blood draws for determination of hormone levels were performed on these cohorts of mice (see below).

Food Intake

Mice were individually housed at week 4 (Fig 1e, 4e) and week 6 (Fig. 2b) and food intake was assessed for the weeks indicated (weeks 5-25 for P322S mice fed normal chow; week 27 for P322S mice fed a high fat diet; weeks 18-20 for ΔPR mice). Food was added at the start of each week. At the end of the week, the remaining food was removed and weighed, including that in the bedding, and new food was weighed and added for the following week. Bedding was changed each week. Nibblers, defined as mice that nibble on the food but do not necessarily eat it, were excluded from the study. Food intake for Figures 1e and 4e is shown as cumulative

intake meaning that after the first week, new food weight from each week was added to the food weight from previous weeks.

Glucose tolerance tests, insulin tolerance tests, and hormone levels

For glucose tolerance tests, mice were fasted for 4 hours (9:00 – 13:00), D-glucose (2 g/kg of body weight) was injected intraperitoneally, and blood glucose was monitored at 0, 15, 30, 60, and 120 minutes after injection. Glucose was assessed using a Bayer contour glucometer and glucose strips (part # 7097C). For insulin tolerance tests, mice were fasted for 6 hours (8:00 – 14:00), human insulin (1 IU/kg of body weight) was injected intraperitoneally and blood glucose was monitored at 0, 15, 30, and 60 minutes after injection. To assess insulin levels, mice were fasted for 6h (8:00-14:00). Blood was collected in a heparin-coated capillary tube from the tail vein of the mice and plasma insulin assessed using an UltraSensitive Mouse Insulin ELISA kit (catalog # 90080, Crystal Chem, Inc). To assess leptin levels, blood was either collected between 9:00- 10:00am from the tail vein of fed mice into heparin-coated capillary tubes (plasma) or at euthanasia trunk blood was collected between 10:00 – 13:00 (serum) from fed mice. Leptin was assessed using a Mouse Leptin ELISA kit (catalog # 90030, Crystal Chem, Inc).

Tissue collection

Mice were euthanized at 12-13 or 31-32 weeks of age using isoflurane followed by decapitation. Mice were sacrificed between 10:00 – 13:00. Trunk blood was collected and the serum was stored at -80°C for future analysis. Tissues were collected, weighed, snap-frozen in liquid nitrogen and stored at -80°C.

Body composition

Body composition was measured in 30 week-old mice at room temperature in the morning using a Minispec LF90 II Bruker Optics by the University of Michigan Animal Phenotyping Core.

Comprehensive Lab Animal Monitoring System (CLAMS)

For automated metabolic assessment (n= 10-15 per group), animals were first acclimated to single housing in home cages for 3 days and then tested in the CLAMS apparatus (Columbus Instruments) for 72 hours. O_2 consumption (VO_2), CO_2 production (VCO_2), X activity, and Z activity were collected in 20-minute bins. The final 24 hours of recordings are presented. Subsequent to CLAMS analysis, body composition was measured by nuclear magnetic resonance.

Plasmids

GFP-tagged rat SH2B1β (GenBank accession number NM_001048180) (8) and SH2B1β P322S (92) have been described previously. The ΔPR deletion was introduced into GFP-SH2B1β using the QuikChange II site-directed mutagenesis kit (Stratagene) according to the manufacturer's protocol. Deletion of P317 and R318 was confirmed by Sanger sequencing (University of Michigan DNA Sequencing Core).

Cell culture and transfections

293T cells (CRL- 3216; AATCC) were maintained at 37°C with humidified air at 5% CO_2 in Dulbecco's modified Eagle's medium (DMEM) (11965-092; Life Technologies) supplemented with 1 mM L-glutamine, 0.25 μg/ml amphotericin, 100 U/ml penicillin, 100 μg/ml streptomycin (DMEM culture medium), and 8% bovine serum (BS; Life Technologies). 293T cells were transiently transfected using calcium phosphate precipitation (66). Cells were used after 24 or 48 hours. PC12 cells (CRL-1721; ATCC) were plated on dishes coated with rat tail type I collagen (BD Biosciences) and maintained at 37°C with humidified air at 5% CO_2 in in normal growth medium (RPMI 1640 medium (A10491-01; Life Technologies) containing 10% horse serum (HS; Atlanta Biologicals) and 5% fetal bovine serum (FBS; Life Technologies)). PC12 cells

were transiently transfected using Lipofectamine LTX (Life Technologies) for 24 hours according to the manufacturer's instructions.

Immunoblotting

Tissues: Tissue lysates were prepared from frozen tissues in L-RIPA lysis buffer (50 mM Tris-HCl, 150 mM NaCl, 2 mM EGTA, 0.1% Triton X-100, pH 7.2, 1 mM Na_3VO_4, 1 mM phenylmethylsulfonylfluoride [PMSF], 10 μg/ml aprotinin, and 10 μg/ml leupeptin). Protein concentration was determined by a DC Protein Assay kit from Bio-Rad Laboratories, Inc. (USA) (#500-0112). Equal amounts of proteins were separated by SDS-PAGE (9% or 7% acrylamide gels). Proteins were then transferred to low-fluorescence PVDF membrane (Bio-Rad; #162-0264). Membranes were incubated with monoclonal antibody to SH2B1 (46, Santa Cruz Biotechnology; Cat #sc-136065, RRID:AB_2301871) or β-tubulin (G-8, Santa Cruz Biotechnology; Cat #sc-55529, RRID:AB_2210962) in 10 mM Tris, 150 mM NaCl, pH 7.4, 0.1% Tween 20, 3% BSA overnight at 4 °C with constant rocking followed by incubation with IRDye-conjugated mouse secondary antibody was added (1:20,000 dilution) for 1 hour at room temperature. Protein signal was detected using the Odyssey infrared imaging system (Li-Cor Biosciences). For immunoprecipitations, cell lysates containing equal amounts of protein were incubated with monoclonal antibody 46 to SH2B1 (1:100) (Santa Cruz Biotechnology; Cat #sc-136065, RRID:AB_2301871) at 4 °C overnight followed by incubation with protein A-agarose beads (RepliGen; #7489) at 4 °C for 1 hour. Samples were centrifuged at 3000 x g at 4 °C for 1 minute. The beads were washed three times with L-RIPA lysis buffer. Samples were resuspended in 62.5 mM Tris/HCl (pH 6.8), 2% (w/v) SDS, 0.05% (w/v) bromophenol blue, 10% (v/v) glycerol, and 5% (v/v) β-mercaptoethanol and boiled at 95 °C for 10 minutes.

PC12 cells: Cells were seeded at ~40-50% confluency per 10-cm collagen-coated dish in normal growth medium. Cells were then transfected either the same day or the next day. 24 hours after transfection, cells were incubated overnight in RPMI 1640 medium with 2% horse serum and 1% fetal bovine serum (deprivation medium). Cells were incubated at 37°C with 25 ng/ml NGF (Harlan Envigo; BT.5025) as indicated, placed on ice, and washed two times with phosphate-buffered saline (PBS; 10 mM $NaPO_4$, 140 mM NaCl, pH 7.4) containing 1 mM Na_3VO_4, pH 7.3 (PBSV). Cells were lysed with boiling L-RIPA lysis buffer supplemented with 20 mM NaF in Laemmli loading buffer for 10 min on ice. Whole cell lysates were centrifuged at 15,000 x g for 10 min at 4°C, and proteins were resolved using 9% SDS-PAGE gels and transferred to low-fluorescence PVDF (Bio-Rad) membranes. Blots were incubated overnight at 4°C with antibodies in 10 mM Tris, 150 mM NaCl, pH 7.4, 0.1% Tween 20, 3% BSA followed by secondary antibody for 1 hour at room temperature. Bands were visualized using the Odyssey infrared imaging system (Li-Cor Biosciences).

Neurite outgrowth

PC12 cells were plated in 6-well dishes and transiently transfected with the indicated construct. Cells were incubated overnight in deprivation medium and then treated with 25 ng/ml mouse NGF. After 2 days, GFP-positive cells were visualized by fluorescence microscopy (40X objective, Nikon Eclipse TE200). One hundred GFP-positive cells in three different areas of each plate were scored for the presence of neurites 2 times the length of the cell body (total of 300 cells per condition per experiment). Each experiment was carried out 3 times. The percentage of GFP-positive cells with neurites was determined by dividing the number of GFP-positive cells with neurites by the total number of GFP-positive cells counted.

Live cell imaging

GFP, GFP-tagged SH2B1, or GFP-tagged SH2B ΔPR mutant was transiently expressed in 293T cells or PC12 cells seeded on 35-mm glass-bottom dishes (MatTek) in normal growth medium. Cells were imaged in normal growth medium using a 60X water immersion objective on an Olympus FV500 laser-scanning confocal microscope and FluoView version 5.0 software (Morphology and Image Analysis Core of the Michigan Diabetes Research Center). A multiline argon blue laser was used to excite GFP fluorescence at 488 nm. For each condition, 18 to 30 cells were counted. Dying or dead cells and cells with a particularly high or low expression level were excluded (usually ~10% of the cells).

Structural modeling and ClustalW analysis

The structural modeling of the PH domain of SH2B1 was based on the NMR structure of SH2B2/APS (1V5M) (reference Li H) as visualized using the PyMOL Molecular Graphics System, version 2.2.3) (http://www.pymol.org). The numbering of the residues in the SH2B2/APS structure are offset from the numbering in SH2B2 (translated from NM_020979.1) (eg., the first residue in the PH domain of APS (Q19) is Q195 in human SH2B2.) Residue numbering with 2 digits refers to the numbering in the APS structure. ClustalW alignments were performed using LaserGene, version 14.0.0 (DNASTAR, Madison, WI). Functional homology was determined using the PAM250 mutation probability matrix. Functional homology was defined as residues that match the consensus within 1 distance unit using the PAM250 mutation probability matrix.

Statistics

All analyses were carried out using GraphPad Prism software. Body weight, glucose tolerance tests, and insulin tolerance tests were analyzed by 2-way ANOVA followed by Fisher's Least Significant Difference post-test. Food intake curves for P322S mice on standard chow and ΔPR

mice were analyzed by linear regression. For other physiological parameters, experimental animals were independently compared with their WT littermates by two-tailed Student's *t* test. Survival phenotype for P322S or ΔPR mice was analyzed by a Chi-square test. Neurite outgrowth was analyzed by a two-tailed Student's *t* test. For all comparisons, *P <0.05 was considered significant.

Note: The work described in this chapter, in modified form, will be submitted for publication under the title "Crucial Role of SH2B1 PH Domain Function for the Control of Energy Balance and Metabolism" by Anabel Flores, Lawrence S. Argetsinger, Alvaro Malaga, Paul Vander, Lauren C. DeSantis, Ray M. Joe, Gowri Chandrashekar, Joel C. Cline, Erik Clutter, Yixin Hu, Jeanne Stuckey, Martin G. Myers Jr., Christin Carter-Su. A.F., (with the help of) L.S.A., M.G.M., and C.C-S. developed the concept, designed experiments, interpreted the data, helped direct experiments, conducted most experiments, analyzed the data, and prepared the manuscript. A.M., L.D., G.C., and Y.H. helped measure body weight and food intake (Figures 2.1d-e, 2.2a-b, 2.4d-e). A.M. helped re-genotype the mice. P.V. conducted neurite outgrowth experiments (Figure 2.8d) and helped with experiments for Figure 2.8a and c. R.M.J. conducted preliminary experiments for Figure 2.8b. E.S.C. maintained mouse colonies and helped collect blood samples (Figures 2.12c and 2.14a). J.M.C. made the GFP-SH2B1 WT and GFP-SH2B1 ΔPR constructs (Figure 2.8). J.S. and L.S.A. analyzed the model of the PH domain (Figure 2.18).

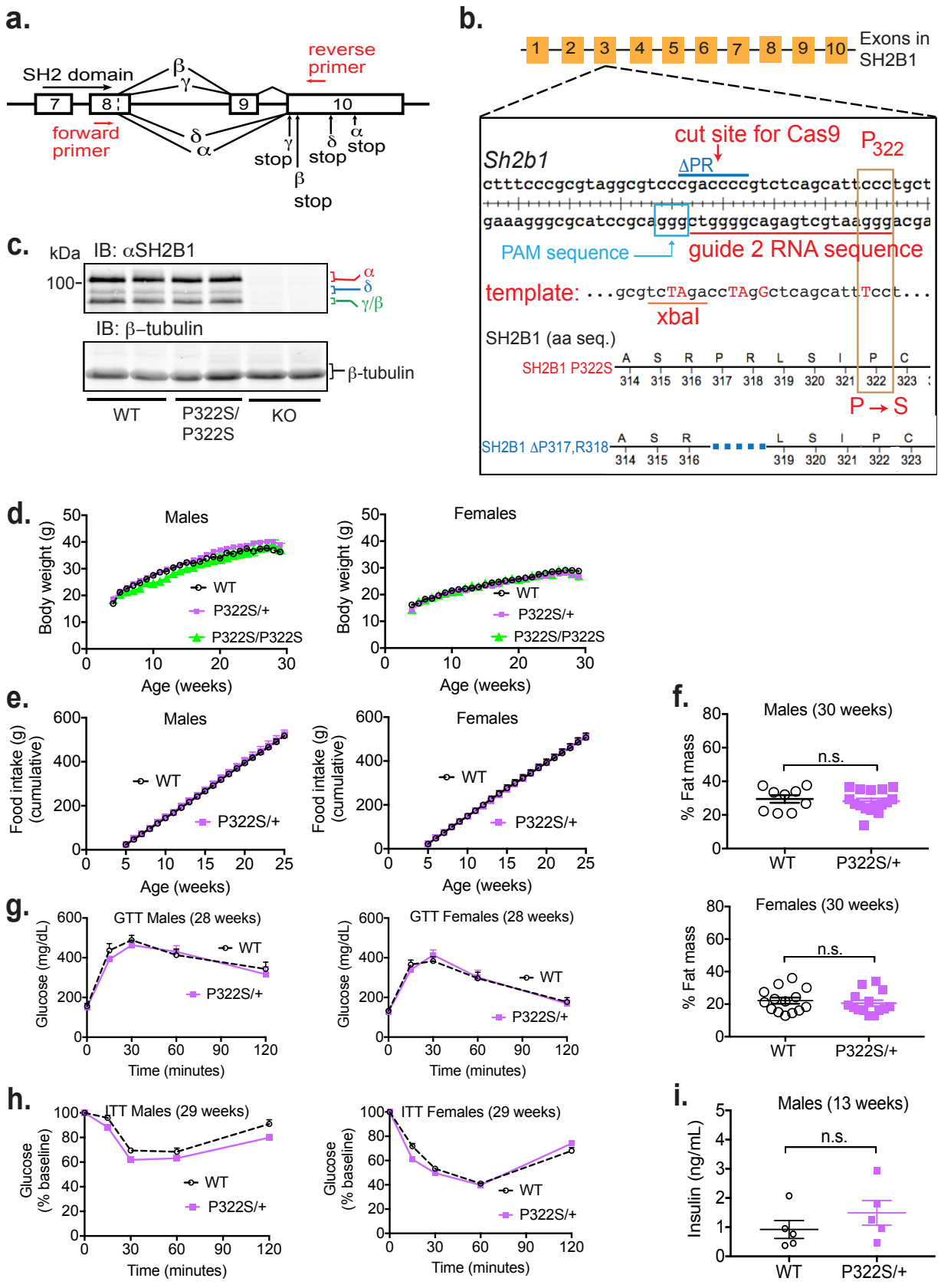
a.
SH2 domain
reverse primer
forward primer
stop
b.
Exons in SH2B1
Sh2b1
cut site for Cas9
P322
ΔPR
PAM sequence
guide 2 RNA sequence
template:
xbaI
SH2B1 (aa seq.)
SH2B1 P322S
SH2B1 ΔP317,R318
P→S
c.
kDa
IB: αSH2B1
IB: β–tubulin
β-tubulin
WT
P322S/ P322S
KO
d.
Males
Females
Body weight (g)
Age (weeks)
WT
P322S/+
P322S/P322S
e.
Food intake (g) (cumulative)
f.
Males (30 weeks)
Females (30 weeks)
% Fat mass
n.s.
g.
GTT Males (28 weeks)
GTT Females (28 weeks)
Glucose (mg/dL)
Time (minutes)
h.
ITT Males (29 weeks)
ITT Females (29 weeks)
Glucose (% baseline)
i.
Males (13 weeks)
Insulin (ng/mL)

Figure 2.1 The effect of the P322S mutation in SH2B1 on body weight, food intake, body composition and glucose metabolism of mice fed standard chow.

a) *Sh2b1* gene structure and position of primers used to assess isoform-specific mRNAs. Exons are noted by numerals. Stop codons for each isoform are noted. **b**) CRISPR-cas9 schematic for SH2B1 P322S gene editing. Shown are the RNA sequence of guide 2, PAM sequence for this guide, cut site for Cas9, the sequence of the 180 nt oligo donor template directing homology-directed repair in the region of the cut site, and the sequence of *Sh2b1* in the regions of the codon for both P322 and the ΔP317, R318 deletion. Mutations in the donor template that introduce the C>T mutation to code for P322S and silent mutations to create a diagnostic XbaI site and disrupt guide RNA binding following repair are highlighted in red. **c**) Proteins in brain tissue lysates from WT, P322S/P322S, and KO male mice were immunoblotted with αSH2B1 or αβ-tubulin. Migration of the 100 kDa protein standard and the four known isoforms of SH2B1 are shown. **d**) Body weight was assessed at weeks 4-29. Means ±SEM. Males: n=8 (WT), 16 (P322S/+), 4 (P322S/P322S). Females n=10 (WT), 14 (P322S/+), 3 (P322S/P322S). **e**) Food intake was assessed at weeks 5-25. Means ± SEM. Males n=7 (WT), 8 (P322S/+). Females n=7 (WT), 9 (P322S/+). **f**) Body fat mass was determined at week 30. Percent fat mass was determined by dividing fat mass by body weight. Means ± SEM. Males: n=9 (WT), 16 (P322S/+); females: n=14 (WT, P322S/+). **g**) GTT was assessed at 28 weeks. After a 4-hour fast, mice were injected intraperitoneally with D-glucose (2 mg/kg of body weight). Blood glucose was monitored at indicated times. Means ± SEM. Males: n=8 (WT), 14 (P322S/+). Females: n=9 (WT), 14 (P322S/+). **h**) ITT was assessed at 29 weeks. After a 6-hour fast, mice were injected intraperitoneally with insulin (1 IU/kg of body weight). Blood glucose was monitored at indicated times. Means ± SEM. Males: n=8 (WT), 15 (P322S/+). Females: n=9 (WT), 13 (P322S/+). **i**) 13-week-old male mice were fasted overnight and insulin levels were determined. Means ± SEM, n=5.

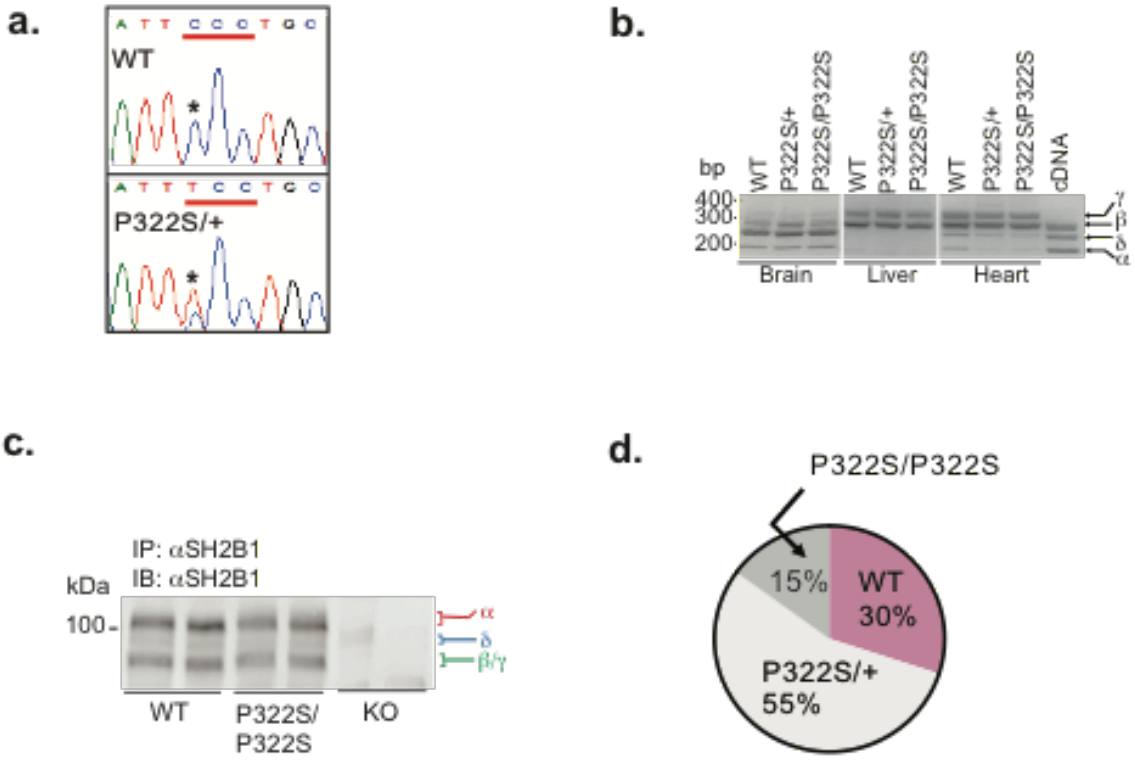

Figure 2.2 The P322S mutation does not affect mRNA or protein levels of the 4 known isoforms of SH2B1.

a) Sequencing of DNA from mice from the N1 generation confirms germline transmission of the SH2B1 P322S mutation. The relevant region of DNA sequence from one of the P322S/+ mice and a WT littermate are shown. The codons for P322 (upper panel) and S322 (lower panel) are underlined. The peaks corresponding to the C >T mutation are denoted by asterisks. **b**) mRNA was extracted from brain, liver, and heart tissue of SH2B1 WT, P322S/+, and P322S/P322S male mice. A ladder of DNA standards and isoform-specific PCR products are shown on the left and right, respectively. Location of forward and reverse primers are shown in Fig. 1a. **c**) Proteins in lysates from brain tissues from WT, P322S/P322S and KO mice were immunoprecipitated and immunoblotted with αSH2B1. The migration of the 100 kDa protein standard and four known isoforms of SH2B1 are shown on the left and right, respectively. **d**) P322S/P322S mice from intercrosses of heterozygous mice are born at approximately half (1 out of 7) of the expected (1 out of 4) Mendelian ratio. n = 179 mice. Chi-Square Test, *P<0.05.

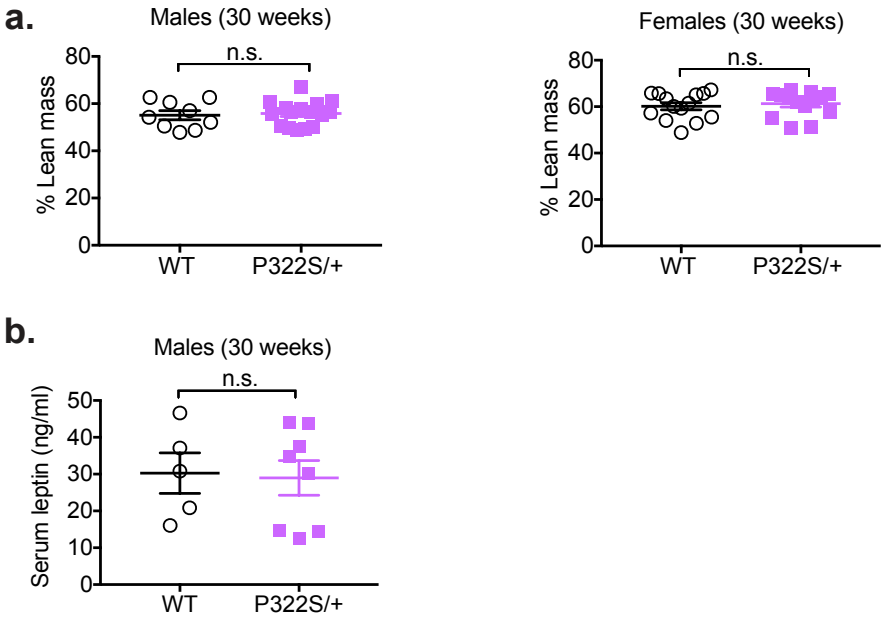

Figure 2.3 The P322S mutation does not affect lean body mass of mice fed standard chow.

a) Lean body mass was determined using NMR at week 30. Percent lean mass was determined by dividing fat mass by body weight. Means ± SEM. Males: n=9 (WT), 16 (P322S/+); females: n=14. **b**) At week 30, serum from P322S/+ and control male mice was assayed for leptin. Means ± SEM. n=5 (WT), 8 (P322S/+).

Table 2.1 Weight of organs in SH2B1 P322S/+ mice fed standard chow

Males	WT (n=8)	P322S/+ (n=13)	Females	WT (n=10)	P322S/+ (n=13)
brain	0.45 ± 0.02 g	0.46 ± 0.01 g	brain	0.47 ± 0.01 g	0.47 ± 0.01 g
heart	0.18 ± 0.01 g	0.18 ± 0.01 g	heart	0.17 ± 0.01 g	0.16 ± 0.01 g
kidney	0.23 ± 0.01 g	0.21 ± 0.01 g	kidney	0.16 ± 0.01 g	0.16 ± 0.01 g
perigonadal fat	2.06 ± 0.19 g	1.49 ± 0.14 g	perigonadal fat	0.83 ± 0.18 g	0.68 ± 0.15 g
testis	0.10 ± 0.01 g	0.12 ± 0.01 g			

Table 2.1 Weight of organs is similar at week 32-33 in SH2B1 P322S/+ mice and their WT littermates fed standard chow. Means ±SEM are shown.

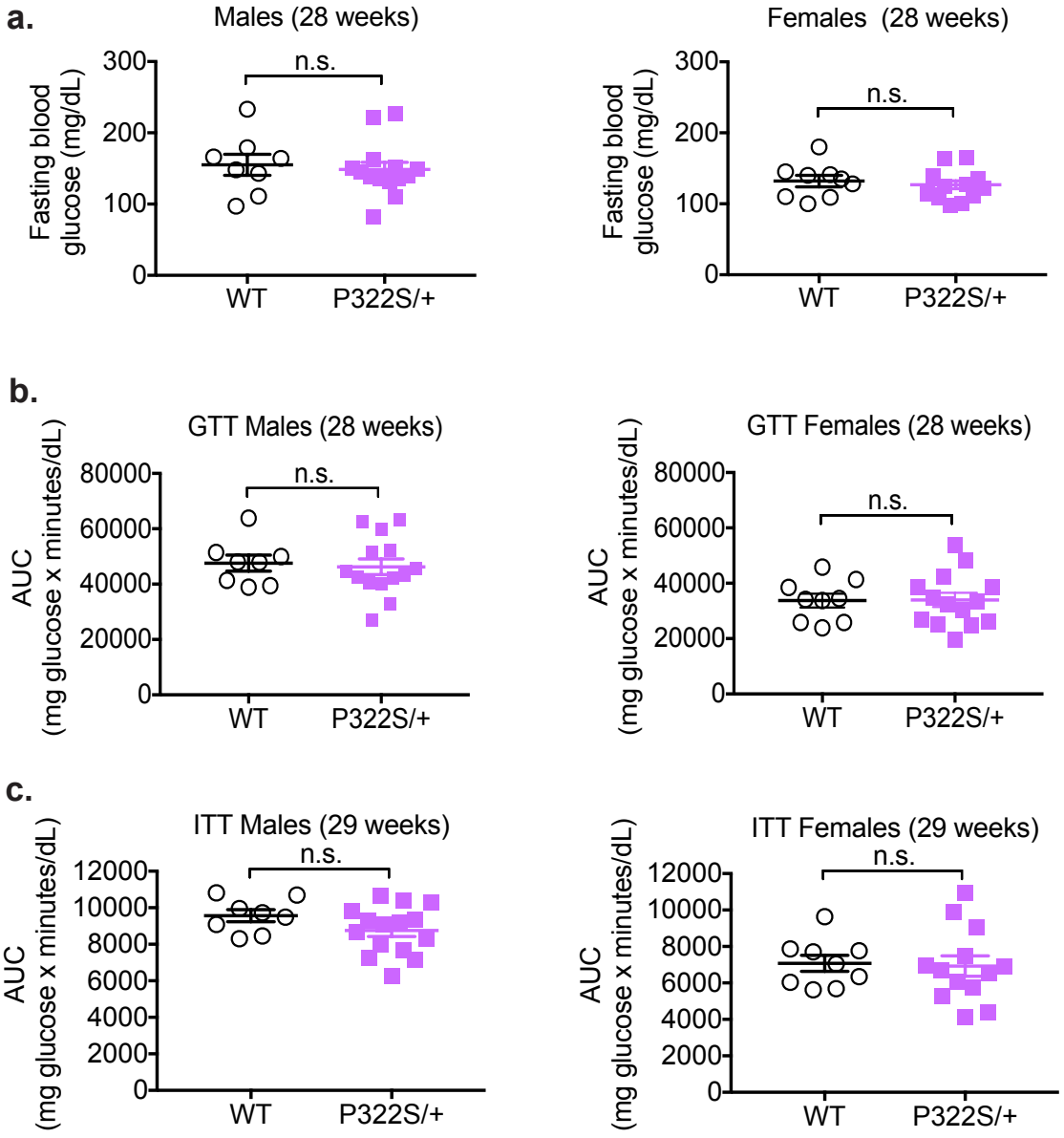
a.
Males (28 weeks)
Fasting blood glucose (mg/dL)
300
200
100
0
n.s.
WT
P322S/+
Females (28 weeks)
Fasting blood glucose (mg/dL)
300
200
100
0
n.s.
WT
P322S/+
b.
GTT Males (28 weeks)
AUC (mg glucose x minutes/dL)
80000
60000
40000
20000
0
n.s.
WT
P322S/+
GTT Females (28 weeks)
AUC (mg glucose x minutes/dL)
80000
60000
40000
20000
0
n.s.
WT
P322S/+
c.
ITT Males (29 weeks)
AUC (mg glucose x minutes/dL)
12000
10000
8000
6000
4000
2000
0
n.s.
WT
P322S/+
ITT Females (29 weeks)
AUC (mg glucose x minutes/dL)
12000
10000
8000
6000
4000
2000
0
n.s.
WT
P322S/+

Figure 2.4 The P322S mutation does not affect glucose tolerance or insulin sensitivity in mice fed standard chow.

a) 28-week-old mice were fasted for 4 hours and blood glucose was measured. **b**) GTT was assessed at 28 weeks. Mice fed standard chow were fasted for 4 hours and then injected intraperitoneally with D-glucose (2 mg/kg of body weight). Blood glucose was monitored (see Fig. 1g) and the area under the curve (AUC) was calculated. Means ± SEM. Males: n=8 (WT), 14 (P322S/+). Females: n=9 (WT), 14 (P322S/+). **c**) ITT was assessed at 29 weeks. Mice were fasted for 6 hours then injected intraperitoneally with human insulin (1 IU/kg of body weight). Blood glucose was monitored (see Fig. 1h) and the area under the curve (AUC) was calculated. Means ± SEM are shown. Males: n=8 (WT), 15 (P322S/+). Females: n=9 (WT), 13 (P322S/+).

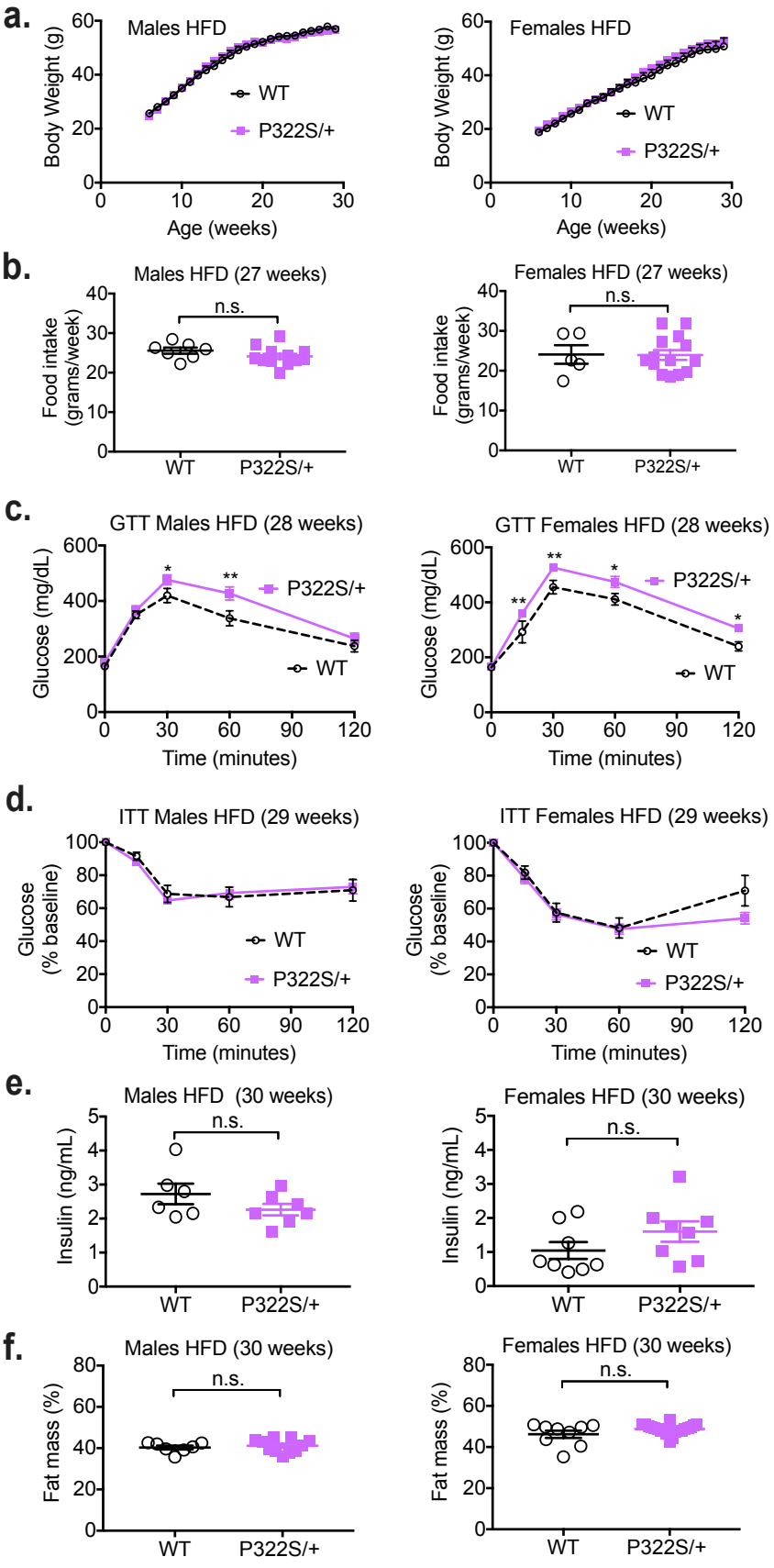
a.
Males HFD
Body Weight (g)
Age (weeks)
WT
P322S/+
Females HFD
b.
Males HFD (27 weeks)
Food intake (grams/week)
n.s.
Females HFD (27 weeks)
c.
GTT Males HFD (28 weeks)
Glucose (mg/dL)
Time (minutes)
GTT Females HFD (28 weeks)
d.
ITT Males HFD (29 weeks)
Glucose (% baseline)
ITT Females HFD (29 weeks)
e.
Males HFD (30 weeks)
Insulin (ng/mL)
Females HFD (30 weeks)
f.
Males HFD (30 weeks)
Fat mass (%)
Females HFD (30 weeks)

Figure 2.5 The P322S mutation in SH2B1 leads to impaired glucose homeostasis in mice challenged with a high fat diet.

a) Starting at week 6, body weight was assessed weekly. Means ±SEM. Males: n=7 (WT), 12 (P322S/+). Females: n=9 (WT), 20 (P322S/+). **b**) Food intake was measured during week 27. Means ± SEM are shown. Males: n=7 (WT), 12 (P322S/+). Females: n=5 (WT), 14 (P322S/+). **c**) GTT was assessed at 28 weeks. Mice were fasted for 4 hours and then injected intraperitoneally with D-glucose (2 mg/kg of body weight). Blood glucose was monitored at times indicated. Means ± SEM. Males: n=7 (WT), 12 (P322S/+). Females: n=9 (WT), 20 (P322S/+). **d**) ITT was assessed at 29 weeks-old. Mice were fasted for 6 hours and then injected intraperitoneally with human insulin (1 IU/kg of body weight). Blood glucose was monitored at the times indicated. Means ± SEM. Males: n=6 (WT), 10 (P322S/+). Females: n=9 (WT), 20 (P322S/+). **e**) At week 30, mice were fasted overnight and insulin levels were determined. Means ± SEM. Males: n=6 (WT), 7 (P322S/+). Females: n=8 (WT, P322S/+). **f**) Body fat mass was determined at week 30. Means ± SEM. Males: n=7 (WT), 11 (P322S/+). Females: n=9 (WT), 20 (P322S/+). For all comparisons: * $P<0.05$, ** $P<0.01$.

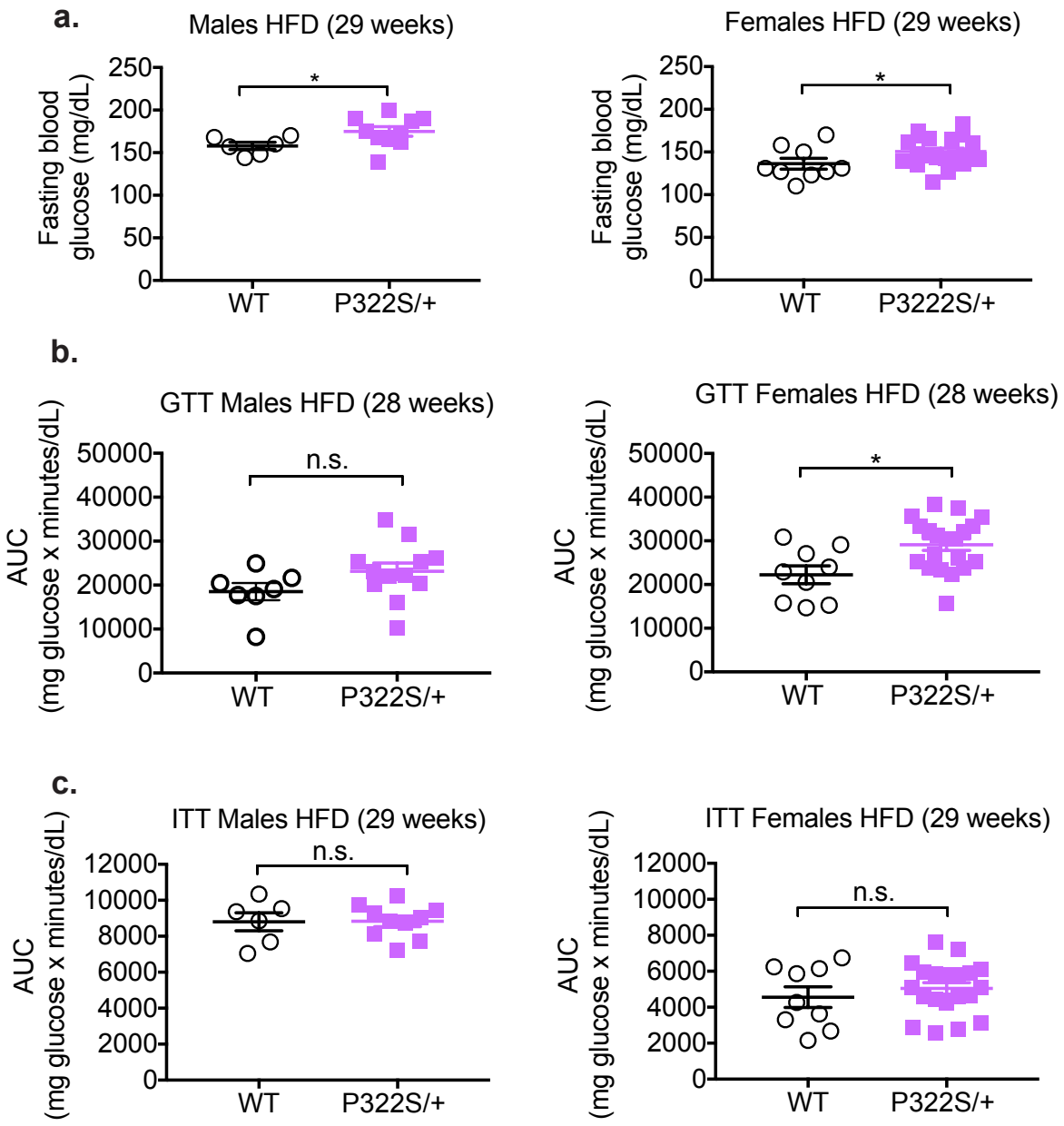
a.
Males HFD (29 weeks)
Fasting blood glucose (mg/dL)
250
200
150
100
50
0
*
WT
P322S/+
Females HFD (29 weeks)
Fasting blood glucose (mg/dL)
250
200
150
100
50
0
*
WT
P3222S/+
b.
GTT Males HFD (28 weeks)
AUC (mg glucose x minutes/dL)
50000
40000
30000
20000
10000
0
n.s.
WT
P322S/+
GTT Females HFD (28 weeks)
AUC (mg glucose x minutes/dL)
50000
40000
30000
20000
10000
0
*
WT
P322S/+
c.
ITT Males HFD (29 weeks)
AUC (mg glucose x minutes/dL)
12000
10000
8000
6000
4000
2000
0
n.s.
WT
P322S/+
ITT Females HFD (29 weeks)
AUC (mg glucose x minutes/dL)
12000
10000
8000
6000
4000
2000
0
n.s.
WT
P322S/+

Figure 2.6 The P322S mutation in SH2B1 leads to impaired glucose homeostasis in mice challenged with a high fat diet.

a) 29-week-old mice were fasted for 6 hours and blood glucose was measured. Means ± SEM. Males: n=6 (WT), 10 (P322S/+). Females: n=9 (WT), 20 (P322S/+). **b)** GTT was assessed at 28 weeks. Mice were fasted for 4 hours and then injected intraperitoneally with D-glucose (2 mg/kg of body weight). Blood glucose was monitored (see Fig. 2d) and the area under the curve (AUC) was calculated. Means ± SEM. Males: n=7 (WT), 12 (P322S/+). Females: n=9 (WT), 20 (P322S/+). **c**) ITT was assessed at 29 weeks. Mice were fasted for 6 hours and then injected intraperitoneally with human insulin (1 IU/kg of body weight). Blood glucose was monitored (see Fig. 2e) and the area under the curve (AUC) was calculated. Means ± SEM. Males: n=6 (WT), 10 (P322S/+). Females: n=9 (WT), 20 (P322S/+). For all comparisons: *P<0.05 and **P<0.01 when compared to WT littermates.

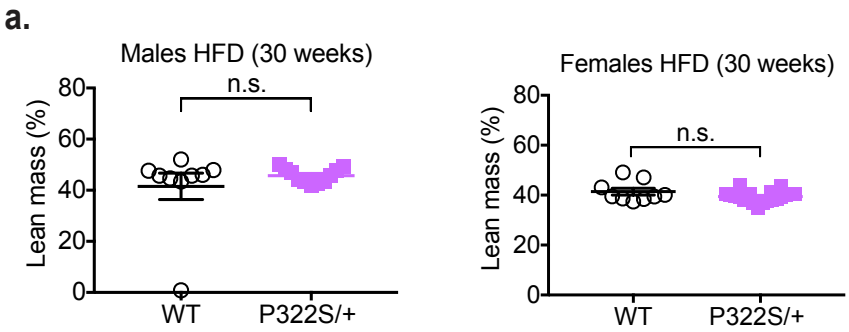

Figure 2.7 The P322S mutation does not affect lean mass in mice fed a high fat diet.

a) Lean body mass of mice fed a high fat diet (cohort used in Fig. 2) was determined at week 30. Percent lean mass was determined by dividing fat mass by body weight. Means ± SEM. Males: n=7 (WT), 11 (P322S/+). Females: n=9 (WT), 20 (P322S/+).

Table 2.2 Weight of organs in SH2B1 P322S/+ mice fed a high fat diet.

Males	WT (n=7)	P322S/+ (n=11)	Females	WT (n=9)	P322S/+ (n=20)
brain	0.45 ± 0.01 g	0.46 ± 0.004 g	brain	0.47 ± 0.01 g	0.47 ± 0.00 g
heart	0.22 ± 0.02 g	0.19 ± 0.01 g	heart	0.17 ± 0.01 g	0.17 ± 0.00 g
kidney	0.24 ± 0.02 g	0.23 ± 0.01 g	kidney	0.18 ± 0.01 g	0.19 ± 0.01 g
perigonadal fat	1.47 ± 0.16 g	1.21 ± 0.11 g	perigonadal fat	3.27 ± 0.32 g	3.63 ± 0.11 g
testis	0.10 ± 0.01 g	0.11 ± 0.01 g			

Table 2.2 Weight of organs is similar at week 32-33 in SH2B1 P322S/+ mice and their WT littermates fed a high fat diet. Means ±SEM are shown.

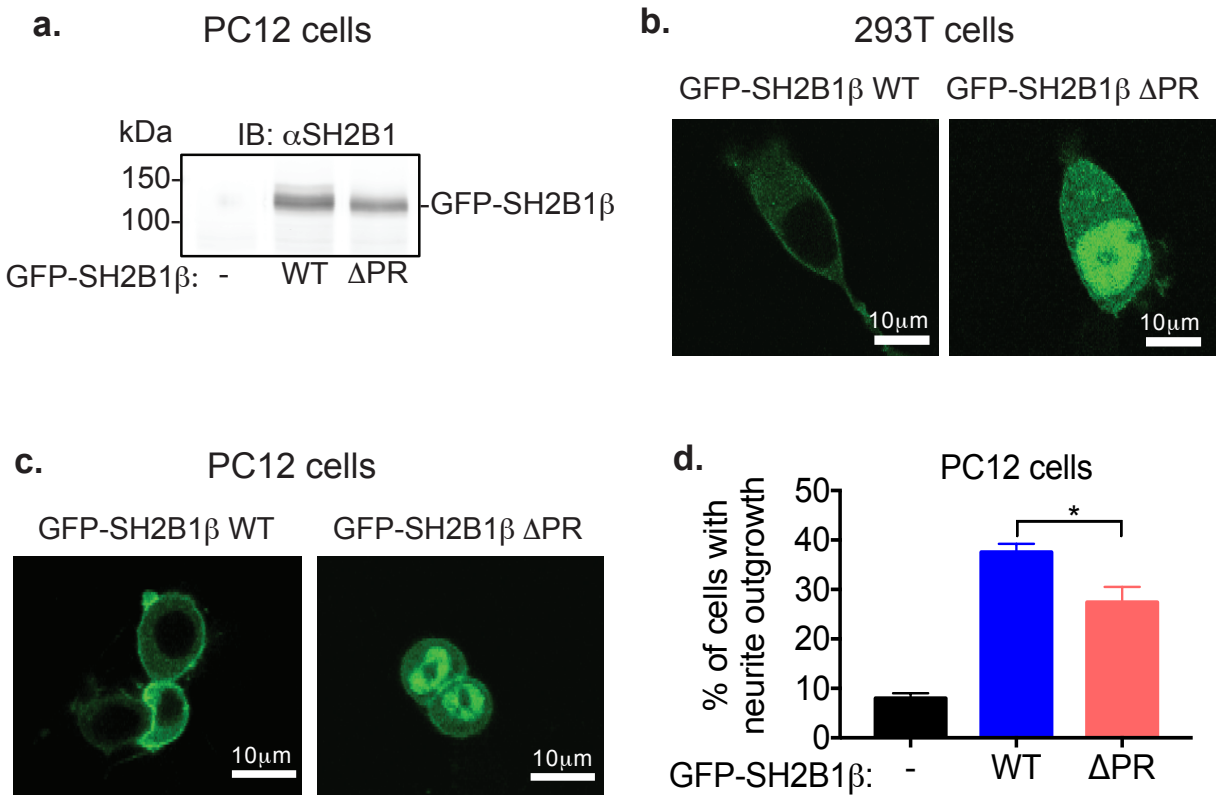

Figure 2.8 Disruption of the PH domain changes the subcellular localization of SH2B1 and impairs the ability of SH2B1 to enhance NGF-induced neurite outgrowth.

a) Proteins in whole cell lysates from PC12 cells transiently expressing the indicated GFP-SH2B1β mutants were immunoblotted with αSH2B1. Migration of molecular weight standards are on the left. **b**) and **c**) Live 293T cells (b) and PC12 cells (c) transiently expressing the indicated GFP-SH2B1β WT or GFP-SH2B1βΔPR were imaged by confocal microscopy. **d**) Live PC12 cells transiently expressing GFP-SH2B1β WT or GFP-SH2B1βΔPR were treated with 25 ng/ml mouse NGF for 2 days after which neurite outgrowth was assessed. GFP-positive cells were scored for the presence of neurites 2 times the length of the cell body (total of 300 cells per condition per experiment). The percentage of cells with neurites was determined by dividing the number of GFP-positive cells with neurites by the total number of GFP-positive cells. Means ± SEM, *P<0.05, n=3.

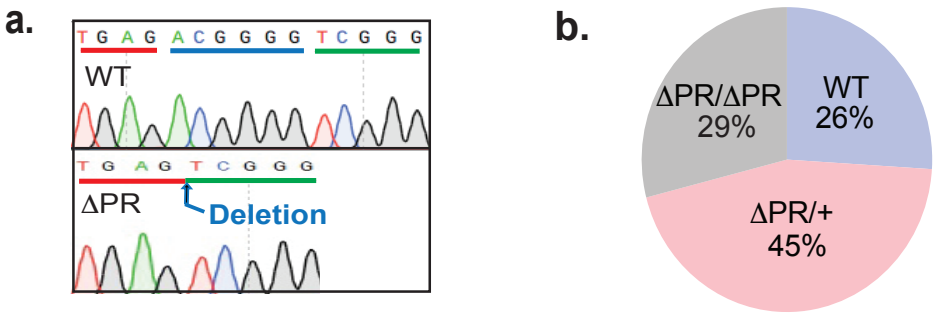

Figure 2.9 Sequencing of mice from the N1 generation confirms germline transmission of the SH2B1 ΔPR (P317, R318) mutation.

a) The relevant DNA sequence from one of the ΔPR/ΔPR mice and a WT littermate are shown. The codons for P317, R318 are underlined in blue. The missing codons for P317, R318 in the *Sh2b1* $^{\Delta PR/\Delta PR}$ mice are shown by an arrow. **b**) The ΔPR mice are born at the expected (1 out of 4) Mendelian ratio. n = 183 mice.

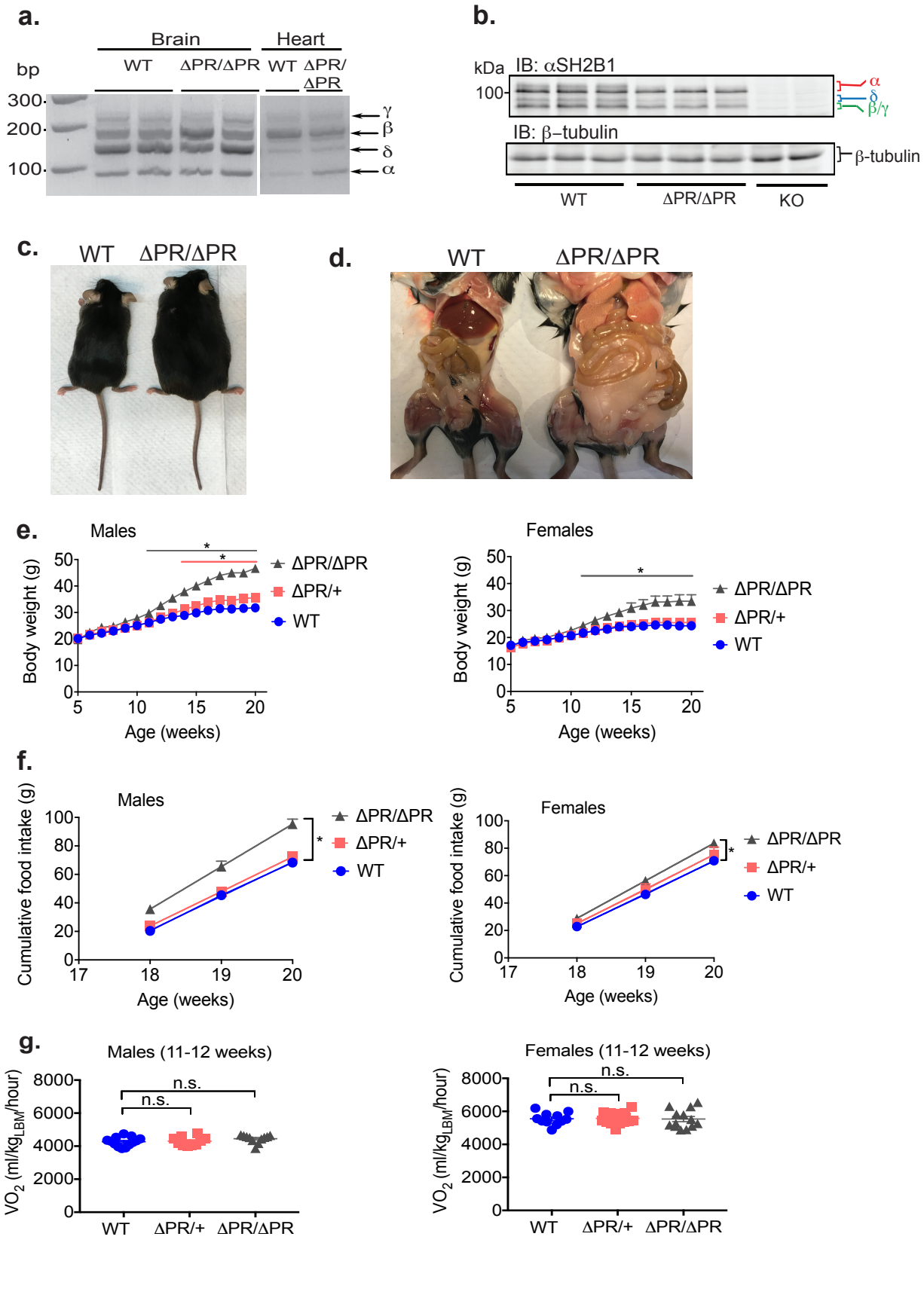
a.
Brain
Heart
WT
ΔPR/ΔPR
WT
ΔPR/ΔPR
bp
300
200
100
γ
β
δ
α
b.
kDa
IB: αSH2B1
100
α
δ
β/γ
IB: β–tubulin
β-tubulin
WT
ΔPR/ΔPR
KO
c.
WT
ΔPR/ΔPR
d.
WT
ΔPR/ΔPR
e.
Males
Body weight (g)
Age (weeks)
ΔPR/ΔPR
ΔPR/+
WT
Females
Body weight (g)
Age (weeks)
ΔPR/ΔPR
ΔPR/+
WT
f.
Males
Cumulative food intake (g)
Age (weeks)
ΔPR/ΔPR
ΔPR/+
WT
Females
Cumulative food intake (g)
Age (weeks)
ΔPR/ΔPR
ΔPR/+
WT
g.
Males (11-12 weeks)
VO2 (ml/kgLBM/hour)
n.s.
n.s.
WT
ΔPR/+
ΔPR/ΔPR
Females (11-12 weeks)
VO2 (ml/kgLBM/hour)
n.s.
n.s.
WT
ΔPR/+
ΔPR/ΔPR

Figure 2.10 Disruption of the PH domain in SH2B1 results in obesity.

a) mRNA was extracted from brain and heart tissue of WT and ΔPR/ΔPR male mice. The migration of a ladder of DNA standards and isoform-specific PCR products are shown on the left and right, respectively. **b**) Proteins in brain lysates from SH2B1 WT, ΔPR/ΔPR, and KO male mice were immunoblotted with αSH2B1 and αβ-tubulin. The migration of the 100 kDa protein standard and the four known isoforms of SH2B1 or β-tubulin are shown on the left and right, respectively. **c**) Representative male WT and ΔPR/ΔPR mice (6 months). **d**) Perigonadal fat of representative male wild-type littermate and ΔPR/ΔPR mouse (6 months). **e**) Body weight was assessed weekly starting at week 5. Means ±SEM. Males: n= 9 (WT, ΔPR/ΔPR), 14 (ΔPR/+). Females: n=7 (WT), 16 (ΔPR/+), 11 (ΔPR/ΔPR). **f**) Food intake was measured between weeks 17-20. Means ± SEM. Males: n= 11 (WT), 10 (ΔPR/+), 7 (ΔPR/ΔPR). Females: n=6 (WT), 9 (ΔPR/+, ΔPR/ΔPR). **g**) Oxygen consumption was assessed at 11-12 weeks using CLAMS. VO_2 normalized to lean body mass (LBM). For all comparisons: * $P<0.05$.

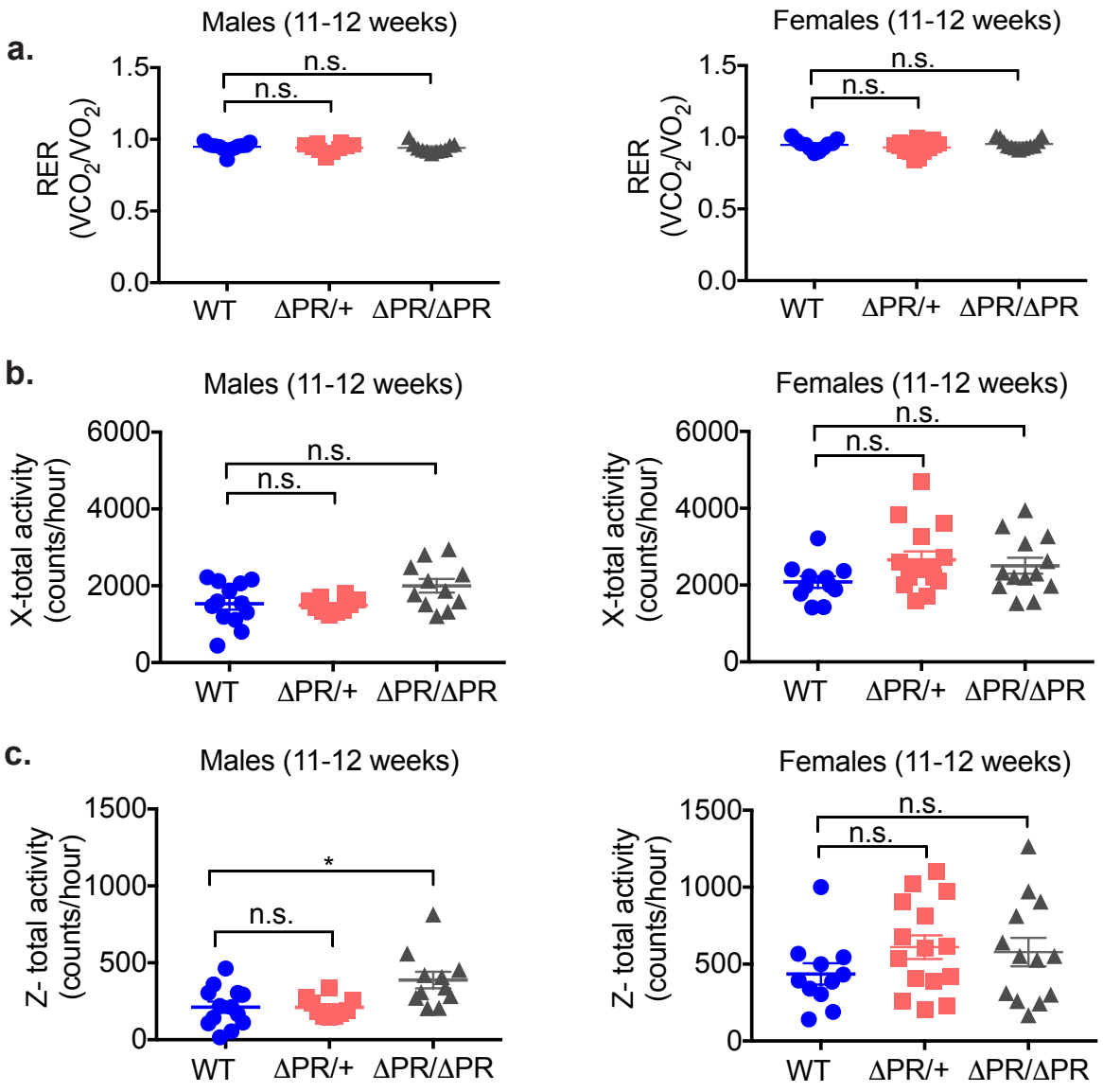

Figure 2.11 Energy expenditure and locomotor activity in ΔPR mice.

Energy expenditure and locomotor activity were assessed at 11-12 weeks using CLAMS. **a**) Respiratory exchange ratio (RER) (VCO_2/VO_2). **b**) Horizontal activity. **c**) Vertical (rearing) activity. Means ± SEM. Males: n=13 (WT), 10 (ΔPR/+), 11 (ΔPR/ΔPR). Females: n=11 (WT), 15 (ΔPR/+), 13 (ΔPR/ΔPR). For all comparisons: *P<0.05 when compared to WT littermates.

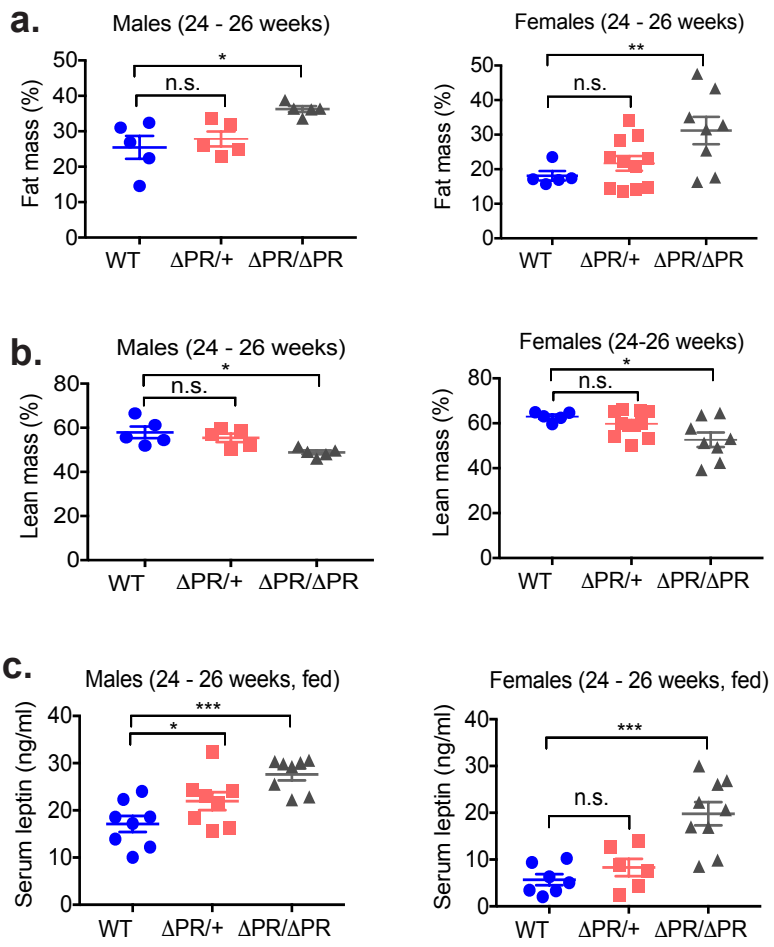

Figure 2.12 Disruption of the PH domain in SH2B1 results in increased adiposity.

a, b) Body fat and lean mass was determined at weeks 24-26. Percent fat or lean mass was determined by dividing fat mass by body weight. Means ± SEM. Males: n=5 (WT, PR/+, ΔPR/ΔPR). Females: n= 5 (WT), 11 (ΔPR/+), 8 (ΔPR/ΔPR). **c**) At week 24-26, serum from WT, ΔPR/+, and ΔPR/ΔPR male and female mice was assayed for leptin. Means ± SEM. Males: n= 8 (WT, PR/+, PR/ΔPR). Females: n=7 (WT), 6 (ΔPR/+), 9 (ΔPR/ΔPR). For all comparisons: * P<0.05, **P<0.01, and ***P<0.001.

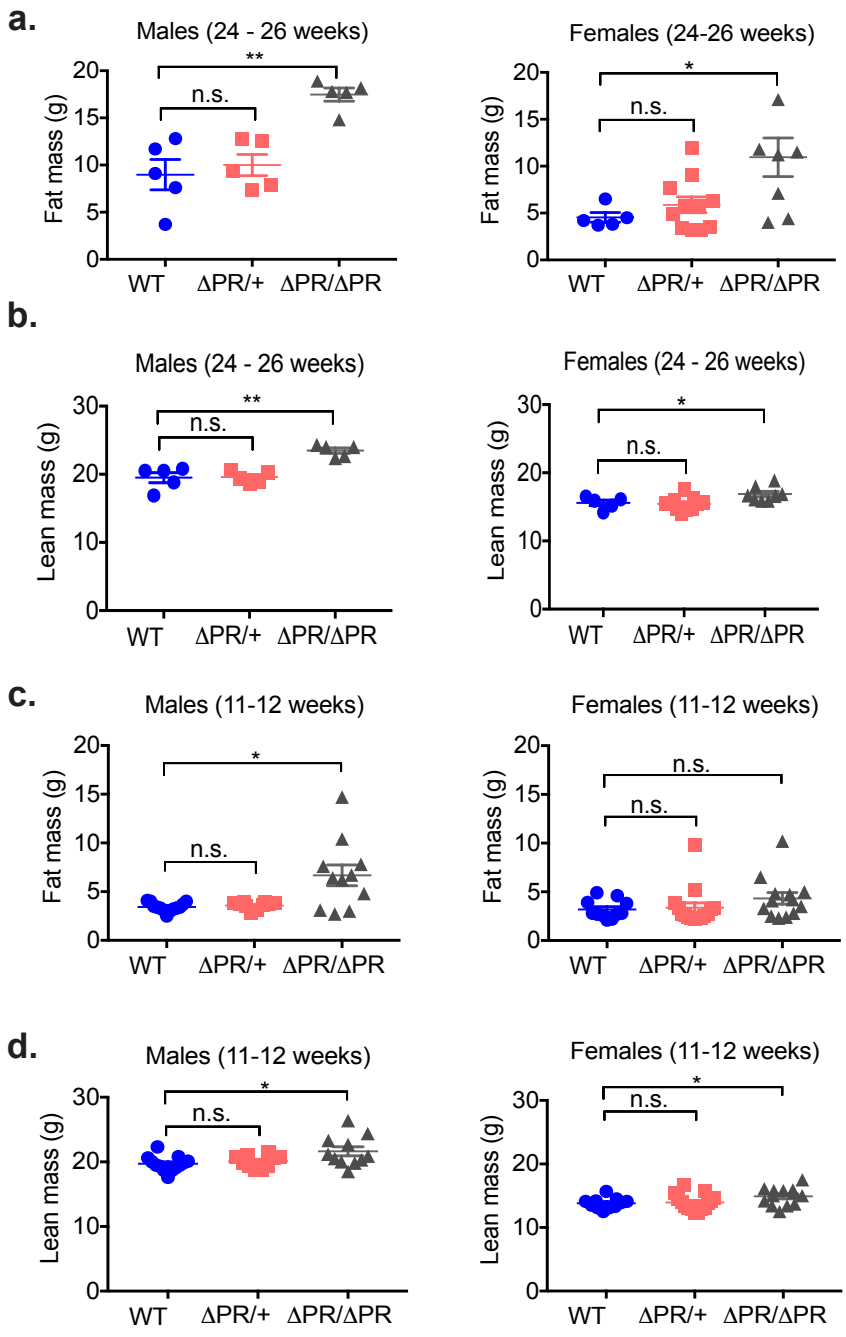

Figure 2.13 Disruption of the PH domain in SH2B1 results in increased adiposity in young male mice.

a, b) Body fat and lean mass was determined at weeks 24-26. Means ± SEM. Males: n=5 (WT, PR/+, ΔPR/ΔPR). Females: n= 5 (WT), 11 (ΔPR/+), 8 (ΔPR/ΔPR). **c**) Body fat and (**d**) lean mass were determined at week 11-12. Means ± SEM. Males: n=13 (WT), 10 (ΔPR/+), 11 (ΔPR/ΔPR). Females: n=11 (WT), 15 (ΔPR/+), 13 (ΔPR/ΔPR). For all comparisons: * P<0.05 and **P<0.01.

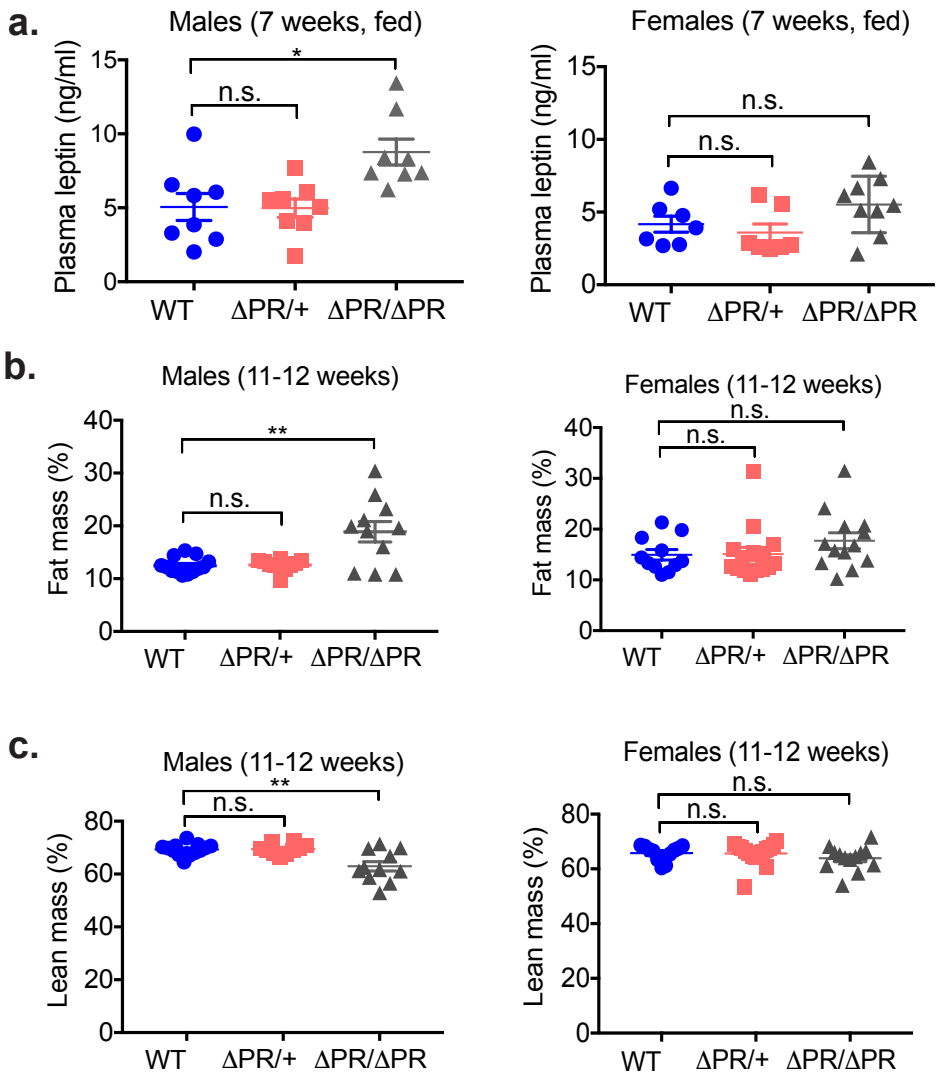

Figure 2.14 Adiposity correlates with increased leptin levels in SH2B1 ΔPR mice.

a) At week 7, serum from WT, ΔPR/+, and ΔPR/ΔPR male mice was assayed for leptin. Means ± SEM. Males: n=8 (WT, ΔPR/ΔPR), 7 (ΔPR/+). Females: n=8 (WT), 5 (ΔPR/+), 12 (ΔPR/ΔPR). **b**) Body fat and (**c**) lean mass were determined at week 11-12. Percent fat or lean mass was determined by dividing the mass by body weight. Means ± SEM. Males: n=13 (WT), 10 (ΔPR/+), 11 (ΔPR/ΔPR). Females: n=11 (WT), 15 (ΔPR/+), 13 (ΔPR/ΔPR). For all comparisons: * $P<0.05$ and ** $P<0.01$.

Table 2.3 Weight of organs from 26-27-week-old ΔPR mice.

Males	WT (n=8)	ΔPR/+ (n=15)	ΔPR/ΔPR (n=10)
brain	0.46 ± 0.01 g	0.46 ± 0.01 g	0.44 ± 0.00 g
heart	0.14 ± 0.01 g	0.15 ± 0.00 g	0.16 ± 0.01 g
liver	1.48 ± 0.05 g	1.51 ± 0.06 g	2.96 ± 0.19 g ****
perigonadal fat	1.42 ± 0.21 g	1.97 ± 0.14 g *	2.12 ± 0.13 g *
inguinal fat	0.82 ± 0.12 g	1.13 ± 0.08 g *	1.82 ± 0.09 g ****
brown fat	0.11 ± .01 g	0.15 ± .02 g	0.19 ± 0.01 g ***
Females	**WT (n=7)**	**ΔPR/+ (n=15)**	**ΔPR/ΔPR (n=11)**
brain	0.46 ± 0.01 g	0.46 ± 0.00 g	0.45 ± 0.00 g
heart	0.13 ± 0.02 g	0.13 ± 0.00 g	0.13 ± 0.01 g
liver	1.14 ± 0.06 g	1.20 ± 0.04 g	1.14 ± 0.12 g
perigonadal fat	0.52 ± 0.09 g	0.84 ± 0.16 g	1.96 ± 0.35 g **
inguinal fat	0.43 ± 0.07 g	0.60 ± 0.09 g	1.36 ± 0.25 g **
brown fat	0.08 ± 0.01 g	0.08 ± 0.01 g	0.14 ± 0.03 g

Table 2.3 Weight of organs at week 26-27 in *Sh2b1*$^{\Delta PR/+}$, *Sh2b1*$^{\Delta PR/\Delta PR}$ mice and their WT littermates fed standard chow. Means ±SEM are shown. *P< 0.05, **P<0.01, ***P<0.001 and ****P<0.0001 when compared to wild-type littermates.

Table 2.4 Weight of organs from 12-14-week-old ΔPR mice.

Males	WT (n=10)	ΔPR/+ (n=10)	ΔPR/ΔPR (n=7)
brain	0.46 ± 0.00 g	0.45 ± 0.00 g	0.45 ± 0.00 g
liver	1.22 ± 0.04 g	1.28 ± 0.08 g	1.37 ± 0.10 g
perigonadal fat	0.50 ± 0.03 g	0.54 ± 0.04 g	1.06 ± 0.18 g *
Females	**WT (n=11)**	**ΔPR/+ (n=14)**	**ΔPR/ΔPR (n=12)**
brain	0.46 ± 0.00 g	0.45 ± 0.00 g	0.45 ± 0.00 g
liver	0.97 ± 0.03 g	0.99 ± 0.05 g	1.06 ± 0.03 g *
perigonadal fat	0.19 ± 0.02 g	0.30 ± 0.07 g	0.44 ± 0.11 g *

Table 2.4 Weight of organs at week 12-14 in *Sh2b1*$^{\Delta PR/+}$, *Sh2b1*$^{\Delta PR/\Delta PR}$ mice and their WT littermates fed standard chow. Means ±SEM are shown. * $p < 0.05$ when compared to wild-type littermates.

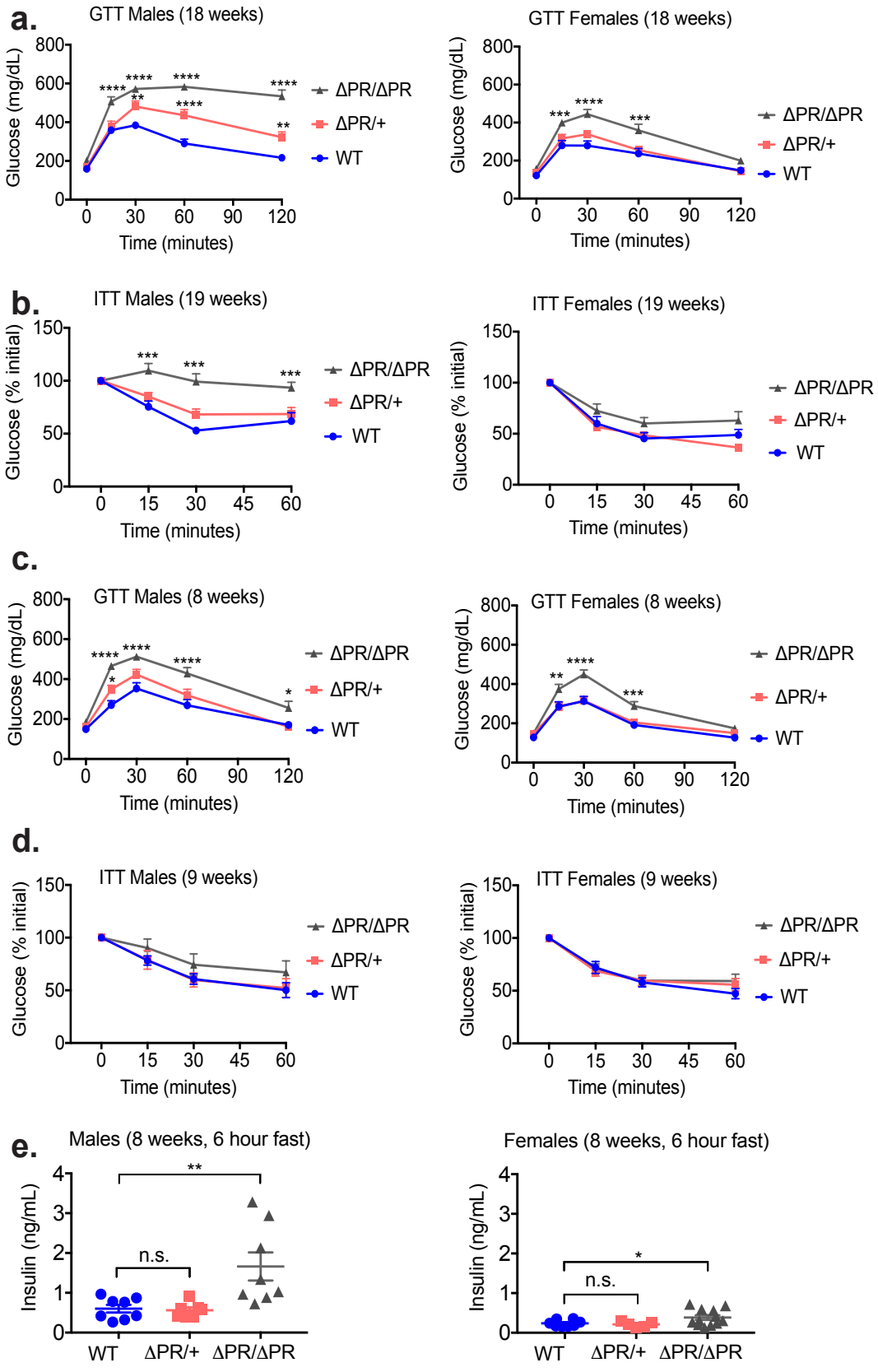
a.
GTT Males (18 weeks)
Glucose (mg/dL)
Time (minutes)
ΔPR/ΔPR
ΔPR/+
WT
GTT Females (18 weeks)
b.
ITT Males (19 weeks)
Glucose (% initial)
ITT Females (19 weeks)
c.
GTT Males (8 weeks)
GTT Females (8 weeks)
d.
ITT Males (9 weeks)
ITT Females (9 weeks)
e.
Males (8 weeks, 6 hour fast)
Insulin (ng/mL)
n.s.
Females (8 weeks, 6 hour fast)

Figure 2.15 SH2B1 ΔPR mice exhibit reduced glucose tolerance and insulin sensitivity.

a) GTT was assessed at 18 weeks. Mice were fasted for 4 hours and then injected intraperitoneally with D-glucose (2 mg/kg of body weight). Blood glucose was monitored at times indicated. Means ± SEM. Males: n= 8 (WT), 12 (ΔPR/+), 10 (ΔPR/ΔPR). Females: n=7 (WT), 14 (ΔPR/+), 10 (ΔPR/ΔPR). **b**) ITT was assessed at 19 weeks. Mice were fasted for 6 hours and then injected intraperitoneally with human insulin (1 IU/kg of body weight). Blood glucose was monitored at the times indicated. Means ± SEM. Males: n= 9 (WT), 14 (ΔPR/+), 11 (ΔPR/ΔPR). Females: n=6 (WT), 13 (ΔPR/+), 11 (ΔPR/ΔPR). **c**) In a separate study, GTT was assessed at 8 weeks. Mice were fasted for 4 hours and then injected intraperitoneally with D-glucose (2 mg/kg of body weight). Blood glucose was monitored at the times indicated. Means ± SEM. Males: n= 13 (WT), 10 (ΔPR/+), 11 (ΔPR/ΔPR). Females: n=10 (WT), 13 (ΔPR/+), 12 (ΔPR/ΔPR). **d**) 9-week-old mice were fasted for 6 hours and then injected intraperitoneally with human insulin (1 IU/kg of body weight). Blood glucose was monitored at the times indicated. Means ± SEM. Males: n=11 (WT), 9 (ΔPR/+), 10 (ΔPR/ΔPR). Females: n=9 (WT), 11 (ΔPR/+), 13 (ΔPR/ΔPR). **e**) 8-week-old mice were fasted for 6 hours and insulin levels were determined. Means ± SEM. Males: n=11 (WT), 9 (ΔPR/+), 10 (ΔPR/ΔPR). Females: n=9 (WT), 11 (ΔPR/+), 13 (ΔPR/ΔPR). For all comparisons: * $P<0.05$, ** $P<0.01$, *** $P<0.001$, **** $P<0.0001$ when compared to WT littermates.

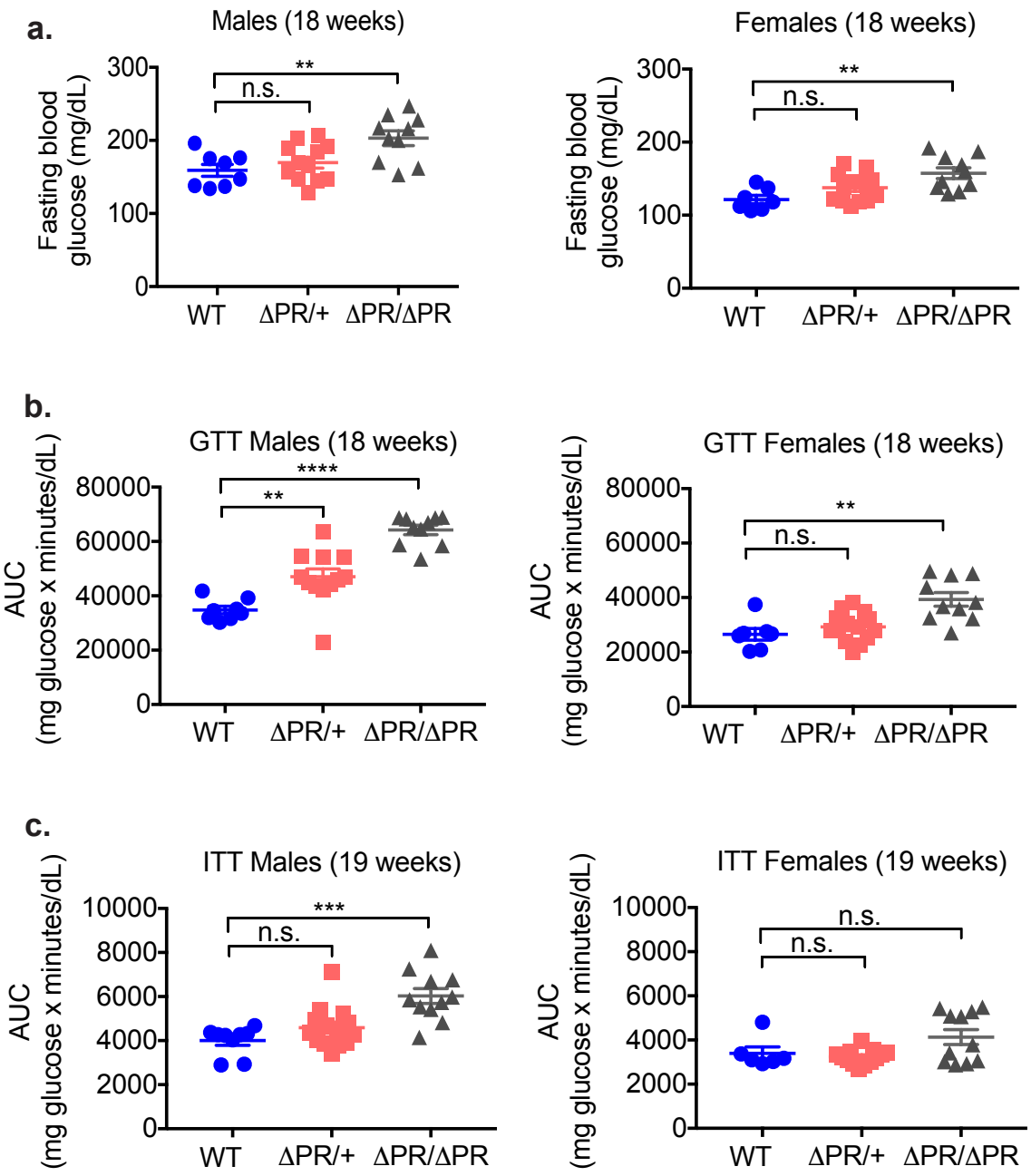
a.
Males (18 weeks)
Fasting blood glucose (mg/dL)
300
200
100
0
n.s.
**
WT
ΔPR/+
ΔPR/ΔPR
Females (18 weeks)
Fasting blood glucose (mg/dL)
300
200
100
0
n.s.
**
WT
ΔPR/+
ΔPR/ΔPR
b.
GTT Males (18 weeks)
AUC (mg glucose x minutes/dL)
80000
60000
40000
20000
0
**
****
WT
ΔPR/+
ΔPR/ΔPR
GTT Females (18 weeks)
AUC (mg glucose x minutes/dL)
80000
60000
40000
20000
0
n.s.
**
WT
ΔPR/+
ΔPR/ΔPR
c.
ITT Males (19 weeks)
AUC (mg glucose x minutes/dL)
10000
8000
6000
4000
2000
0
n.s.
***
WT
ΔPR/+
ΔPR/ΔPR
ITT Females (19 weeks)
AUC (mg glucose x minutes/dL)
10000
8000
6000
4000
2000
0
n.s.
n.s.
WT
ΔPR/+
ΔPR/ΔPR

Figure 2.16 ΔPR mice exhibit reduced glucose tolerance and insulin sensitivity.

a) At week 18, mice were fasted for 4 hours and blood glucose was measured. Means ± SEM. Males: n= 8 (WT), 12 (ΔPR/+), 10 (ΔPR/ΔPR). Females: n=7 (WT), 14 (ΔPR/+), 10 (ΔPR/ΔPR). **b**) GTT was assessed at 18 weeks. Mice were fasted for 4 hours and then injected intraperitoneally with D-glucose (2 mg/kg of body weight). Blood glucose was monitored at the times indicated (see Fig. 7a) and the area under the curve (AUC) was calculated. Means ± SEM. Males: n= 8 (WT), 12 (ΔPR/+), 10 (ΔPR/ΔPR). Females: n=7 (WT), 14 (ΔPR/+), 10 (ΔPR/ΔPR). **c**) ITT was assessed at 19 weeks. Mice were fasted for 6 hours and then injected intraperitoneally with human insulin (1 IU/kg of body weight). Blood glucose was monitored at the times indicated (see Fig. 7b) and the area under the curve (AUC) was calculated. Means ± SEM. Males: n=9 (WT), 14 (ΔPR/+), 11 (ΔPR/ΔPR). Females: n=6 (WT), 13 (ΔPR/+), 11 (ΔPR/ΔPR). For all comparisons: **P<0.01, ***P<0.001, and ****P<0.0001 when compared to WT littermates.

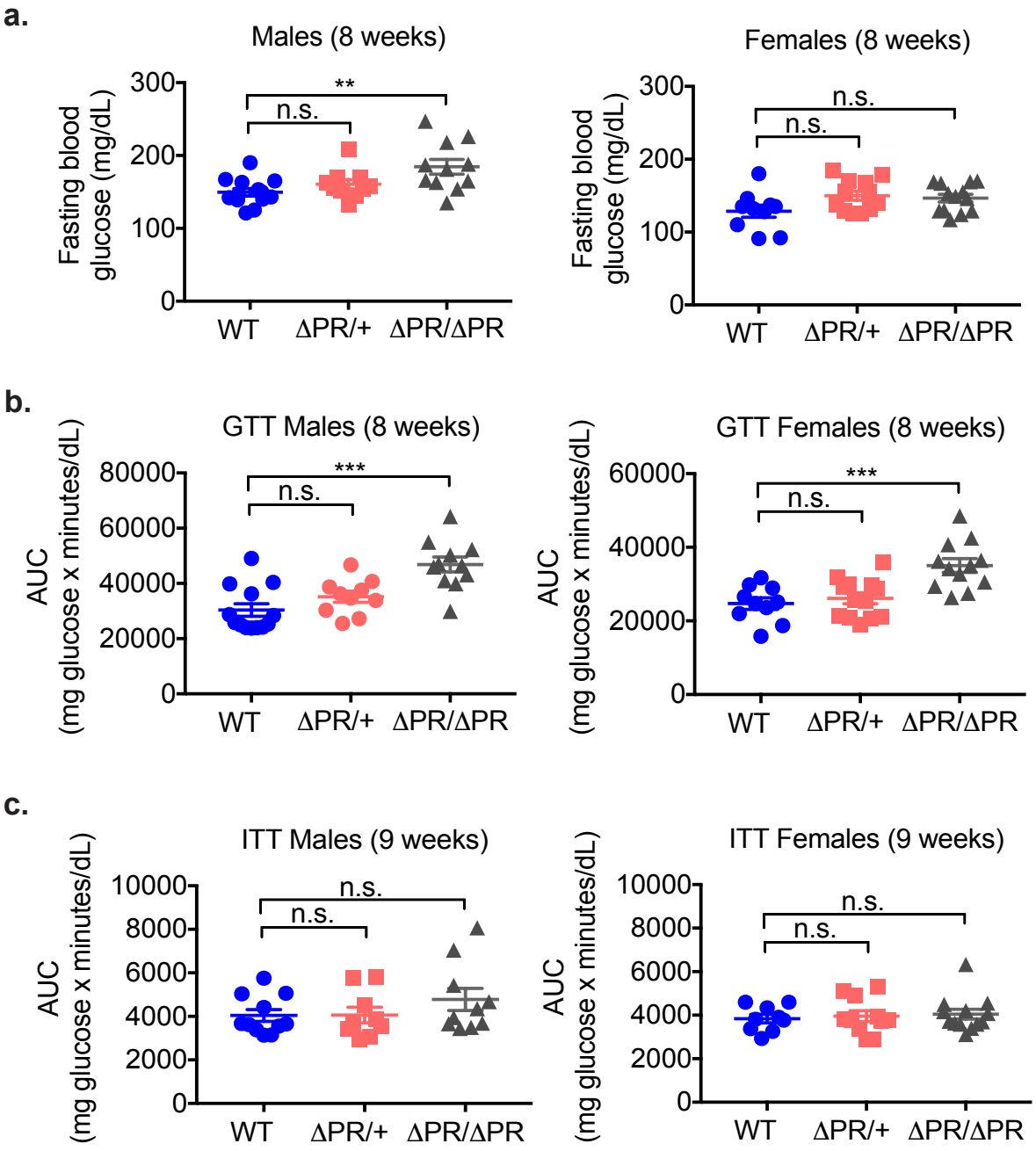
a.
Males (8 weeks)
Fasting blood glucose (mg/dL)
300
200
100
0
**
n.s.
WT
ΔPR/+
ΔPR/ΔPR
Females (8 weeks)
n.s.
n.s.
b.
GTT Males (8 weeks)
AUC (mg glucose x minutes/dL)
80000
60000
40000
20000
***
GTT Females (8 weeks)
c.
ITT Males (9 weeks)
10000
8000
6000
4000
2000
ITT Females (9 weeks)

Figure 2.17 ΔPR mice exhibit reduced glucose tolerance prior to the onset of obesity.

a) At week 18, mice were fasted for 4 hours and blood glucose was measured. Means ± SEM. Males: n=13 (WT), 10 (ΔPR/+), 11 (ΔPR/ΔPR). Females: n=10 (WT), 13 (ΔPR/+), 12 (ΔPR/ΔPR). **b**) GTT was assessed at 8 weeks. Mice were fasted for 4 hours and then injected intraperitoneally with D-glucose (2 mg/kg of body weight). Blood glucose was monitored at times indicated (see Fig. 7c) and the area under the curve (AUC) was calculated. Means ± SEM. Males: n=13 (WT), 10 (ΔPR/+), 11 (ΔPR/ΔPR). Females: n=10 (WT), 13 (ΔPR/+), 12 (ΔPR/ΔPR). **c**) ITT was assessed at 9 weeks. Mice were fasted for 6 h and then injected intraperitoneally with human insulin (1 IU/kg of body weight). Blood glucose was monitored at the times indicated (see Fig. 7d) and the area under the curve (AUC) was calculated. Means ± SEM. Males: n=11 (WT), 9 (ΔPR/+), 10 (ΔPR/ΔPR). Females: n=9 (WT), 11 (ΔPR/+), 13 (ΔPR/ΔPR). For all comparisons: **P<0.01 and ***P<0.001 when compared to WT littermates.

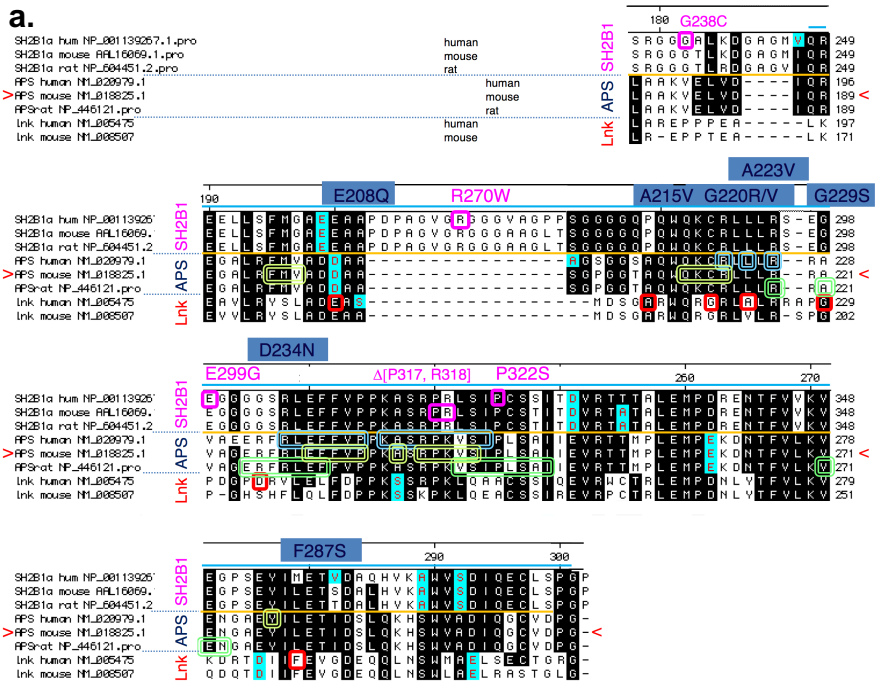
a.
G238C
E208Q
R270W
A215V G220R/V
G229S
A223V
D234N
E299G
Δ[P317, R318]
P322S
F287S
SH2B1
APS
Lnk
human
mouse
rat

b.

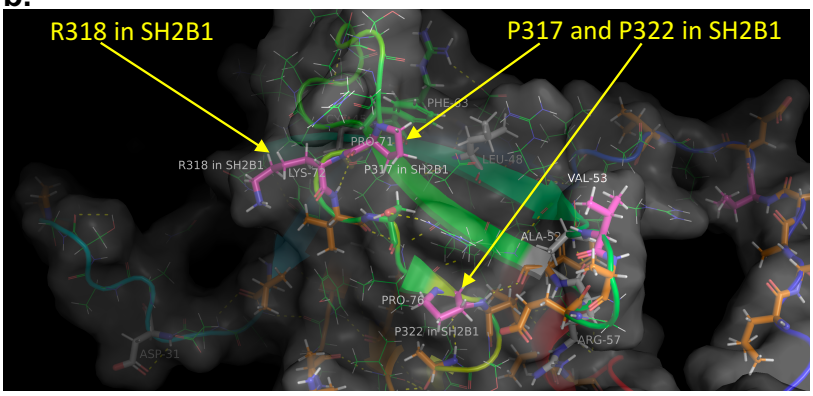
R318 in SH2B1
P317 and P322 in SH2B1
PHE-63
PRO-71
LEU-48
VAL-53
ALA-52
PRO-76
ARG-57
ASP-31

c.

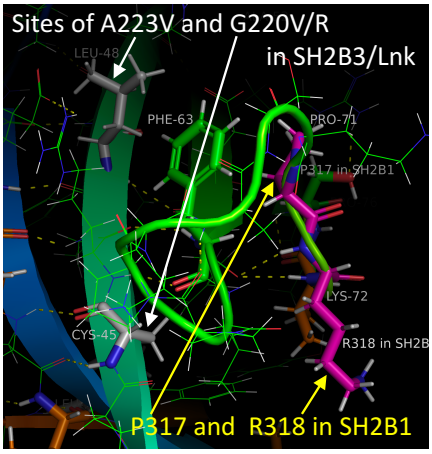
Sites of A223V and G220V/R
in SH2B3/Lnk
LEU-48
PHE-63
PRO-71
P317 in SH2B1
LYS-72
CYS-45
R318 in SH2B
P317 and R318 in SH2B1

d.

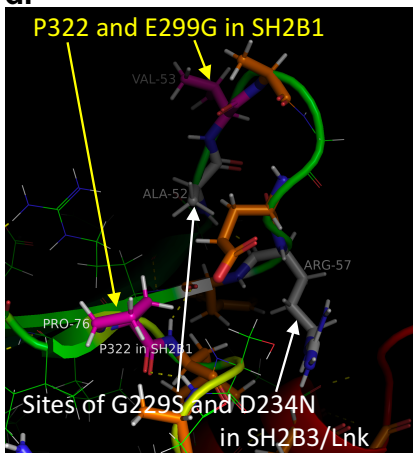
P322 and E299G in SH2B1
VAL-53
ALA-52
ARG-57
PRO-76
P322 in SH2B1
Sites of G229S and D234N
in SH2B3/Lnk

Figure 2.18 Modeling and analysis of the 3-D structure of the PH domain of SH2B1 in the region of P317, R318, and P322.

a. ClustalW of SH2B1, SH2B2/APS, and SH2B3/Lnk. The region included in the NMR structure of APS (1V5M) is shown. Homologous residues are highlighted in black, functionally homologous residues are cyan. The PH domain is indicated by the blue line above the sequences. Locations of the human mutations in SH2B1 associated with obesity and P317, R318 in SH2B1 are indicated in magenta. The mutations in Lnk associated with myeloproliferative neoplasms are indicated in blue boxes. Residues within 6Å of P71 in APS (P317 in SH2B1, P240 in SH2B3/Lnk) are denoted by a blue double rectangle. Residues within 6Å of K72 in APS (R318 in SH2B1, K241 in SH2B3/Lnk) are denoted by a light green double rectangle. Residues within 6Å of P76 (P322 in SH2B1, P245 in SH2B3/Lnk) are denoted by a green double rectangle. **b-c.** Residues in SH2B2/APS that correspond to human mutations in SH2B1 and residues P317, R318 in SH2B1 are magenta. Residues corresponding to human mutations in Lnk are grey. Residues that are homologous or functionally homologous in human SH2B1 and SH2B2/APS are denoted by green lines. The non-homologous residues are denoted by orange sticks. Oxygen atoms are red, nitrogen blue, sulfur orange, hydrogen grey. β-pleated sheets, α-helices, and connecting loops are indicated. **b.** Region in the APS structure in the vicinity of P71 and K72 (P317, R318 in SH2B1) and P76 (P322 in SH2B1). The exterior surface of the PH domain is tinted grey. **c.** Region in the APS structure in the vicinity of P71 and K72 (P317, R318 in SH2B1), F63 (F309 in SH2B1; F240 in Lnk), and C45 and L48 (sites of the human mutations G220V, G220R and A223V in Lnk). Compared to the image in b), the image in c) is rotated ~90^{o} counter-clockwise and ~90^{o} back. **d.** Region in the APS structure in the vicinity of P76 (P322 in SH2B1), R57 and A52 (sites of the human mutations D234N and G229S in Lnk), and V53 (the site of the human E299G mutation in SH2B1).

Chapter 3

Conclusions and Future Directions

The overall goal of my thesis research was to elucidate the contribution of the PH domain to SH2B1 regulation of energy balance and glucose homeostasis. One approach took advantage of the human mutations identified in patients with severe obesity, insulin resistance, and maladaptive behavior. The second approach introduced a two-amino acid deletion in the PH domain of SH2B1. Both approaches took advantage of CRISPR/Cas9 genome editing in mice to disrupt the PH domain of SH2B1, by introducing either a point mutation associated with human obesity P322S or the 2-amino acid deletion of P317 and R318 (ΔPR).

Regarding the first approach of introducing the PH domain-located P322S point mutation into SH2B1 in mice, we show that the P322S human obesity-associated mutation does not affect body weight, food intake or insulin sensitivity of heterozygote mice. Studies using a smaller cohort (3-4 animals) of homozygote mice fed a standard chow gave similar results. Although the P322S mutation in SH2B1 in mice also did not seem to affect glucose tolerance or insulin sensitivity under standard chow conditions, the P322S mutation did decrease glucose tolerance when the mice were challenged with a high fat diet. Since glucose tolerance, but not insulin tolerance, was reduced on a high fat diet, future experiments should test whether the P322S mice have impaired insulin secretion from β-cells. In order to help address this possibility, insulin concentrations should be measured during a glucose tolerance test to assess if the β-cells have the same or decreased ability to secrete insulin into the blood compared to WT mice. An additional experiment to address if P322S mice have impaired insulin secretion from β-cells is to

isolate islets from the mice and measure insulin content, insulin secretion from islets in the presence of glucose, and levels of insulin mRNA. It is also possible that the P322S mice may have reduced insulin tolerance and that the insulin tolerance test is not sensitive enough to detect this. A more sensitive test to check the insulin tolerance in the P322S mice would be the use of hyperinsulinemic-euglycemic clamps.

Our findings suggest that, in mice, the P322S mutation does not replicate the full spectrum of effects seen in humans with the SH2B1 P322S mutation. Because environmental factors such as diet, exercise and other behavioral patterns greatly increase the prevalence of obesity in a population (181), it is possible that other environmental conditions or genetic backgrounds may reveal a phenotype in mice with the SH2B1 P322S mutation that more closely resembles the obese, insulin-resistant phenotype ascribed to humans with the P322S mutation. To further investigate whether one of these alternative factors (e.g. a diet high in fructose) may work in concert with the P322S mutation to cause obesity, I challenged P322S mice with a 70% high fructose diet. The P322S mice did not exhibit obesity compared to their WT littermates (Figure 3.1), suggesting that there may be other factors contributing to the penetrance of the pathogenicity of the P322S mutation in humans. The impact of genetic background could also be tested using breeding or CRISPR/Cas9 to introduce the P322S mutation into another breed of mice or using CRISPR/Cas9 to introduce the P322S mutation into another animal species. The finding that the P322S homozygous mice are born at lower frequencies than the homozygous ΔPR mice raises the possibility that the ability of SH2B1 to enter the nucleus, as seen with the P322S mutation (92) and not with the ΔPR mutation (shown here), affects the function of SH2B1 in the implantation/development of the pups.

In contrast to the P322S mutation, the relatively small deletion in the PH domain present

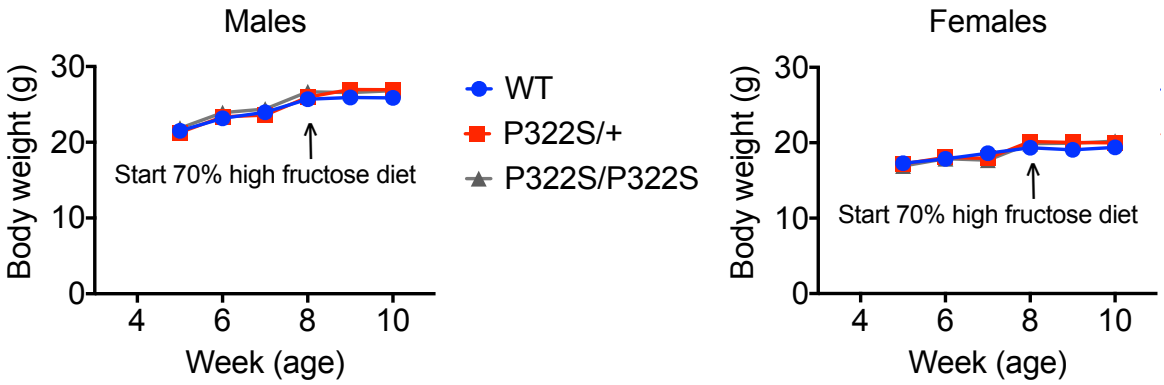

Figure 3.1 The P322S mutation does not affect body weight of mice fed a high fructose diet.

Starting at week 5, body weight was assessed weekly. Means ±SEM. Males: n=10 (WT), 16 (P322S/+), 12 (P322S/P322S). Females: n=9 (WT), 16 (P322S/+), 12 (P322S/P322S).

in ΔPR, causes a rather profound effect on both SH2B1β localization at the cellular level and energy balance and glucose homeostasis at the whole animal level. This is despite the fact it is predicted to have only a minor effect on the structure of the PH domain based on PH domain modeling using NMR structure data for the PH domain of family member SH2B2, The ΔPR mice show increased body weight, adiposity, food intake, and reduced glucose tolerance and insulin sensitivity. At the cellular level, the ΔPR mutation alters the subcellular localization of SH2B1 and impairs the ability of SH2B1 to enhance NGF-induced neurite outgrowth in PC12 cells. It is still not clear if the ΔPR deletion affects the subcellular localization of other isoforms of SH2B1. In preliminary experiments, I found that SH2B1δ ΔPR localized to nuclear bodies in PC12 cells (Figure 3.2a), in addition to localizing in the nucleus, nucleolus, and plasma membrane as is seen with SH2B1δ WT. SH2B1 enhancement of NGF-induced neuronal differentiation of PC12 cells was also impaired, as was found when the ΔPR mutation was introduced into SH2B1β (Figure 3.2b). I am in the process of testing if the ΔPR deletion also affects the subcellular localization of the α and γ isoforms of SH2B1.

The neuronal assays utilized here focused on the effect of SH2B1 on NGF signaling in PC12 cells. However, SH2B1 has also been shown to interact with the activated receptors for BDNF (TrkB) and GDNF (RET) (182), interactions that are likely to be more relevant than the SH2B1 effects on NGF signaling in regards to energy balance. Investigating the effect of the PH domain mutations of SH2B1 in BDNF signaling is particularly relevant for these studies because genetic variations that cause reduced BDNF or TrkB expression or activity lead to hyperphagia and obesity in humans and mice (110). A role for SH2B1 in neuronal development, architecture and/or neuronal signaling using BDNF and GDNF in cortical and hippocampal neurons or PC12 cells has been shown (20,12). Assessing the effect of the SH2B1 mutations on these neuronal

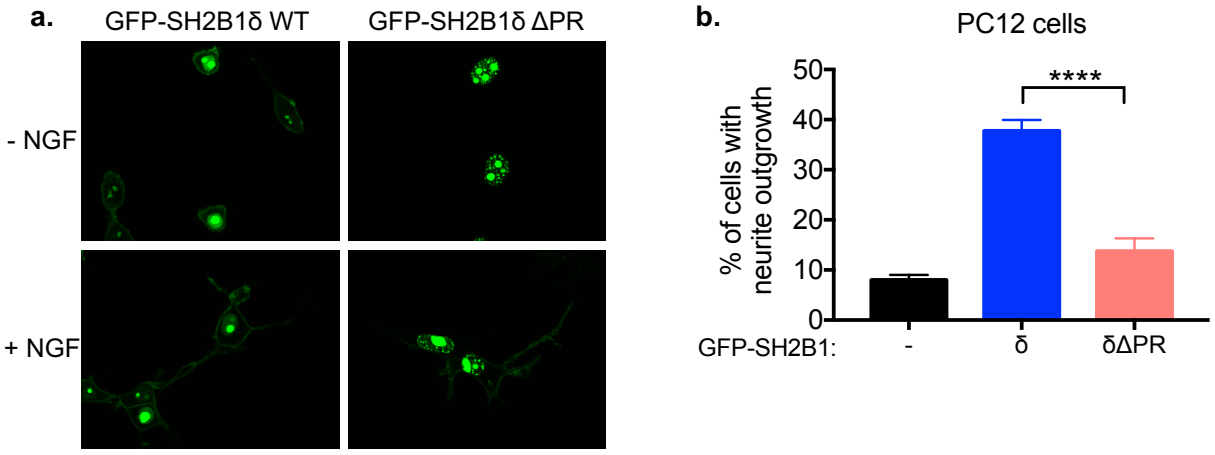

Figure 3.2 Disruption of the PH domain changes the subcellular localization of SH2B1δ and impairs the ability of SH2B1δ to enhance NGF-induced neurite outgrowth.

a) PC12 cells transiently expressing the indicated GFP-SH2B1δ WT or GFP-SH2B1δΔPR were imaged by confocal microscopy. **b**) Live PC12 cells transiently expressing GFP-SH2B1δ WT or GFP-SH2B1δΔPR were treated with 25 ng/ml mouse NGF for 2 days after which neurite outgrowth was assessed. GFP-positive cells were scored for the presence of neurites 2 times the length of the cell body (total of 300 cells per condition per experiment). The percentage of cells with neurites was determined by dividing the number of GFP-positive cells with neurites by the total number of GFP-positive cells. Means ± SEM, ****P<0.0001, n=3.

functions would broaden the scope of my work and give insight into whether the PH domain is important for neuronal function for other neurotrophic factors.

I have not yet been able to identify a mechanism by which the ΔPR mutation in the PH domain of SH2B1 impairs the ability of SH2B1β or SH2B1δ to enhance neuronal differentiation. To continue to gain understanding of how the ΔPR deletion affects the function of SH2B1, future experiments in this project should focus on the following: 1) identifying binding partners of SH2B1, 2) determining the role of SH2B1 in gene expression, 3) determining if the ΔPR deletion affects neuronal projections that regulate energy balance, and 4) determining the effect of the ΔPR deletion on SH2B1 function in other tissues involved in energy balance and glucose homeostasis (liver, β-cells, fat). I have discussed these experiments in more detail in the following paragraphs.

Identifying binding partners of SH2B1 in the nucleus

Identifying binding partners of SH2B1β or SH2B1δ in the nucleus and how the ΔPR mutation affects the ability of SH2B1β and SH2B1δ to enhance neuronal differentiation should further elucidate the role of SH2B1 in neuronal development. There are a number of proteins in the nucleus that regulate neurogenesis that may be affected by the PH domain mutations in SH2B1 (183). Phosphorylation of cellular proteins in response to NGF or BDNF in cells expressing WT or ΔPR mutant SH2B1β/δ should be investigated. A global, non-biased phosphoproteomics approach can be used to identify cellular proteins whose phosphorylation is differentially altered by SH2B1 WT vs the SH2B1β or δ ΔPR mutants. Phosphoproteomics might be particularly effective in identifying phosphoproteins whose phosphorylation is differentially regulated by SH2B1 β/δ WT vs ΔPR, particularly if the ΔPR mutation has modest effects on signaling pathways that are amplified in more downstream targets. Use of iTRAQ-

based mass spectrometry will enable us to simultaneously analyze the results from different treatment groups, improving the ability to compare the phosphorylation sites identified. Priority should be given to proteins that are signaling proteins, proteins that regulate neurite outgrowth or other aspects of neuronal function, cytoskeletal proteins or proteins known to regulate cytoskeletal proteins (e.g. kinases, phosphatases) expected to affect neurite outgrowth, and nuclear proteins of potential relevance to the human disease phenotype. I would expect that phosphorylation of one or more of these proteins essential for neuronal differentiation would be altered in cells expressing mutant SH2B1β ΔPR or SH2B1δ ΔPR compared to WT SH2B1β or δ respectively.

Determining the role of SH2B1 in gene expression

Another way to gain insight into how the ΔPR PH domain mutation affects the cellular function of SH2B1β would be to investigate gene expression. A critical function of neurotrophic ligands is to initiate a highly-orchestrated response that alters the gene expression profile of neuronal precursors to promote differentiation into a mature neuron and formation of proper neuronal circuitry. SH2B1β greatly enhances expression of a subset of NGF-regulated genes in PC12 cells (29). Maximal stimulation appears to require nuclear cycling of SH2B1 (27,25) and is reduced by the P322S mutation for the two genes tested, *Plaur* and *Mmp3* (Cline et al., personal communication). However, exactly how SH2B1 regulates gene expression and how the pathogenic mutations in SH2B1 impair that regulation are not known. It would be interesting to test if the ΔPR mutation reduces the expression of NGF-regulated genes in PC12 cells. I would expect the ΔPR mutation to reduce the expression of NGF-regulated genes involved in neuronal differentiation and survival in PC12 cells. To test this, I would propose to make PC12 cells stably expressing GFP, GFP-SH2B1β WT or GFP-SH2B1β ΔPR, treat the cells with or without

NGF, perform RNA seq and look for NGF- and SH2B1β-sensitive genes expressed differentially in ΔPR vs WT cells.

I would next determine whether the PH domain mutations similarly affect expression of genes regulated by other neurotrophic ligands implicated in feeding behavior (e.g. BDNF) in the context of primary neurons. It could be particularly informative to determine the impact of the ΔPR mutation and other human obesity mutations on SH2B1 function in the context of BDNF. SH2B1 has been shown to interact with the BDNF receptor, TrkB, and to enhance the number of BDNF-induced neurite outgrowths in PC12 cells stably expressing TrkB and SH2B1β (7,182). More recently, overexpression of SH2B1β was shown to promote neurite outgrowth and branching in cultured hippocampal neurons supplemented with BDNF (20). Additionally, it would be interesting to study the roles of the other isoforms (α, γ, and δ) of SH2B1in BDNF signaling and the effect of any of the human obesity-associated mutations on BDNF function. I expect the human obesity mutations to have a bigger impact on SH2B1 regulation of BDNF than NGF signaling since BDNF is known to mediate signaling involved in the regulation of energy balance. Studying the effects of the different isoforms and the human mutations on BDNF signaling should provide critical insight into SH2B1 regulation of neuronal function critical for energy balance.

Neuronal projections

Most experiments to elucidate the specific cellular functions of SH2B1 and to understand how the cellular functions are affected by human mutations in SH2B1 have used *in vitro* model systems. I showed that the ΔPR mutation impairs the ability of SH2B1 to enhance NGF-induced neurite outgrowth of cultured PC12 cells. However, it has not been determined whether SH2B1 affects the ability to promote axonal projections and synapses in neurons implicated in energy

balance in the hypothalamus. Based on previous lab findings implicating SH2B1 in neurite outgrowth, I predict that SH2B1 affects the neuronal projections from, or the number of neurons in, brain circuits that are involved in energy balance. The next experiment to carry out would be to define the role for SH2B1 in the control of circuit formation in neurons involved in energy balance.

In the hypothalamus, leptin activates LepRb on the surface of specialized neurons to control food intake and neuroendocrine processes that modulate energy expenditure. The crucial role of leptin in the control of energy balance is underscored by the severe obesity in human patients and animal models with mutations in leptin or LepRb (184). Lifelong energy balance depends on the proper developmental formation of axonal projections from the LepRb-expressing POMC and AgRP neurons in the arcuate nucleus to their crucial targets in the paraventricular hypothalamic nucleus (94). Disruption of *Sh2b1* in LepRb neurons in mice promotes obesity and metabolic dysfunction, suggesting that SH2B1 signaling in LepRb neurons is crucial for the control of energy balance and metabolism (personal communication from L. Rui). I expect SH2B1 to play a role in the projection of leptin receptor-expressing neurons in the arcuate nucleus to the paraventricular hypothalamic nucleus based on previous findings that SH2B1 enhances neurite outgrowth in multiple types of neurons (185). Next, the impact of SH2B1 and the ΔPR PH domain deletion on the formation of POMC and AgRP circuits in the hypothalamus should be determined. Brain sections from these mice could be used for immunohistochemical analysis and fiber density can be determined. I expect that the density of the AgRP and/or POMC projections to the PVH will be impaired.

BDNF has been shown to play a critical role in directing projections from TrkB expressing neurons in the arcuate nucleus to the paraventricular hypothalamic nucleus (186) and

SH2B1β enhances BDNF-dependent neurite outgrowth in PC12 cells (20). Based on these findings, I hypothesize that SH2B1 in TrkB neurons is also crucial for establishing these circuits between the arcuate nucleus and paraventricular hypothalamic nucleus, and that this process may be dysregulated by the ΔPR and/or human mutations in SH2B1. To test this, I would generate 3 sets of mice to look at the effect of SH2B1 on projections of TrkB neurons: WT, ΔPR and KO mice expressing tamoxifen-inducible mNeonGreen in TrkB neurons. I expect that the density of the AgRP and/or POMC projections to the PVH (or a subset) will be impaired in the *Sh2b1 ΔPR* and *Sh2b1 KO* mice compared to the *Sh2b1 WT* mice. It would also be interesting to examine whether the lack of SH2B1 in non-AgRP and non-POMC neurons impairs the projections of other TrkB neurons in the arcuate nucleus to other regions of the brain implicated in energy balance.

Effect of ΔPR deletion in other tissues involved in energy balance and glucose homeostasis

Here, I show that in addition to becoming obese, the *Sh2b1 ΔPR* mice develop hyperglycemia, hyperinsulinemia, reduced glucose tolerance, and insulin resistance, a metabolic phenotype similar to that of the *Sh2b1 KO* mice. Whether the phenotype seen in the *Sh2b1 KO* mice is due to developmental abnormalities still remains to be determined. The Cre-lox system can be used to generate *Sh2b1* conditional *KO* mice to delete SH2B1 in adulthood to determine if the phenotype is developmental, adult onset, or both. Furthermore, Cre-lox mice can also be used to delete SH2B1 in specific cell types in adulthood and determine the contribution of SH2B1 in these specific cells to the phenotype seen in the *Sh2b1 KO* mice. Neuron-specific restoration of SH2B1β via the neuron-specific enolase promoter largely rescues the impaired glucose homeostasis seen in the SH2B1 KO mice (56). However, SH2B1 also binds via its SH2 domain directly to the activation loop of the insulin receptor (9,44,10) and deletion of SH2B1 inhibits

activation of the insulin receptor in liver, β-cells, and fat, including insulin-dependent tyrosine phosphorylation of IRS1 and IRS2 and activation of the PI3K/Akt and Erk1/2 pathways (41). These findings indicate that while neuronal SH2B1 is required for maintaining normal glucose homeostasis *in vivo*, peripheral SH2B1 may also be contributing to glucose homeostasis, at least in part, by enhancing IR activation and signaling in the liver, muscle, and/or fat. The mechanism by which the ΔPR or the P322S mutations in the PH domain of SH2B1 affect glucose homeostasis has not been extensively investigated. Whether the ΔPR deletion affects the activation of the insulin receptor and downstream targets should be tested in different tissues involved in glucose homeostasis (e.g. liver, β-cells).

Glucose homeostasis may be dysregulated in one or more of these tissues in *Sh2b1 ΔPR* mice. In support of this, the ΔPR mice on standard chow exhibit increased liver weight and pale livers consistent with lipid accumulation. Increased lipid accumulation may be a factor contributing to impaired glucose metabolism, since high lipids have been shown to contribute to insulin resistance (187). To confirm that the increased liver weights in the ΔPR mice are due to increased lipid accumulation, H & E staining should be done. Triglyceride levels in the liver should also be measured. I expect SH2B1 activation of the insulin receptor to be impaired and that the livers from *Sh2b1 ΔPR* mice will show increased lipid accumulation.

Several lines of evidence demonstrate that SH2B1 in β-cells is a novel pro-survival and pro-proliferative signaling molecule that directly promotes activation of the PI3K/Akt pathway *in vitro* and *in vivo* (142). Furthermore, SH2B1 has been proposed to sustain the ability of IRS proteins to activate the PI3K pathway by protecting IRS proteins from tyrosine dephosphorylation (48). Additionally, SH2B1 cell-autonomously promotes insulin expression by enhancing JAK2 activation and the ability of JAK2 to stimulate insulin promoter activity in β-

cells (141). As a key experiment, the survival, proliferation, and insulin secretion in β-cells of the *Sh2b1 ΔPR* and *P322S* mice should be determined. Based on the published data of the role of SH2B1 in β-cells, I would expect the P322S and ΔPR mutations to impair the function of SH2B1 in β-cells.

Modeling of the PH domain of SH2B1

We analyzed the SH2B1 PH domain in the context of the NMR structure of the PH domain of the SH2B family member SH2B2/APS (179) to gain insight into potential alterations mediated by the mutants that we studied (Figure 8). In the SH2B2/APS structure, the residues corresponding to P317, R318, and P322S in SH2B1 (P71, K72 and P76, respectively) lie on an exterior surface of the PH domain (Figure 2.18) that represents a likely binding interface (e.g., for a different region of SH2B1 or another protein). Because the residues corresponding to P317 and R318 in SH2B1 are on the surface of the PH domain and do not substantially change the direction of the loop, the P317, R318 deletion in SH2B1 is not expected to severely damage the structure, although the deletion would be expected to substantially alter the shape of the interface surface. The P317, R318 deletion is also predicted to possibly affect the ability of nearby S320 to be phosphorylated. I am now trying to determine whether a change in the ability of S320 to be phosphorylated is contributing to the cellular and physiological phenotype seen with the ΔP317, R318 deletion. In preliminary studies, mutating S320 to an alanine, thereby preventing phosphorylation at this position, did not alter the subcellular localization of SH2B1β or SH2B1β ΔPR nor did it affect the ability of SH2B1β or SH2B1β ΔPR to promote NGF-induced neurite outgrowth. I am confirming these results and testing whether mutating S320 to the phosphomimetic E320 alters either the subcellular localization of SH2B1β or SH2B1β ΔPR or their ability to promote neurite outgrowth.

In summary, carrying out these experiments will provide important insight into how the different SH2B1 isoforms act to regulate growth factor signaling, gene expression, neuronal circuits and peripheral tissues involved in energy balance and glucose metabolism and how they are affected by the P322S mutation and ΔPR disruption in the PH domain of SH2B1. Further understanding of the mechanism of action of SH2B1 may provide basis for therapeutic intervention to treat obesity and/or insulin resistance in humans.

Bibliography

1. Good MC, Zalatan JG, Lim WA. 2011 Scaffold proteins: hubs for controlling the flow of cellular information. *Science*. 332(6030):680-686.
2. Kuriyan J, Cowburn D. 1997 Modular peptide recognition domains in eukaryotic signaling. *Ann Rev Biophys Biomol Struct*. 26:259-288.
3. Huang X, Li Y, Tanaka K, Moore KG, Hayashi JI. 1995 Cloning and characterization of Lnk, a signal transduction protein that links T-cell receptor activation signal to phospholipase C g 1, Grb2, and phosphatidylinositol 3-kinase. *Proc Nat Acad Sci USA*. 92(25):11618-11622.
4. Osborne MA, Dalton S, Kochan JP. 1995 The Yeast Tribrid System - Genetic Detection of *trans*-phosphorylated ITAM-SH2-Interactions. *BioTechnology*. 13:1474-1478.
5. Yokouchi M, Suzuki R, Masuhara M, Komiya S, Inoue A, Yoshimura A. 1997 Cloning and characterization of APS, an adaptor molecule containing PH and SH2 domains that is tyrosine phosphorylated upon B-cell receptor stimulation. *Oncogene*. 15(1):7-15.
6. Yousaf N, Deng Y, Kang Y, Riedel H. 2001 Four PSM/SH2-B alternative splice variants and their differential roles in mitogenesis. *J Biol Chem*. 276(44):40940-40948.
7. Qian X, Riccio A, Zhang Y, Ginty DD. 1998 Identification and characterization of novel substrates of Trk receptors in developing neurons. *Neuron*. 21(5):1017-1029.
8. Rui L, Herrington J, Carter-Su C. 1999 SH2-B is required for nerve growth factor-induced neuronal differentiation. *J Biol Chem*. 274(15):10590-10594.
9. Kotani K, Wilden P, Pillay TS. 1998 SH2-Bα is an insulin-receptor adapter protein and substrate that interacts with the activation loop of the insulin-receptor kinase. *Biochem J*. 335(Pt 1):103-109.
10. Riedel H, Wang J, Hansen H, Yousaf N. 1997 PSM, an insulin-dependent, pro-rich, PH, SH2 domain containing partner of the insulin receptor. *J Biochem*. 122(6):1105-1113.
11. Wang J, Riedel H. 1998 Insulin-like growth factor-I receptor and insulin receptor association with a Src homology-2 domain-containing putative adapter. *J Biol Chem*. 273(6):3136-3139.
12. Zhang Y, Zhu W, Wang YG, Liu XJ, Jiao L, Liu X, Zhang ZH, Lu CL, He C. 2006 Interaction of SH2-Bβ with RET is involved in signaling of GDNF-induced neurite outgrowth. *J Cell Sci*. 119(Pt 8):1666-1676.
13. Rui L, Carter-Su C. 1998 Platelet-derived growth factor (PDGF) stimulates the association of SH2-Bβ with PDGF receptor and phosphorylation of SH2-Bβ. *J Biol Chem*. 273(33):21239-21245.
14. Kong M, Wang CS, Donoghue DJ. 2002 Interaction of fibroblast growth factor receptor 3 and the adapter protein SH2-B. *J Biol Chem*. 277(18):15962-15970.
15. Nishi M, Werner ED, Oh BC, Frantz JD, Dhe-Paganon S, Hansen L, Lee J, Shoelson SE. 2005 Kinase activation through dimerization by human SH2-B. *Mol Cell Biol*. 25(7):2607-2621.

16. O'Brien KB, O'Shea JJ, Carter-Su C. 2002 SH2-B family members differentially regulate JAK family tyrosine kinases. *J Biol Chem*. 277(10):8673-8681.
17. Rui L, Carter-Su C. 1999 Identification of SH2-Bβ as a potent cytoplasmic activator of the tyrosine kinase Janus kinase 2. *Proc Nat Acad Sci USA*. 96(13):7172-7177.
18. Rui L, Mathews LS, Hotta K, Gustafson TA, Carter-Su C. 1997 Identification of SH2-Bβ as a substrate of the tyrosine kinase JAK2 involved in growth hormone signaling. *Mol Cell Biol*. 17(11):6633-6644.
19. Joe RM, Flores A, Doche ME, Cline JM, Clutter ES, Vander PB, Riedel H, Argetsinger LS, Carter-Su C. 2017 Phosphorylation of the Unique C-terminal Tail of the Alpha Isoform of the Scaffold Protein SH2B1 Controls the Ability of SH2B1alpha to Enhance Nerve Growth Factor Function. *Mol Cell Biol*.
20. Shih CH, Chen CJ, Chen L. 2013 New function of the adaptor protein SH2B1 in brain-derived neurotrophic factor-induced neurite outgrowth. *PloS one*. 8(11):e79619.
21. Jing S, Tapley P, Barbacid M. 1992 Nerve growth factor mediates signal transduction through trk homodimer receptors. *Neuron*. 9(6):1067-1079.
22. Stephens RM, Loeb DM, Copeland TD, Pawson T, Greene LA, Kaplan DR. 1994 Trk receptors use redundant signal transduction pathways involving SHC and PLC-γ 1 to mediate NGF responses. *Neuron*. 12(3):691-705.
23. Vetter ML, Martin-Zanca D, Parada LF, Bishop JM, Kaplan DR. 1991 Nerve growth factor rapidly stimulates tyrosine phosphorylation of phospholipase C-gamma 1 by a kinase activity associated with the product of the trk protooncogene. *Proc Nat Acad Sci USA*. 88(13):5650-5654.
24. Obermeier A, Bradshaw RA, Seedorf K, Choidas A, Schlessinger J, Ullrich A. 1994 Neuronal differentiation signals are controlled by nerve growth factor receptor/Trk binding sites for SHC and PLC gamma. *EMBO J*. 13(7):1585-1590.
25. Maures TJ, Chen L, Carter-Su C. 2009 Nucleocytoplasmic shuttling of the adapter protein SH2B1β (SH2-Bβ) is required for nerve growth factor (NGF)-dependent neurite outgrowth and enhancement of expression of a subset of NGF-responsive genes. *Mol Endocrinol*. 23:1077-1091.
26. Pearce LR, Joe R, Doche MD, Su HW, Keogh JM, Henning E, Argetsinger LS, Bochukova EG, Cline JM, Garg S, Saeed S, Shoelson S, O'Rahilly S, Barroso I, Rui L, Farooqi IS, Carter-Su C. 2014 Functional characterisation of obesity-associated variants involving the alpha and beta isoforms of human SH2B1. *Endocrinology*. 9(Sept;155):3219-3226.
27. Chen L, Carter-Su C. 2004 Adapter protein SH2-Bβ undergoes nucleocytoplasmic shuttling: implications for nerve growth factor induction of neuronal differentiation. *Mol Cell Biol*. 24(9):3633-3647.
28. Maures TJ, Su H-W, Argetsinger LS, Grinstein S, Carter-Su C. 2011 Phosphorylation controls a dual function polybasic NLS in the adapter protein SH2B1β to regulate its cellular function and distribution between the plasma membrane, cytoplasm and nucleus. *J Cell Sci*. 124(Pt9):1542-1552.
29. Chen L, Maures TJ, Jin H, Huo JS, Rabbani SA, Schwartz J, Carter-Su C. 2008 SH2B1β (SH2-Bβ) enhances expression of a subset of nerve growth factor-regulated genes important for neuronal differentiation including genes encoding uPAR and MMP3/10. *Mol Endocrinol*. 22(2):454-476.

30. Farias-Eisner R, Vician L, Reddy S, Basconcillo R, Rabbani SA, Wu YY, Bradshaw RA, Herschman HR. 2001 Expression of the urokinase plasminogen activator receptor is transiently required during "priming" of PC12 cells in nerve growth factor-directed cellular differentiation. *J Neurosci Res*. 63(4):341-346.
31. Farias-Eisner R, Vician L, Silver A, Reddy S, Rabbani SA, Herschman HR. 2000 The urokinase plasminogen activator receptor (UPAR) is preferentially induced by nerve growth factor in PC12 pheochromocytoma cells and is required for NGF-driven differentiation. *J Neurosci*. 20(1):230-239.
32. Nordstrom LA, Lochner J, Yeung W, Ciment G. 1995 The metalloproteinase stromelysin-1 (transin) mediates PC12 cell growth cone invasiveness through basal laminae. *Mol Cell Neurosci*. 6(1):56-68.
33. Sternlicht MD, Werb Z. 2001 How matrix metalloproteinases regulate cell behavior. *Ann Rev Cell Dev Biol*. 17:463-516.
34. Basbaum CB, Werb Z. 1996 Focalized proteolysis: spatial and temporal regulation of extracellular matrix degradation at the cell surface. *Curr Opin Cell Biol*. 8(5):731-738.
35. Vician L, Basconcillo R, Herschman HR. 1997 Identification of genes preferentially induced by nerve growth factor versus epidermal growth factor in PC12 pheochromocytoma cells by means of representational difference analysis. *J Neurosci Res*. 50(1):32-43.
36. Kurzer JH, Argetsinger LS, Zhou Y-J, Kouadio J-L, O'Shea JJ, Carter-Su C. 2004 Tyrosine 813 is a site of JAK2 autophosphorylation critical for activation of JAK2 by SH2-Bβ. *Mol Cell Biol*. 24(10):4557-4570.
37. Maures TJ, Kurzer JH, Carter-Su C. 2007 SH2B1 (SH2-B) and JAK2: a multifunctional adaptor protein and kinase made for each other. *Trends Endocrinol Metab*. 18(1):38-45.
38. O'Brien KB, Argetsinger LS, Diakonova M, Carter-Su C. 2003 YXXL motifs in SH2-Bb are phosphorylated by JAK2, JAK1, and platelet-derived growth factor receptor and are required for membrane ruffling. *J Biol Chem*. 278(14):11970-11978.
39. Carvalheira JB, Ribeiro EB, Folli F, Velloso LA, Saad MJ. 2003 Interaction between leptin and insulin signaling pathways differentially affects JAK-STAT and PI 3-kinase-mediated signaling in rat liver. *Biol Chem*. 384(1):151-159.
40. Clement K, Vaisse C, Lahlou N, Cabrol S, Pelloux V, Cassuto D, Gourmelen M, Dina C, Chambaz J, Lacorte JM, Basdevant A, Bougneres P, Lebouc Y, Froguel P, Guy-Grand B. 1998 A mutation in the human leptin receptor gene causes obesity and pituitary dysfunction. *Nature*. 392(6674):398-401.
41. Duan C, Li M, Rui L. 2004 SH2-B promotes insulin receptor substrate 1 (IRS1)- and IRS2-mediated activation of the phosphatidylinositol 3-kinase pathway in response to leptin. *J Biol Chem*. 279(42):43684-43691.
42. Bates SH, Stearns WH, Dundon TA, Schubert M, Tso AW, Wang Y, Banks AS, Lavery HJ, Haq AK, Maratos-Flier E, Neel BG, Schwartz MW, Myers Jr. MG. 2003 STAT3 signalling is required for leptin regulation of energy balance but not reproduction. *Nature*. 421(6925):856-859.
43. Hu J, Hubbard SR. 2006 Structural basis for phosphotyrosine recognition by the Src homology-2 domains of the adapter proteins SH2-B and APS. *J Mol Biol*. 361(1):69-79.
44. Nelms K, O'Neill TJ, Li S, Hubbard SR, Gustafson TA, Paul WE. 1999 Alternative splicing, gene localization, and binding of SH2-B to the insulin receptor kinase domain. *Mammalian Genome*. 10(12):1160-1167.

45. Riedel H, Yousaf N, Zhao Y, Dai H, Deng Y, Wang J. 2000 PSM, a mediator of PDGF-BB-, IGF-I-, and insulin-stimulated mitogenesis. *Oncogene*. 19(1):39-50.
46. Zhang M, Deng Y, Tandon R, Bai C, Riedel H. 2008 Essential role of PSM/SH2-B variants in insulin receptor catalytic activation and the resulting cellular responses. *J Cell Biochem*. 103(1):162-181.
47. Ahmed Z, Pillay TS. 2003 Adapter protein with a pleckstrin homology (PH) and an Src homology 2 (SH2) domain (APS) and SH2-B enhance insulin-receptor autophosphorylation, extracellular-signal-regulated kinase and phosphoinositide 3-kinase-dependent signalling. *Biochem J*. 371(Pt 2):405-412.
48. Morris DL, Cho KW, Zhou Y, Rui L. 2009 SH2B1 enhances insulin sensitivity by both stimulating the insulin receptor and inhibiting tyrosine dephosphorylation of insulin receptor substrate proteins. *Diabetes*. 58(9):2039-2047.
49. Ohtsuka S, Takaki S, Iseki M, Miyoshi K, Nakagata N, Kataoka Y, Yoshida N, Takatsu K, Yoshimura A. 2002 SH2-B is required for both male and female reproduction. *Mol Cell Biol*. 22(9):3066-3077.
50. Pelicci G, Lanfrancone L, Grignani F, McGlade J, Cavallo FF, G., Nicoletti I, Grignani F, Pawson T, Pelicci PG. 1992 A novel transforming protein (SHC) with an SH2 domain is implicated in mitogeic signal transduction. *Cell*. 70(1):93-104.
51. Smith TR, Elmendorf JS, David TS, Turinsky J. 1997 Growth hormone-induced insulin resistance: role of the insulin receptor, IRS-1, GLUT-1, and GLUT-4. *Am J Physiol*. 272(6 Pt 1):E1071-E1079.
52. Sun X-J, Wang L-M, Zhang Y, Yenush L, Myers Jr. MG, Giasheen E, Lane WS, Pierce JH, White MF. 1995 Role of IRS-2 in insulin and cytokine signalling. *Nature*. 377:173-177.
53. Sun XJ, Rothenberg P, Kahn CR, Backer JM, Araki E, Wilden PA, Cahill DA, Goldstein BJ, White MF. 1991 Structure of the insulin receptor substrate IRS-1 defines a unique signal transduction protein. *Nature*. 352:73-77.
54. Duan C, Yang H, White MF, Rui L. 2004 Disruption of SH2-B causes age-dependent insulin resistance and glucose intolerance. *Mol Cell Biol*. 24(17):7435-7443.
55. Minami A, Iseki M, Kishi K, Wang M, Ogura M, Furukawa N, Hayashi S, Yamada M, Obata T, Takeshita Y, Nakaya Y, Bando Y, Izumi K, Moodie SA, Kajiura F, Matsumoto M, Takatsu K, Takaki S, Ebina Y. 2003 Increased insulin sensitivity and hypoinsulinemia in APS knockout mice. *Diabetes*. 52(11):2657-2665.
56. Ren D, Li M, Duan C, Rui L. 2005 Identification of SH2-B as a key regulator of leptin sensitivity, energy balance and body weight in mice. *Cell Metab*. 2:95-104.
57. Takaki S, Morita H, Tezuka Y, Takatsu K. 2002 Enhanced hematopoiesis by hematopoietic progenitor cells lacking intracellular adaptor protein, Lnk. *J Exp Med*. 195(2):151-160.
58. Wang TC, Chiu H, Chang YJ, Hsu TY, Chiu IM, Chen L. 2011 The adaptor protein SH2B3 (Lnk) negatively regulates neurite outgrowth of PC12 cells and cortical neurons. *PloS one*. 6(10):e26433.
59. Rui L, Gunter DR, Herrington J, Carter-Su C. 2000 Differential binding to and regulation of JAK2 by the SH2 domain and N-terminal region of SH2-Bβ. *Mol Cell Biol*. 20(9):3168-3177.

60. Kurzer JH, Saharinen P, Silvennoinen O, Carter-Su C. 2006 Binding of SH2-B family members within a potential negative regulatory region maintains JAK2 in an active state. *Mol Cell Biol*. 26(17):6381-6394.
61. Li M, Ren D, Iseki M, Takaki S, Rui L. 2006 Differential role of SH2-B and APS in regulating energy and glucose homeostasis. *Endocrinology*. 147(5):2163-2170.
62. Hu J, Liu J, Ghirlando R, Saltiel AR, Hubbard SR. 2003 Structural basis for recruitment of the adapter protein APS to the activated insulin receptor. *Mol Cell*. 12(6):1379-1389.
63. Liu J, Kimura A, Baumann CA, Saltiel AR. 2002 APS facilitates c-Cbl tyrosine phosphorylation and GLUT4 translocation in response to insulin in 3T3-L1 adipocytes. *Mol Cell Biol*. 22(11):3599-3609.
64. Ahn MY, Katsanakis KD, Bheda F, Pillay TS. 2004 Primary and essential role of the adaptor protein APS for recruitment of both c-Cbl and its associated protein CAP in insulin signaling. *J Biol Chem*. 279(20):21526-21532.
65. Baumann CA, Ribon V, Kanzaki M, Thurmond DC, Mora S, Shigematsu S, Bickel PE, Pessin JE, Saltiel AR. 2000 CAP defines a second signalling pathway required for insulin-stimulated glucose transport. *Nature*. 407(6801):202-207.
66. Chiang SH, Baumann CA, Kanzaki M, Thurmond DC, Watson RT, Neudauer CL, Macara IG, Pessin JE, Saltiel AR. 2001 Insulin-stimulated GLUT4 translocation requires the CAP-dependent activation of TC10. *Nature*. 410(6831):944-948.
67. Yokouchi M, Wakioka T, Sakamoto H, Yasukawa H, Ohtsuka S, Sasaki A, Ohtsubo M, Valius M, Inoue A, Komiya S, Yoshimura A. 1999 APS, an adaptor protein containing PH and SH2 domains, is associated with the PDGF receptor and c-Cbl and inhibits PDGF-induced mitogenesis. *Oncogene*. 18(3):759-767.
68. Li M, Li Z, Morris DL, Rui L. 2007 Identification of SH2B2β as an inhibitor for SH2B1- and SH2B2α-promoted Janus kinase-2 activation and insulin signaling. *Endocrinology*. 148(4):1615-1621.
69. Iseki M, Takaki S, Takatsu K. 2000 Molecular cloning of the mouse APS as a member of the Lnk family adaptor proteins. *Biophys Res Commun*. 272(1):45-54.
70. Wakioka T, Sasaki A, Mitsui K, Yokouchi M, Inoue A, Komiya S, Yoshimura A. 1999 APS, an adaptor protein containing Pleckstrin homology (PH) and Src homology-2 (SH2) domains inhibits the JAK-STAT pathway in collaboration with c-Cbl. *Leukemia*. 13(5):760-767.
71. McMullin MF, Cario H. 2016 LNK mutations and myeloproliferative disorders. *Am J Hematol*. 91(2):248-251.
72. Iseki M, Kubo-Akashi C, Kwon SM, Yamaguchi A, Takatsu K, Takaki S. 2005 APS, an adaptor molecule containing PH and SH2 domains, has a negative regulatory role in B cell proliferation. *Biochem Biophys Res Commun*. 330(3):1005-1013.
73. Kubo-Akashi C, Iseki M, Kwon SM, Takizawa H, Takatsu K, Takaki S. 2004 Roles of a conserved family of adaptor proteins, Lnk, SH2-B, and APS, for mast cell development, growth, and functions: APS-deficiency causes augmented degranulation and reduced actin assembly. *Biochem Biophys Res Commun*. 315(2):356-362.
74. Takizawa H, Kubo-Akashi C, Nobuhisa I, Kwon SM, Iseki M, Taga T, Takatsu K, Takaki S. 2006 Enhanced engraftment of hematopoietic stem/progenitor cells by the transient inhibition of an adaptor protein, Lnk. *Blood*. 107(7):2968-2975.
75. Mori T, Suzuki-Yamazaki N, Takaki S. 2018 Lnk/Sh2b3 Regulates Adipose Inflammation and Glucose Tolerance through Group 1 ILCs. *Cell Rep*. 24(7):1830-1841.

76. Bersenev A, Wu C, Balcerek J, Tong W. 2008 Lnk controls mouse hematopoietic stem cell self-renewal and quiescence through direct interactions with JAK2. *J Clin Invest*. 118(8):2832-2844.
77. Simon C, Dondi E, Chaix A, de Sepulveda P, Kubiseski TJ, Varin-Blank N, Velazquez L. 2008 Lnk adaptor protein down-regulates specific Kit-induced signaling pathways in primary mast cells. *Blood*. 112(10):4039-4047.
78. Tong W, Zhang J, Lodish HF. 2005 Lnk inhibits erythropoiesis and Epo-dependent JAK2 activation and downstream signaling pathways. *Blood*. 105(12):4604-4612.
79. Seita J, Ema H, Ooehara J, Yamazaki S, Tadokoro Y, Yamasaki A, Eto K, Takaki S, Takatsu K, Nakauchi H. 2007 Lnk negatively regulates self-renewal of hematopoietic stem cells by modifying thrombopoietin-mediated signal transduction. *Proc Nat Acad Sci USA*. 104(7):2349-2354.
80. Takaki S, Sauer K, Iritani BM, Chien S, Ebihara Y, Tsuji K, Takatsu K, Perlmutter RM. 2000 Control of B cell production by the adaptor protein lnk. *Immunity*. 13(5):599-609.
81. Velazquez L, Cheng AM, Fleming HE, Furlonger C, Vesely S, Bernstein A, Paige CJ, Pawson T. 2002 Cytokine signaling and hematopoietic homeostasis are disrupted in *Lnk*-deficient mice. *J Exp Med*. 195(12):1599-1611.
82. Buza-Vidas N, Antonchuk J, Qian H, Mansson R, Luc S, Zandi S, Anderson K, Takaki S, Nygren JM, Jensen CT, Jacobsen SE. 2006 Cytokines regulate postnatal hematopoietic stem cell expansion: opposing roles of thrombopoietin and LNK. *Genes Dev*. 20(15):2018-2023.
83. Baran-Marszak F, Magdoud H, Desterke C, Alvarado A, Roger C, Harel S, Mazoyer E, Cassinat B, Chevret S, Tonetti C, Giraudier S, Fenaux P, Cymbalista F, Varin-Blank N, Le Bousse-Kerdiles MC, Kiladjian JJ, Velazquez L. 2010 Expression level and differential JAK2-V617F-binding of the adaptor protein Lnk regulates JAK2-mediated signals in myeloproliferative neoplasms. *Blood*. 116(26):5961-5971.
84. Pardanani A. 2008 JAK2 inhibitor therapy in myeloproliferative disorders: rationale, preclinical studies and ongoing clinical trials. *Leukemia*. 22(1):23-30.
85. Gery S, Cao Q, Gueller S, Xing H, Tefferi A, Koeffler HP. 2009 Lnk inhibits myeloproliferative disorder-associated JAK2 mutant, JAK2V617F. *J Leukoc Biol*. 85(6):957-965.
86. Oh ST, Simonds EF, Jones C, Hale MB, Goltsev Y, Gibbs KD, Jr., Merker JD, Zehnder JL, Nolan GP, Gotlib J. 2010 Novel mutations in the inhibitory adaptor protein LNK drive JAK-STAT signaling in patients with myeloproliferative neoplasms. *Blood*. 116(6):988-992.
87. Hurtado C, Erquiaga I, Aranaz P, Migueliz I, Garcia-Delgado M, Novo FJ, Vizmanos JL. 2011 LNK can also be mutated outside PH and SH2 domains in myeloproliferative neoplasms with and without V617FJAK2 mutation. *Leuk Res*. 35(11):1537-1539.
88. Lasho TL, Mudireddy M, Finke CM, Hanson CA, Ketterling RP, Szuber N, Begna KH, Patnaik MM, Gangat N, Pardanani A, Tefferi A. 2018 Targeted next-generation sequencing in blast phase myeloproliferative neoplasms. *Blood Adv*. 2(4):370-380.
89. Oh ST, Gotlib J. 2010 JAK2 V617F and beyond: role of genetics and aberrant signaling in the pathogenesis of myeloproliferative neoplasms. *Expert Rev Hematol*. 3(3):323-337.
90. Pardanani A, Lasho T, Finke C, Oh ST, Gotlib J, Tefferi A. 2010 LNK mutation studies in blast-phase myeloproliferative neoplasms, and in chronic-phase disease with TET2, IDH, JAK2 or MPL mutations. *Leukemia*. 24(10):1713-1718.

91. Tefferi A, Lasho TL, Guglielmelli P, Finke CM, Rotunno G, Elala Y, Pacilli A, Hanson CA, Pancrazzi A, Ketterling RP, Mannarelli C, Barraco D, Fanelli T, Pardanani A, Gangat N, Vannucchi AM. 2016 Targeted deep sequencing in polycythemia vera and essential thrombocythemia. *Blood Adv*. 1(1):21-30.
92. Doche MD, Bochukova EG, Su HW, Pearce L, Keogh JM, Henning E, Cline JM, Dale A, Cheetham T, Barroso I, Argetsinger LS, O'Rahilly SO, Rui L, Carter-Su C, Farooqi IS. 2012 *SH2B1* mutations are associated with maladaptive behavior and obesity. *J Clin Invest*. 122(12):4732-4736.
93. Morton GJ, Meek, T. H., Schwartz, M. W. 2014 Neurobiology of food intake in health and disease. *Nat Rev Neurosci*. 15(6):367-378.
94. Myers Jr. MG, Olson DP. 2012 Central nervous system control of metabolism. *Nature*. 491(7424):357-363.
95. Crowley VE, Yeo GS, O'Rahilly S. 2002 Obesity therapy: altering the energy intake-and-expenditure balance sheet. *Nat Rev Drug Discov*. 1(4):276-286.
96. Rodriguez EM, Blazquez JL, Guerra M. 2010 The design of barriers in the hypothalamus allows the median eminence and the arcuate nucleus to enjoy private milieus: the former opens to the portal blood and the latter to the cerebrospinal fluid. *Peptides*. 31(4):757-776.
97. Zhao AZ, Huan JN, Gupta S, Pal R, Sahu A. 2002 A phosphatidylinositol 3-kinase phosphodiesterase 3B-cyclic AMP pathway in hypothalamic action of leptin on feeding. *Nat Neurosci*. 5(8):727-728.
98. Zhao R, Guerrah A, Tang H, Zhao ZJ. 2002 Cell surface glycoprotein PZR is a major mediator of concanavalin A-induced cell signaling. *J Biol Chem*. 277(10):7882-7888.
99. Gao Q, Wolfgang MJ, Neschen S, Morino K, Horvath TL, Shulman GI, Fu XY. 2004 Disruption of neural signal transducer and activator of transcription 3 causes obesity, diabetes, infertility, and thermal dysregulation. *Proc Nat Acad Sci USA*. 101(13):4661-4666.
100. Farooqi IS, Keogh JM, Kamath S, Jones S, Gibson WT, Trussell R, Jebb SA, Lip GY, O'Rahilly S. 2001 Partial leptin deficiency and human adiposity. *Nature*. 414(6859):34-35.
101. Gibson WT, Farooqi IS, Moreau M, DePaoli AM, Lawrence E, O'Rahilly S, Trussell RA. 2004 Congenital leptin deficiency due to homozygosity for the Δ133G mutation: report of another case and evaluation of response to four years of leptin therapy. *J Clin Endo Metab*. 89(10):4821-4826.
102. Konner AC, Klockener T, Bruning JC. 2009 Control of energy homeostasis by insulin and leptin: targeting the arcuate nucleus and beyond. *Physiol Behav*. 97(5):632-638.
103. Waterson MJ, Horvath TL. 2015 Neuronal Regulation of Energy Homeostasis: Beyond the Hypothalamus and Feeding. *Cell Metab*. 22(6):962-970.
104. Schwartz MW, Woods SC, Porte Jr. D, Seeley RJ, Baskin DG. 2000 Central nervous system control of food intake. *Nature*. 404(6778):661-671.
105. Coll AP, Farooqi IS, Challis BG, Yeo GS, O'Rahilly S. 2004 Proopiomelanocortin and energy balance: insights from human and murine genetics. *J Clin Endo Metab*. 89(6):2557-2562.
106. Robinson SL, Thiele TE. 2017 The Role of Neuropeptide Y (NPY) in Alcohol and Drug Abuse Disorders. *Int Rev Neurobiol*. 136:177-197.

107. Minor RK, Lopez M, Younts CM, Jones B, Pearson KJ, Anson RM, Dieguez C, de Cabo R. 2011 The arcuate nucleus and neuropeptide Y contribute to the antitumorigenic effect of calorie restriction. *Aging Cell*. 10(3):483-492.
108. Betley JN, Cao ZF, Ritola KD, Sternson SM. 2013 Parallel, redundant circuit organization for homeostatic control of feeding behavior. *Cell*. 155(6):1337-1350.
109. Farooqi S, O'Rahilly S. 2006 Genetics of obesity in humans. *Endocrine Reviews*. 27(7):710-718.
110. Xu B, Goulding EH, Zang K, Cepoi D, Cone RD, Jones KR, Tecott LH, Reichardt LF. 2003 Brain-derived neurotrophic factor regulates energy balance downstream of melanocortin-4 receptor. *Nat Neurosci*. 6(7):736-742.
111. Cohen-Cory S, Kidane AH, Shirkey NJ, Marshak S. 2010 Brain-derived neurotrophic factor and the development of structural neuronal connectivity. *Dev Neurobiol*. 70(5):271-288.
112. Lipsky RH, Marini AM. 2007 Brain-derived neurotrophic factor in neuronal survival and behavior-related plasticity. *Ann N Y Acad Sci*. 1122:130-143.
113. Jellinger PS. 2007 Metabolic consequences of hyperglycemia and insulin resistance. *Clin Cornerstone*. 8 Suppl 7:S30-42.
114. Unger TJ, Calderon GA, Bradley LC, Sena-Esteves M, Rios M. 2007 Selective deletion of *Bdnf* in the ventromedial and dorsomedial hypothalamus of adult mice results in hyperphagic behavior and obesity. *J Neurosci*. 27(52):14265-14274.
115. Xu B, Xie X. 2016 Neurotrophic factor control of satiety and body weight. *Nat Rev Neurosci*. 17(5):282-292.
116. Han JC, Liu QR, Jones M, Levinn RL, Menzie CM, Jefferson-George KS, Adler-Wailes DC, Sanford EL, Lacbawan FL, Uhl GR, Rennert OM, Yanovski JA. 2008 Brain-derived neurotrophic factor and obesity in the WAGR syndrome. *N Engl J Med*. 359(9):918-927.
117. Rios M, Fan G, Fekete C, Kelly J, Bates B, Kuehn R, Lechan RM, Jaenisch R. 2001 Conditional deletion of brain-derived neurotrophic factor in the postnatal brain leads to obesity and hyperactivity. *Mol Endocrinol*. 15(10):1748-1757.
118. Prentki M, Matschinsky FM, Madiraju SR. 2013 Metabolic signaling in fuel-induced insulin secretion. *Cell Metab*. 18(2):162-185.
119. Belgardt BF, Bruning JC. 2010 CNS leptin and insulin action in the control of energy homeostasis. *Ann N Y Acad Sci*. 1212:97-113.
120. Rui L. 2014 Energy metabolism in the liver. *Compr Physiol*. 4(1):177-197.
121. Air EL, Strowski MZ, Benoit SC, Conarello SL, Salituro GM, Guan X-M, Liu K, Woods SC, Zhang BB. 2002 Small molecule insulin mimetics reduce food intake and body weight and prevent development of obesity. *Nat Med*. 8(2):179-183.
122. Benoit SC, Air EL, Coolen LM, Strauss R, Jackman A, Clegg DJ, Seeley RJ, Woods SC. 2002 The catabolic action of insulin in the brain is mediated by melanocortins. *J Neurosci*. 22(20):9048-9052.
123. Sipols AJ, Baskin DG, Schwartz MW. 1995 Effect of intracerebroventricular insulin infusion on diabetic hyperphagia and hypothalamic neuropeptide gene expression. *Diabetes*. 44(2):147-151.
124. Konner AC, Janoschek R, Plum L, Jordan SD, Rother E, Ma X, Xu C, Enriori P, Hampel B, Barsh GS, Kahn CR, Cowley MA, Ashcroft FM, Bruning JC. 2007 Insulin action in AgRP-expressing neurons is required for suppression of hepatic glucose production. *Cell Metab*. 5(6):438-449.

125. Russell JW, Feldman EL. 2001 Impaired glucose tolerance--does it cause neuropathy? *Muscle & Nerve*. 24(9):1109-1112.
126. Hill JW, Elias CF, Fukuda M, Williams KW, Berglund ED, Holland WL, Cho YR, Chuang JC, Xu Y, Choi M, Lauzon D, Lee CE, Coppari R, Richardson JA, Zigman JM, Chua S, Scherer PE, Lowell BB, Bruning JC, Elmquist JK. 2010 Direct insulin and leptin action on pro-opiomelanocortin neurons is required for normal glucose homeostasis and fertility. *Cell Metab*. 11(4):286-297.
127. Williams KW, Margatho LO, Lee CE, Choi M, Lee S, Scott MM, Elias CF, Elmquist JK. 2010 Segregation of acute leptin and insulin effects in distinct populations of arcuate proopiomelanocortin neurons. *J Neurosci*. 30(7):2472-2479.
128. Morton GJ, Schwartz MW. 2011 Leptin and the central nervous system control of glucose metabolism. *Physiol Rev*. 91(2):389-411.
129. Jo YH, Chua SC, Jr. 2013 The brain-liver connection between BDNF and glucose control. *Diabetes*. 62(5):1367-1368.
130. Jo YH. 2012 Endogenous BDNF regulates inhibitory synaptic transmission in the ventromedial nucleus of the hypothalamus. *J Neurophysiol*. 107(1):42-49.
131. Komori T, Morikawa Y, Nanjo K, Senba E. 2006 Induction of brain-derived neurotrophic factor by leptin in the ventromedial hypothalamus. *Neuroscience*. 139(3):1107-1115.
132. Li Z, Zhou Y, Carter-Su C, Myers Jr. MG, Rui L. 2007 SH2B1 enhances leptin signaling by both Janus kinase 2 Tyr^{813} phosphorylation-dependent and -independent mechanisms. *Mol Endocrinol*. 21(9):2270-2281.
133. Ren D, Zhou Y, Morris D, Li M, Li Z, Rui L. 2007 Neuronal SH2B1 is essential for controlling energy and glucose homeostasis. *J Clin Invest*. 117(2):397-406.
134. Duan C, Tang C, Liao L, Li C, Su T, Chen Z. 2010 [Molecular mechanism of SH2B1 in regulating JAK2/IRS2 during obesity development]. *Zhong Nan Da Xue Xue Bao Yi Xue Ban*. 35(3):209-214.
135. Yoshiga D, Sato N, Torisu T, Mori H, Yoshida R, Nakamura S, Takaesu G, Kobayashi T, Yoshimura A. 2007 Adaptor protein SH2-B linking receptor-tyrosine kinase and Akt promotes adipocyte differentiation by regulating peroxisome proliferator-activated receptor gamma messenger ribonucleic acid levels. *Mol Endocrinol*. 21(5):1120-1131.
136. Song W, Ren D, Li W, Jiang L, Cho KW, Huang P, Fan C, Song Y, Liu Y, Rui L. 2010 SH2B regulation of growth, metabolism, and longevity in both insects and mammals. *Cell Metab*. 11(5):427-437.
137. Hester JM, Wing MR, Li J, Palmer ND, Xu J, Hicks PJ, Roh BH, Norris JM, Wagenknecht LE, Langefeld CD, Freedman BI, Bowden DW, Ng MC. 2012 Implication of European-derived adiposity loci in African Americans. *Int J Obes (Lond)*. 36(3):465-473.
138. León-Mimila P V-RH, Villalobos-Comparán M, Villarreal-Molina T, Romero-Hidalgo S, López-Contreras B, Gutiérrez-Vidal R, Vega-Badillo J, Jacobo-Albavera L, Posadas-Romeros C, Canizalez-Román A, Río-Navarro BD, Campos-Pérez F, Acuña-Alonzo V, Aguilar-Salinas C, Canizales-Quinteros S. 2013 Contribution of common genetic variants to obesity and obesity-related traits in mexican children and adults. *PloS One*. 8(8):e70640.
139. Ng MC, Tam CH, So WY, Ho JS, Chan AW, Lee HM, Wang Y, Lam VK, Chan JC, Ma RC. 2010 Implication of genetic variants near NEGR1, SEC16B, TMEM18,

ETV5/DGKG, GNPDA2, LIN7C/BDNF, MTCH2, BCDIN3D/FAIM2, SH2B1, FTO, MC4R, and KCTD15 with obesity and type 2 diabetes in 7705 Chinese. *J Clin Endocrinol Metab*. 95(5):2418-2425.
140. Takeuchi F, Yamamoto K, Katsuya T, Nabika T, Sugiyama T, Fujioka A, Isono M, Ohnaka K, Fujisawa T, Nakashima E, Ikegami H, Nakamura J, Yamori Y, Yamaguchi S, Kobayashi S, Ogihara T, Takayanagi R, Kato N. 2011 Association of genetic variants for susceptibility to obesity with type 2 diabetes in Japanese individuals. *Diabetologia*. 54(6):1350-1359.
141. Chen Z, Morris DL, Jiang L, Liu Y, Rui L. 2014 SH2B1 in beta-cells promotes insulin expression and glucose metabolism in mice. *Molecular endocrinology*. 28(5):696-705.
142. Chen Z, Morris DL, Jiang L, Liu Y, Rui L. 2014 SH2B1 in beta-cells regulates glucose metabolism by promoting beta-cell survival and islet expansion. *Diabetes*. 63(2):585-595.
143. Efeyan A, Comb WC, Sabatini DM. 2015 Nutrient-sensing mechanisms and pathways. *Nature*. 517(7534):302-310.
144. Fraenkel M, Ketzinel-Gilad M, Ariav Y, Pappo O, Karaca M, Castel J, Berthault MF, Magnan C, Cerasi E, Kaiser N, Leibowitz G. 2008 mTOR inhibition by rapamycin prevents beta-cell adaptation to hyperglycemia and exacerbates the metabolic state in type 2 diabetes. *Diabetes*. 57(4):945-957.
145. Rachdi L, Balcazar N, Osorio-Duque F, Elghazi L, Weiss A, Gould A, Chang-Chen KJ, Gambello MJ, Bernal-Mizrachi E. 2008 Disruption of Tsc2 in pancreatic beta cells induces beta cell mass expansion and improved glucose tolerance in a TORC1-dependent manner. *Proc Natl Acad Sci U S A*. 105(27):9250-9255.
146. Shimobayashi M, Hall MN. 2014 Making new contacts: the mTOR network in metabolism and signalling crosstalk. *Nat Rev Mol Cell Biol*. 15(3):155-162.
147. Fingar DC, Salama S, Tsou C, Harlow E, Blenis J. 2002 Mammalian cell size is controlled by mTOR and its downstream targets S6K1 and 4EBP1/eIF4E. *Genes Dev*. 16(12):1472-1487.
148. Blandino-Rosano M, Scheys JO, Jimenez-Palomares M, Barbaresso R, Bender AS, Yanagiya A, Liu M, Rui L, Sonenberg N, Bernal-Mizrachi E. 2016 4E-BP2/SH2B1/IRS2 Are Part of a Novel Feedback Loop That Controls beta-Cell Mass. *Diabetes*. 65(8):2235-2248.
149. Postic C, Dentin R, Girard J. 2004 Role of the liver in the control of carbohydrate and lipid homeostasis. *Diabetes Metab*. 30(5):398-408.
150. Sheng L, Liu Y, Jiang L, Chen Z, Zhou Y, Cho KW, Rui L. 2013 Hepatic SH2B1 and SH2B2 regulate liver lipid metabolism and VLDL secretion in mice. *PLoS One*. 8(12):e83269.
151. Jansen R, van Embden JD, Gaastra W, Schouls LM. 2002 Identification of a novel family of sequence repeats among prokaryotes. *OMICS*. 6(1):23-33.
152. Ran FA, Hsu PD, Lin CY, Gootenberg JS, Konermann S, Trevino AE, Scott DA, Inoue A, Matoba S, Zhang Y, Zhang F. 2013 Double nicking by RNA-guided CRISPR Cas9 for enhanced genome editing specificity. *Cell*. 154(6):1380-1389.
153. Deltcheva E, Chylinski K, Sharma CM, Gonzales K, Chao Y, Pirzada ZA, Eckert MR, Vogel J, Charpentier E. 2011 CRISPR RNA maturation by trans-encoded small RNA and host factor RNase III. *Nature*. 471(7340):602-607.
154. Deveau H, Garneau JE, Moineau S. 2010 CRISPR/Cas system and its role in phage-bacteria interactions. *Annu Rev Microbiol*. 64:475-493.

155. Jinek M, Chylinski K, Fonfara I, Hauer M, Doudna JA, Charpentier E. 2012 A programmable dual-RNA-guided DNA endonuclease in adaptive bacterial immunity. *Science*. 337(6096):816-821.
156. Ran FA, Hsu PD, Wright J, Agarwala V, Scott DA, Zhang F. 2013 Genome engineering using the CRISPR-Cas9 system. *Nat Protoc*. 8(11):2281-2308.
157. Cong L, Ran FA, Cox D, Lin S, Barretto R, Habib N, Hsu PD, Wu X, Jiang W, Marraffini LA, Zhang F. 2013 Multiplex genome engineering using CRISPR/Cas systems. *Science*. 339(6121):819-823.
158. Chen F, Pruett-Miller SM, Huang Y, Gjoka M, Duda K, Taunton J, Collingwood TN, Frodin M, Davis GD. 2011 High-frequency genome editing using ssDNA oligonucleotides with zinc-finger nucleases. *Nat Methods*. 8(9):753-755.
159. Saleh-Gohari N, Helleday T. 2004 Conservative homologous recombination preferentially repairs DNA double-strand breaks in the S phase of the cell cycle in human cells. *Nucleic Acids Res*. 32(12):3683-3688.
160. Tyers M, Haslam RJ, Rachubinski RA, Harley CB. 1989 Molecular analysis of pleckstrin: the major protein kinase C substrate of platelets. *J Cell Biochem*. 40(2):133-145.
161. Mayer BJ, Ren R, Clark KL, Baltimore D. 1993 A putative modular domain present in diverse signaling proteins. *Cell*. 73(4):629-630.
162. Scheffzek K, Welti S. 2012 Pleckstrin homology (PH) like domains - versatile modules in protein-protein interaction platforms. *FEBS Lett*. 586(17):2662-2673.
163. Hyvonen M, Macias MJ, Nilges M, Oschkinat H, Saraste M, Wilmanns M. 1995 Structure of the binding site for inositol phosphates in a PH domain. *EMBO J*. 14(19):4676-4685.
164. Yu JW, Mendrola JM, Audhya A, Singh S, Keleti D, DeWald DB, Murray D, Emr SD, Lemmon MA. 2004 Genome-wide analysis of membrane targeting by S. cerevisiae pleckstrin homology domains. *Mol Cell*. 13(5):677-688.
165. Park WS, Heo WD, Whalen JH, O'Rourke NA, Bryan HM, Meyer T, Teruel MN. 2008 Comprehensive identification of PIP3-regulated PH domains from C. elegans to H. sapiens by model prediction and live imaging. *Mol Cell*. 30(3):381-392.
166. Timper K, Bruning JC. 2017 Hypothalamic circuits regulating appetite and energy homeostasis: pathways to obesity. *Dis Model Mech*. 10(6):679-689.
167. Maures TJ. Molecular mechanisms by which adapter protein SH2B1β facilitates NGF-dependent neuronal differentiation. *Cellular and Molecular Biology.* Vol Ph.D. Ann Arbor: University of Michigan; 2008:261.
168. Lemmon MA. 2003 Phosphoinositide recognition domains. *Traffic*. 4(4):201-213.
169. Baumeister MA, Rossman KL, Sondek J, Lemmon MA. 2006 The Dbs PH domain contributes independently to membrane targeting and regulation of guanine nucleotide-exchange activity. *Biochem J*. 400(3):563-572.
170. Klein DE, Lee A, Frank DW, Marks MS, Lemmon MA. 1998 The pleckstrin homology domains of dynamin isoforms require oligomerization for high affinity phosphoinositide binding. *J Biol Chem*. 273(42):27725-27733.
171. Rui L, Herrington J, Carter-Su C. 1999 SH2-B, a membrane-associated adapter, is phosphorylated on multiple serines/threonines in response to nerve growth factor by kinases within the MEK/ERK cascade. *J Biol Chem*. 274(37):26485-26492.

172. Li Q, Cao X, Qiu H-Y, Lu J, Gao R, Liu C, Yuan M-X, Yang G-R, Yang J-K. 2016 A three-step programmed method for the identification of causative gene mutations of maturity onset diabetes of the young (MODY). *Gene*. 588(2):141-148.
173. Volckmar AL, Bolze F, Jarick I, Knoll N, Scherag A, Reinehr T, Illig T, Grallert H, Wichmann HE, Wiegand S, Biebermann H, Krude H, Fischer-Posovszky P, Rief W, Wabitsch M, Klingenspor M, Hebebrand J, Hinney A. 2012 Mutation screen in the GWAS derived obesity gene SH2B1 including functional analyses of detected variants. *BMC Med Genomics*. 5:65.
174. Ahima RS. 2008 Revisiting leptin's role in obesity and weight loss. *J Clin Invest*. 118(7):2380-2383.
175. McLaren L. 2007 Socioeconomic status and obesity. *Epidemiol Rev*. 29:29-48.
176. Himsworth HP. 1934 Dietetic factors influencing the glucose tolerance and the activity of insulin. *J Physiol*. 81(1):29-48.
177. Sweeney JS. Dietary Factors That Influence the Dextrose Tolerance Test, A Preliminary Study. *Departments of Internal Medicine and Physiology, Baylor University, College of Medicine*.818-830.
178. Vaudry D, Stork PJ, Lazarovici P, Eiden LE. 2002 Signaling pathways for PC12 cell differentiation: making the right connections. *Science*. 296(5573):1648-1649.
179. Li H, Tochio N, Koshiba S, Inoue M, Kigawa T, Yokoyama S. 2003 Solution Structure of the Pleckstrin Homology Domain of Mouse APS. *RCSB Protein Data Bank*.
180. Spolverini A, Pieri L, Guglielmelli P, Pancrazzi A, Fanelli T, Paoli C, Bosi A, Nichele I, Ruggeri M, Vannucchi AM. 2013 Infrequent occurrence of mutations in the PH domain of LNK in patients with JAK2 mutation-negative 'idiopathic' erythrocytosis. *Haematologica*. 98(9):e101-102.
181. Krishnan M, Thompson JMD, Mitchell EA, Murphy R, McCowan LME, Shelling AN, On Behalf Of The Children Of Scope Study Group G. 2017 Analysis of association of gene variants with obesity traits in New Zealand European children at 6 years of age. *Mol Biosyst*. 13(8):1524-1533.
182. Suzuki K, Mizutani M, Hitomi Y, Kizaki T, Ohno H, Ishida H, Haga S, Koizumi S. 2002 Association of SH2-B to phosphorylated tyrosine residues in the activation loop of TrkB. *Res Commun Mol Pathol Pharmacol*. 111(1-4):27-39.
183. Segal RA, Greenberg ME. 1996 Intracellular signaling pathways activated by neurotrophic factors. *Ann Rev Neurosci*. 19:463-489.
184. Farooqi IS, O'Rahilly, S. 2014 20 years of leptin: human disorders of leptin action. *J Endocrinol*. 223(1):T63-70.
185. Hsu YC, Chen SL, Wang YJ, Chen YH, Wang DY, Chen L, Chen CH, Chen HH, Chiu IM. 2014 Signaling adaptor protein SH2B1 enhances neurite outgrowth and accelerates the maturation of human induced neurons. *Stem cells translational medicine*. 3(6):713-722.
186. Liao GY, Bouyer K, Kamitakahara A, Sahibzada N, Wang CH, Rutlin M, Simerly RB, Xu B. 2015 Brain-derived neurotrophic factor is required for axonal growth of selective groups of neurons in the arcuate nucleus. *Molecular metabolism*. 4(6):471-482.
187. Boden G, Laakso M. 2004 Lipids and glucose in type 2 diabetes: what is the cause and effect? *Diabetes Care*. 27(9):2253-2259.